Document Version July 1, 2008

The TAM/WASP Modeling Framework for Development of Nutrient and BOD TMDLs in the Tidal Anacostia River

Ross Mandel
Sunghee Kim
Andrea Nagel
Jim Palmer
Cherie Schultz

Interstate Commission on the Potomac River Basin
51 Monroe Street, Suite PE-08
Rockville, MD 20850

and

Kaye Brubaker, Ph.D.
Department of Civil and Environmental Engineering
1173 Glenn L. Martin Hall
University of Maryland
College Park, MD 20742

February 11, 2008

ICPRB Report 08-1

ACKNOWLEDGEMENTS

The authors would like to thank Nauth Panday and Tom Thornton of the Maryland Department of Environment for their valuable input and assistance, and for their encouragement and patience throughout this project.

The authors would also like to thank the following persons who provided data and other information used in model development and model calibration: Brenda Majedi of the U.S. Geological Survey – MD-DE-DC Water Science Center; Meo Curtis and Keith Van Ness of the Montgomery County Department of Environmental Protection; Dr. M. Cheng, Dawn Hawkins-Nixon, Sharon Meigs, and Donna Wilson, Director, Prince George's County Department of Environmental Resources.

The Anacostia Nutrient/BOD TMDLs were a joint effort of MDE; DC Department of the Environment; U. S. Environmental Protection Agency, Headquarters and Region IIII; and the EPA's consultants, Limno-Tech. The authors would like to thank the following participants in the TMDL development effort who guided and reviewed our work: Monir Chowdhury, DDOE; Mike Haire, EPA Headquarters; Tom Henry, EPA Region III; Helene Drago, EPA Region III; Mary Kuo, EPA Region III; Kuo-Liang Lai, EPA Region III; Michael Sullivan, LTI; Scott Hinz, LTI; and David Dilks, LTI.

The opinions expressed in this report are those of the authors and should not be construed as representing the several states of the signatories or Commissioners to the Interstate Commission on the Potomac River Basin: Maryland, Pennsylvania, Virginia, West Virginia, or the District of Columbia.

Funding for this project was provided by the Maryland Department of the Environment and the signatories to the Interstate Commission on the Potomac River Basin.

TABLE OF CONTENTS

LIST OF TABLES

LIST OF FIGURES

EXECUTIVE SUMMARY

The TAM/WASP modeling framework has been successfully updated to develop biochemical oxygen demand (BOD), total nitrogen (TN), and total phosphorus (TP) total maximum daily loads (TMDLs) for the tidal Anacostia River. The updated framework includes revised loads from the Northeast Branch (NEB) , Northwest Branch (NWB), Lower Beaverdam Creek (LBC), and Watts Branch, as well as smaller tributaries, direct drainage to the tidal river, Combined Sewer Overflows (CSOs), and municipal and industrial point sources. The U.S. Geological Survey (USGS) software ESTIMATOR was used to determine total nutrient and BOD loads from NE and NWB. A revised Hydrological Simulation Program Fortran (HSPF) model of the NEB and NWB was used to quantify the sources of these loads. Revised HSPF models of LBC and Watts Branch were used both to determine overall loads to the Anacostia from these tributaries, as well as to quantify the sources of these loads. CSO loads were determined based on information developed for the District of Columbia Water and Sewer Authority's (DCWASA's) Long-Term Control Plan (LTCP), included simulated flows from the LTCP's MOUSE model.

The eutrophication component of the TAM/WASP model was recalibrated for the period 1995-2002. This period encompasses both the TMDL simulation period (1995-1997) and a period (1999-2002) in which chlorophyll *a* (Chla) monitoring data was collected in the Anacostia. The calibration successfully met its two objectives: (1) the minimum simulated dissolved oxygen (DO) concentration should be no greater than the minimum DO observed at the major ambient monitoring stations on an annual basis, and (2) the maximum simulated Chla should be no less than the maximum Chla observed at the major ambient monitoring stations. After meeting these two objectives, the recalibrated model was used to demonstrate that water quality standards for DO, Chla, and water clarity could be met in the Anacostia if BOD loads were reduced by 58% and both TN and TP loads reduced by 80%.

1 INTRODUCTION

This report describes the refinement and recalibration of the TAM/WASP EUTRO Model for use in the joint Maryland-District of Columbia nutrient and biochemical oxygen demand (BOD) Total Maximum Daily Loads (TMDLs) for the tidal Anacostia River (MDE and DDOE, 2008). It constitutes the second volume to the report (Schultz et al, 2007), which similarly described the use of the TAM/WASP model in developing the joint sediment TMDL for the Anacostia (MDE and DDOE, 2007).

The original TAM/WASP Model, which itself was based on the Metropolitan Council of Government's (MWCOG) tidal Anacostia Model (TAM), was developed for use in the District's initial BOD TMDL (DCDOH, 2002). The sediment component of the TAM/WASP modeling framework (Schultz, 2003) was used to develop the sediment TMDL for the District (DCDOH, 2001), which was submitted to, but not approved by, Region III of the U. S. Protection Agency (U.S. EPA). The EPA developed its own sediment TMDL for the tidal Anacostia River using the TAM/WASP modeling framework (U. S. EPA, 2001a). Both the sediment TMDL and the BOD TMDL were voided by the Third Circuit Court of Appeals because the TMDL included only average annual, but not daily, maximum loads. At the time of the court's decision, the Maryland Department of the Environment (MDE) was in the process of developing sediment, nutrient, and BOD TMDLs for its portion of the Anacostia Basin, also based on the TAM/WASP modeling framework. In response to the court's decision, the District of Columbia's Department of the Environment (DDOE) and the EPA joined MDE in the effort to develop revised TMDLs for the Anacostia Basin for both jurisdictions.

The modeling framework associated with the TAM/WASP Model includes Hydrological Simulation Program Fortran (HSPF) models of the non-tidal Anacostia River watershed, representing the Northeast Branch (NEB), the Northwest Branch (NWB), Lower Beaverdam Creek (LBC), and the Watts Branch. Two earlier versions of these models were developed for MDE by Manchester and Mandel (2001) and Mandel et al. (2003). The current version of these models was recalibrated concurrently with TAM/WASP Model to calculate loads and their sources for the sediment, nutrient, and BOD TMDLs. The calibration of the hydrology and sediment simulations is described in Schultz et al. (2007). The calibration of nutrient and BOD loads for the nutrient and BOD TMDLs is described in this report.

1.1 Setting

The Anacostia River watershed covers an area of approximately 174 square miles (mi^2), with 17% of the watershed lying within the boundaries of District of Columbia, and 83% in the State of Maryland. Figure 1.1 shows the location of the river and its watershed. The main channel of the Anacostia River begins in Bladensburg, Maryland, at the confluence of its two largest tributaries, the Northeast Branch and the Northwest Branch, and flows a distance of approximately 8.4 miles before it discharges into the Potomac River in Washington, DC. The drainage areas of the Northeast and Northwest Branch

tributaries, 53 mi^2 and 72 mi^2, respectively, comprise approximately 72% of the total area of the watershed.

Because of its location in the Washington metropolitan area, the majority of the watershed is highly urbanized, with a population of 804,500 in 1990 and a projected population of 838,100 by the year 2010 (Warner *et al*., 1997). Land use in the watershed is approximately 75% urban, 5% agricultural, and 20% forest or wetlands, with 23% of the area of the watershed covered by impervious surfaces.

The Anacostia River is actually an estuary, with tidal influence extending some distance into the Northeast and the Northwest Branch tributaries. The variation in the river's water surface elevation over a tidal cycle is approximately 3 feet. However, water in the tidal portion of the river is fresh, with negligible values of salinity. From an analysis by the National Oceanographic and Atmospheric Administration (NOAA) of sounding data taken by the US Army Corps of Engineers prior to a 1999 dredging project combined with additional bathymetry data taken by the Navy in the summer of 2000, the volume of the tidal portion of the river at mean tide is approximately 10,000,000 cubic meters (m^3), with a surface area of approximately 3,300,000 square meters (m^2). The width of the river varies from approximately 60 meters (m) in some upstream reaches to approximately 500 m near the confluence with the Potomac, and average depths across channel transects vary from approximately 1.2 m upstream of Bladensburg to about 5.6 m just downstream of the South Capital Street Bridge. During non-storm conditions, measured flow velocities during the tidal cycle have been in the range of 0 to 0.3 m/sec (Katz *et al*., 2000; Schultz and Velinsky, 2001).

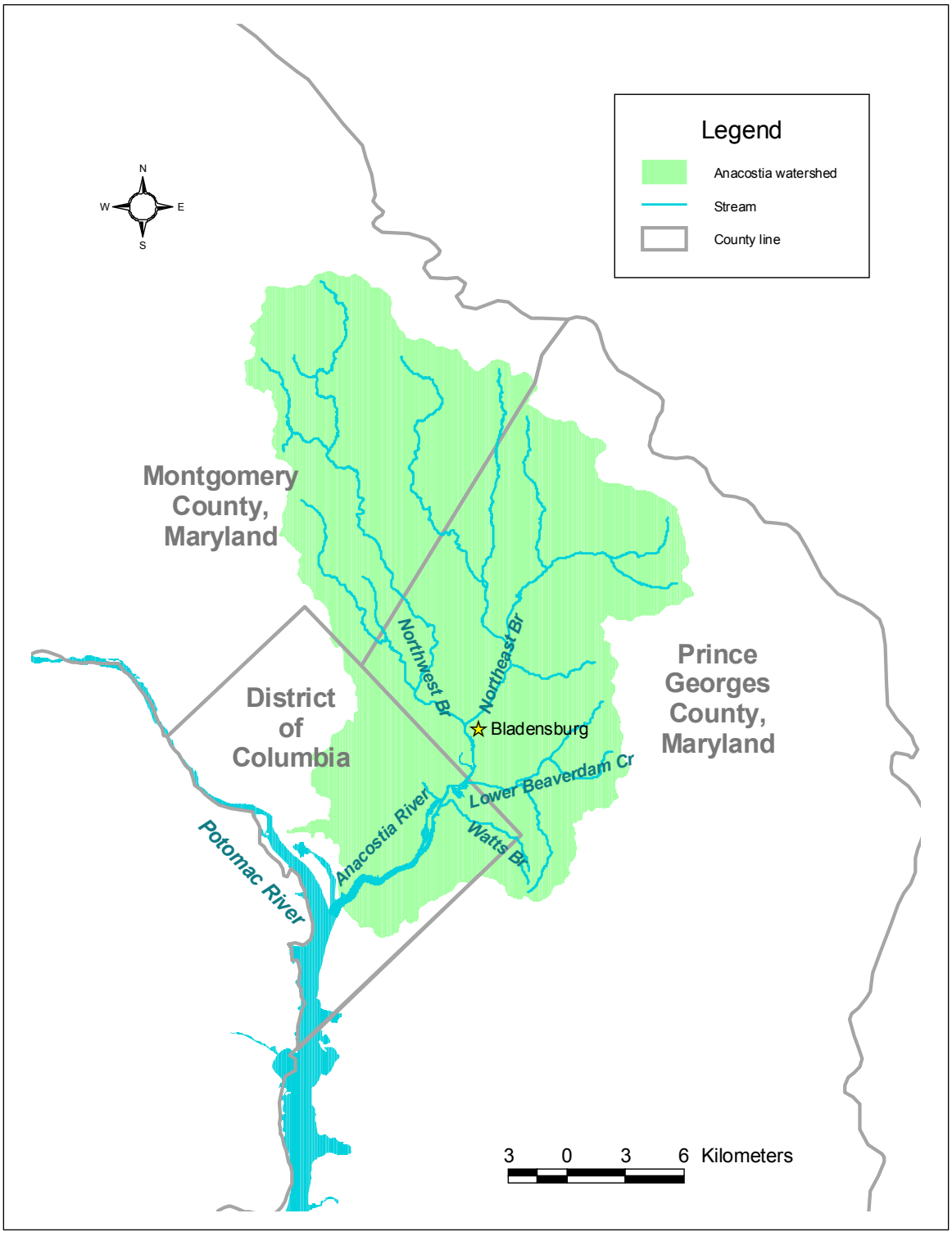

Figure 1.1. The Anacostia River Watershed

2 SOURCE ASSESSMENT AND THE NON-TIDAL ANACOSTIA WATERSHED HSPF MODELS

There are two requirements that the source assessment of nutrient and BOD loads must meet. First, the TMDLs will set load allocations for BOD, total nitrogen (TN), and total phosphorus (TP) by source, so the source assessment must determine loads for these constituents by source. Second, daily input loads must be specified for each of the WASP's state variables: ammonia nitrogen (NH4), nitrate nitrogen (NO3), inorganic phosphorus (PO4), BOD, chlorophyll *a* (Chla), dissolved oxygen (DO), organic nitrogen (ON), and organic phosphorus (OP).

A variety of methods were used to calculate input loads to TAM/WASP and their sources.

- For the Northeast and Northwest Branches, the U. S. Geological Survey (USGS) statistical software, ESTIMATOR, was used to calculate daily input loads, based on monitoring data collected by USGS, MWCOG, and MDE. ESTIMATOR cannot identify the source of the loads, so the HSPF models of the Northeast and Northwest Branches were used to determine the loads by source.

- The HSPF models of Lower Beaverdam Creek and Watts Branch were used to directly calculate input loads for TAM/WASP from these tributaries.

- Daily storm flow and base flow were estimated for smaller tributaries and direct drainage to the tidal Anacostia River from the Watts Branch HSPF model. Loads were determined for these flows using average event mean concentrations (EMCs) calculated from monitoring data collected for the DC, Montgomery County, and Prince George's County municipal separate storm sewer system (MS4) permits.

- Municipal and industrial waste water treatment plants flows and loads were determined from monitored flows and concentrations reported for their permits.

- Simulated Combined Sewer Overflows (CSOs) were determined using the MOUSE model, which was developed for the Washington Sewer Authority's (DCWASA) Long-term Control Plant (LTCP) for DC CSOs (DCWASA, 2002). CSO loads were determined from the average event mean concentrations in the monitoring data collected for Anacostia overflows for the LTCP.

The calculation of loads from these sources is discussed in more detail below.

2.1 Stormwater EMCs

Stormwater EMCs play a key role in estimating nutrient and BOD loads to the tidal Anacostia River. Not only are stormwater loads from small tributaries and direct drainage calculated as a product of simulated stormflow and EMC concentration, but

EMCs also serve as calibration targets for the non-tidal Anacostia HSPF models. Table 2.1.1 shows the average EMCs used in the source assessment. Each EMC is the average of the monitoring station average. Separate estimates were made for (1) NEB, NWB, and Maryland direct drainage, (2) LBC and Watts Branch, and (3) DC small tributaries and direct drainage. In Maryland jurisdictions, stations were classified by dominant land use, where as in DC, stations represent mixed land uses, so averages were calculated by land use for Maryland but not for DC. The monitoring stations used to calculate the averages were restricted to the Anacostia watershed. Prince George's County's monitoring stations in the Anacostia are all located in LBC, so separate average EMCs were calculated for LBC. These were also used as calibration targets in the Watts Branch, since the HSPF models of LBC and Watts Branch use the same calibration parameters for their land processes.

Table 2.1.1. Average Stormwater Event Mean Concentrations (mg/l)

Region	Land Use	BOD5	TKN	NO3	TP
All MD Anacostia	Residential	11.6	1.6	0.9	0.3
	Commercial	20.5	2.9	0.6	0.2
	Industrial	14.8	1.4	1.0	0.2
LBC	Residential	12.6	1.9	1.5	0.5
	Commercial	18.6	2.6	0.7	0.3
	Industrial	13.9	1.8	0.6	0.2
DC	All LUs	42.9	2.6	1.1	0.5

2.2 ESTIMATOR Loads

The USGS has developed the software program, ESTIMATOR, to provide a statistically-sound estimate of constituent loads from monitoring data and observed daily average flow. ESTIMATOR calculates daily, monthly, or annual constituent loads based on observed daily average flows and grab-sample monitoring data. ESTIMATOR has been used to calculate nutrient and sediment loads for the RIM (River Input Monitoring) program for the Chesapeake Bay Program, as well as estimate sediment and nutrient trends in the region. Cohn et al. (1989) and Cohn et al. (1992) give the theory behind ESTIMATOR. Langland et al. (2001, 2005) demonstrate the application of ESTIMATOR in the Chesapeake Bay Watershed.

ESTIMATOR contains three elements. The heart of ESTIMATOR is a multiple regression equation which relates the log of constituent concentrations to flow, time and season. The equation for C, the constituent concentration, takes the following form:

$$\ln[C] = \beta_0 + \beta_1 \ln[Q] + \beta_2 \ln[Q]^2 + \beta_3 T + \beta_4 T^2 + \beta_5 \sin[2\pi T] + \beta_6 \cos[2\pi T] + \varepsilon$$

Where

Q is the daily discharge
T is time, expressed in years

The flow and time variables are centered so that terms are orthogonal. Regression relation is essentially a multivariate rating curve, which takes into account temporal trends and seasonal trends as well as trends in flow.

The second element is the use of a minimum variance unbiased (MVUE) procedure to obtain estimates of concentrations and loads from the log of constituent concentrations determined from the regression. Cohn et al. (1989) describe the motivations for using the MVUE procedure, as opposed to simpler methods.

The transformed constituent concentrations are combined with daily flows to estimate daily, monthly, and annual loads. Standard errors, confidence intervals, and standard errors of prediction can also be calculated.

In order for ESTIMATOR to provide good estimates of nutrient and sediment loads, monitoring data must be available over the range of flows for which loads are to be calculated

2.2.1 Available Monitoring Data in the Anacsotia Watershed

MDE, USGS, and the Metropolitan Washington Council of Governments (MWCOG) have all recently conducted water quality monitoring at the USGS gages on the Northeast Branch (01649500) and Northwest Branch (01651000). Figure 2.2.1 shows the location of these gages. Table 2.2.1 characterizes the sampling programs. Tables 2.2.2 and 2.2.3 give summary statistics for DO, BOD, Chla, and nutrient concentrations observed in their programs for NWB and NEB, respectively.

As described above, ESTIMATOR requires (1) a complete record of average daily flows for the period of interest, and (2) constituent concentrations taken over a range of flows, including storm flows. As Table 2.2.1 shows, both the USGS and MWCOG monitoring programs include storm sampling.

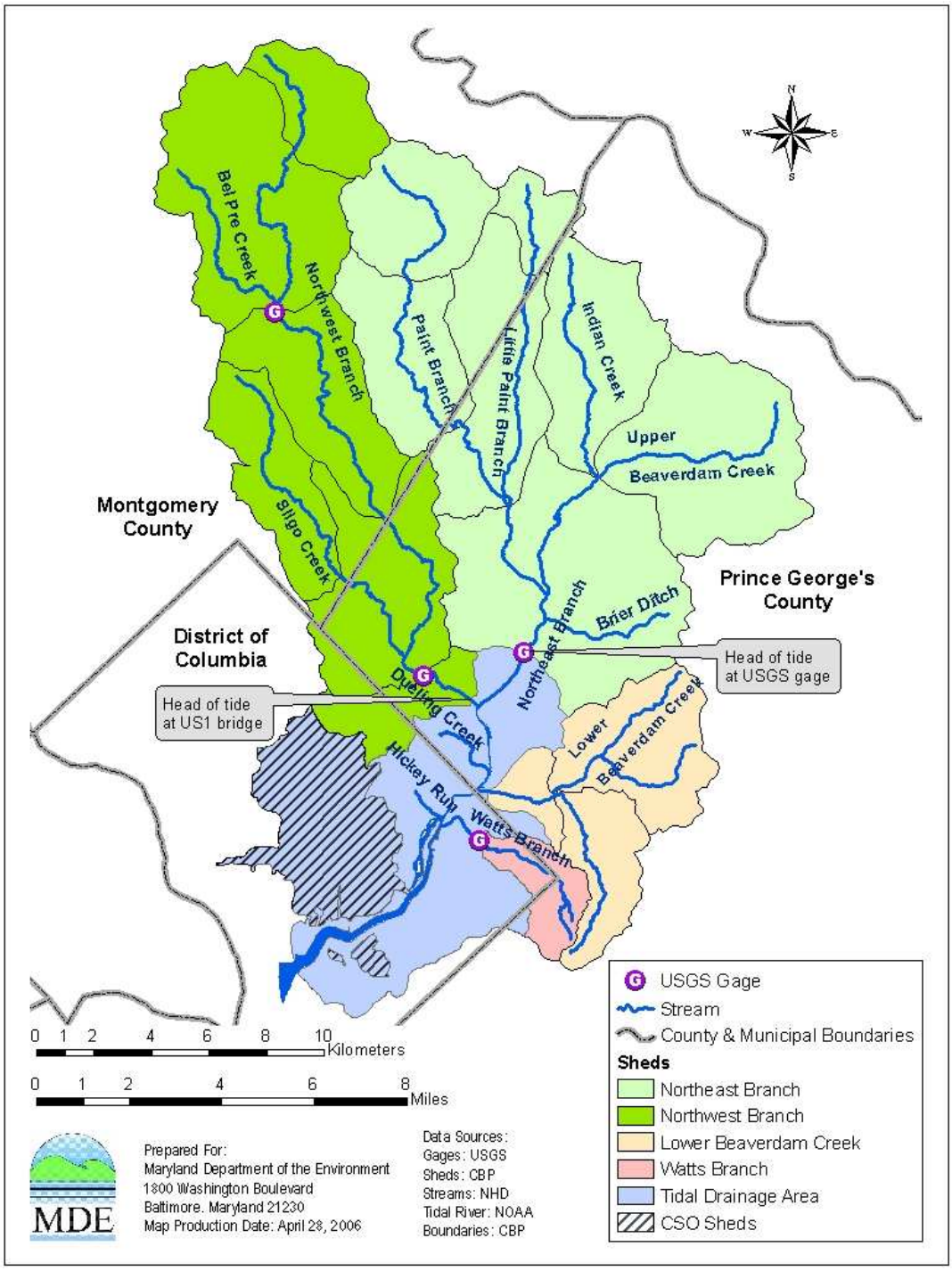

Figure 2.1.1. Location of USGS Gages

Table 2.2.1. Characterization of Non-tidal Anacostia River Watershed Monitoring Programs

Program	Sampling Period	Approx. No. of Nutrient Samples per Location		Description
		NEB	NWB	
LTCP	8/1999 – 3/2000	34	33	Baseflow grab samples and flow-weighted composite storm samples
MDE	8/2004 – 8/2005	15	15	Monthly ambient sampling
USGS	7/2003 – 8/2005	70	65	Instantaneous storm and grab samples

Table 2.2.2. Summary Statistics for Constituent Concentrations (mg/l), NE Branch Anacostia River, 1999-2005

Statistic	BOD5	DO	NH4	NO3	[1]TN	DIP	[1]TP	CHLa
Count	69	103	119	119	118	109	118	13
Min	0.10	7.40	0.00	0.020	0.40	0.003	0.017	0.43
1st Quartile	1.00	8.80	0.02	0.613	1.30	0.009	0.040	1.92
Median	1.00	10.50	0.06	0.803	1.61	0.017	0.118	2.56
3rd Quartile	3.20	11.70	0.10	0.980	2.26	0.022	0.330	3.49
Max	13.00	17.30	0.45	1.440	3.50	0.090	0.670	6.73
Avg	2.09	10.60	0.08	0.780	1.78	0.020	0.187	2.69
Std. Dev.	2.04	2.03	0.09	0.271	0.66	0.017	0.169	1.64

[1] High LTCP outlier excluded

Table 2.2.3. Summary Statistics for Constituent Concentrations (mg/l), NW Branch Anacostia River, 1999-2005

Statistic	BOD5	DO	NH4	[1]NO3	TN	DIP	TP	CHLa
Count	70	121	112	112	112	103	113	11
Min	0.10	7.10	0.00	0.21	0.55	0.003	0.01	1.28
1st Quartile	1.00	8.70	0.01	0.60	1.44	0.005	0.03	1.73
Median	1.00	10.40	0.03	0.85	1.82	0.010	0.10	1.92
3rd Quartile	3.00	12.40	0.09	1.12	2.66	0.020	0.42	3.74
Max	17.50	16.00	0.50	1.99	6.14	0.080	1.07	8.22
Avg	2.38	10.82	0.07	0.88	2.17	0.017	0.24	3.14
Std. Dev.	2.81	2.31	0.09	0.36	1.10	0.017	0.25	2.21

2.2.2 ESTIMATOR Results

Daily loads for the WASP calibration simulation period 1995 through 2002 were calculated using ESTIMATOR for the following constituents: DO, BOD, NH4, NO3, ON, and TP. The time terms were not used in the regression, because the period of record was not long enough to justify estimating temporal trends.

Tables 2.2.4 and 2.2.5 show the results for the NEB and NWB respectively. Each table shows (1) the values of the estimated coefficients for the regression equation, (2) summary statistics, and (3) estimated average annual loads for the period 1995-2002. Generally, the ESTIMATOR regressions have coefficients of determination greater than 0.5, except for NH4 and BOD in the Northeast Branch. With the exception of NO3, residuals from the regression are normally-distributed, and serial correlation between the residuals is less than 0.4, the recommended threshold for concern. The NO3 regression in NEB had non-normal residuals, as determined by the probability plot correlation coefficient, and the NO3 regression in the NWB had a higher degree of serial correlation than recommended. For these reasons, NO3 loads were re-estimated using the Least Absolute Deviation (LAD) method, found in the USGS software package LOADEST. LAD is a non-parametric regression method that does not assume a normally-distributed error term (Runkle, *et al*., 2004). The USGS recommends using this method when regression statistics indicate that the error term is not normally distributed.

Table 2.2.4. Coefficients of Regression Equation and Regression Statistics, Northeast Branch

Coefficient or Statistic	[1] BOD5	[1] DO	[1] NH4	[1] NO3	[3] NO3	[2] ON	[2] TP
Constant	0.32	2.36	-3.06	-0.05	5.91	-0.44	-2.25
log Flow	0.75	* -0.03	* 0.33	0.00	0.90	* 0.36	* 0.56
log Flow^2	-0.07	0.00	-0.01	* -0.11	-0.03	0.04	0.01
sin (2*pi*time)	0.31	* 0.10	* 0.55	0.09	-0.08	* 0.16	-0.01
cos (2*pi*time)	-0.30	* 0.20	0.15	* 0.20	-0.15	* -0.25	* -0.32
Standard Error of Regression (S)	0.96	0.09	0.89	0.41		0.51	0.56
Number of Observations (N)	69	103	119	119	119	117	118
Coefficient of Determination (R^2)	47.5	76.5	42.7	51.7		62.2	75.0
Serial Correlation Coefficient (SCR)	-0.06	0.17	0.30	0.35		0.39	0.35
Probability Plot Correlation Coefficient (PPCC)	0.98	1.00	0.99	0.97		0.98	0.98
Average Annual Load (tons)	499	1,078	9.49	87	78	92	20

[1] ESTIMATOR Model
[2] ESTIMATOR Model, High LTCP outlier excluded
[3] LOADEST Model 6, LAD regression
* Significant at $\alpha = 0.05$

Table 2.2.5. Coefficients of Regression Equation and Regression Statistics, Northwest Branch

Coefficient or Statistic	[1] BOD5	[1] DO	[1] NH4	[1] NO3	[2] NO3	[1] ON	[1] TP
Constant	0.29	2.36	-3.53	-0.12	5.51	-0.31	-2.29
log Flow	* 0.97	-0.01	* 0.29	* -0.11	0.86	* 0.48	* 0.67
log Flow^2	-0.16	* 0.01	* 0.08	* -0.03	-0.05	0.01	0.02
sin (2*pi*time)	-0.01	* 0.15	* 0.54	* 0.21	-0.17	0.01	-0.16
cos (2*pi*time)	0.04	* 0.21	0.02	* 0.13	-0.14	* -0.31	* -0.38
Standard Error of Regression (S)	0.98	0.11	1.00	0.36		0.56	0.72
Number of Observations (N)	70	121	112	112	112	112	113
Coefficients of Determination (R^2)	64.4	74.4	34.8	37.5		69.3	73.0
Serial Correlation Coefficient (SCR)	-0.14	0.17	0.34	0.51		0.23	0.25
Probability Plot Correlation Coefficient (PPCC)	0.96	1.00	0.99	0.99		0.99	0.99
Average Annual Load (tons)	280	664	4.7	54	56	74	17

[1] ESTIMATOR Model
[2] LOADEST Model 6, LAD regression
* Significant at $\alpha = 0.05$

2.3 The Anacostia HSPF Watershed Models

The computer model HSPF was used to develop a computer simulation of the Northwest Branch, Northeast Branch, Lower Beaverdam Creek, and Watts Branch. This is the third version HSPF Model of the Non-tidal Anacostia Watershed developed by ICPRB within the past decade. The Phase I Anacostia Model (Manchester and Mandel, 2001) was developed to confirm the nutrient, sediment, and BOD loading rates used in DC's sediment and BOD TMDLs. It simulated the period 1988-1995, coincident with the simulation period of the TAM/WASP model of the tidal Anacostia. It was calibrated primarily against water quality monitoring data collected by the Coordinated Anacostia Monitoring Program (CAMP). The Phase II Anacostia Model (Mandel *et al*., 2003) was intended to update the Phase I Model. The simulation period was 1996-2000, and it was calibrated against water quality monitoring data collected by the Metropolitan Washington Council of Governments (MWCOG) for the DC combined sewer system overflow (CSO) Long-Term Control Plan (LTCP) 1999-2000. While the LTCP data was more up-to-date than the CAMP data, it was collected during a very dry period punctuated by an extreme event, Hurricane Floyd, in September 1999. The Phase III Anacostia Model fulfills the promise of the Phase II Model. The simulation period is 1995-2004, to cover the simulation period of the Tidal Anacostia Model used in sediment, nutrient, and BOD TMDLs. It is calibrated primarily against ESTIMATOR loads, which are based on water quality monitoring data collected over the last ten years, including the recent automated sampler data collected by the USGS at the Northwest and Northeast gages, as described above.

2.3.1 General Overview of the HSPF Model

The HSPF Model simulates the fate and transport of pollutants over the entire hydrological cycle. Two distinct sets of processes are represented in HSPF: (1) processes that determine the fate and transport of pollutants at the surface or in the subsurface of a watershed, and (2) in-stream processes. The former will be referred to as land or watershed processes, the latter as in-stream or river reach processes.

Constituents can be represented at various levels of detail and simulated both on land and for in-stream environments. These choices are made in part by specifying the modules that are used, and thus the choices establish the model structure used for any one problem. In addition to the choice of modules, other types of information must be supplied for the HSPF calculations, including model parameters and time-series of input data. Time-series of input data include meteorological data, point sources, reservoir information, and other type of continuous data as needed for model development.

A watershed is subdivided into model segments, which are defined as areas with similar hydrologic characteristics. Within a model segment, multiple land use types can be simulated, each using different modules and different model parameters. There are two general types of land uses represented in the model: pervious land, which uses the PERLND module, and impervious land, which uses the IMPLND module. More specific land uses, like forest, crop, or developed land, can be implemented using these two general types. In terms of simulation, all land processes are computed for a spatial unit of one acre. The number or acres of each land use in a given model segment is multiplied by the values (fluxes, concentrations, and other processes) computed for the corresponding acre. These edge-of-stream (EOS) loads are then input into the river reaches. Although the model simulation is performed on a temporal basis, land use information does not change with time.

Within HSPF, the RCHRES module sections are used to simulate hydraulics of river reaches and the sediment transport, water temperature, and water quality processes that result in the delivery of flow and pollutant loading to a bay, reservoir, ocean or any other body of water. Flow through a reach is assumed to be unidirectional. In the solution technique of normal advection, it is assumed that simulated constituents are uniformly dispersed throughout the waters of the RCHRES; constituents move at the same horizontal velocity as the water, and the inflow and outflow of materials are based on a mass balance. HSPF primarily uses the “level pool” method of routing flow through a reach. Outflow from a free-flowing reach is a single-valued function of reach volume, specified by the user in an F-Table, although within a time step, the HSPF model uses a convex routing method to move mass flow and mass within the reach. Outflow may leave the reach through as many as five possible exits, which can represent water withdrawals or other diversions.

Bicknell *et al.* (1996) discuss the HSPF model in more detail.

2.3.2 Segmentation and Land Use

Figure 2.3.1 shows the segmentation used in the HSPF models. Segments 10-40 and 210 comprise the model of the NWB, segments 50-100 and 270 comprise the NEB, segments 120-140 comprise LBC, and segment 150 represents the Watts Branch.

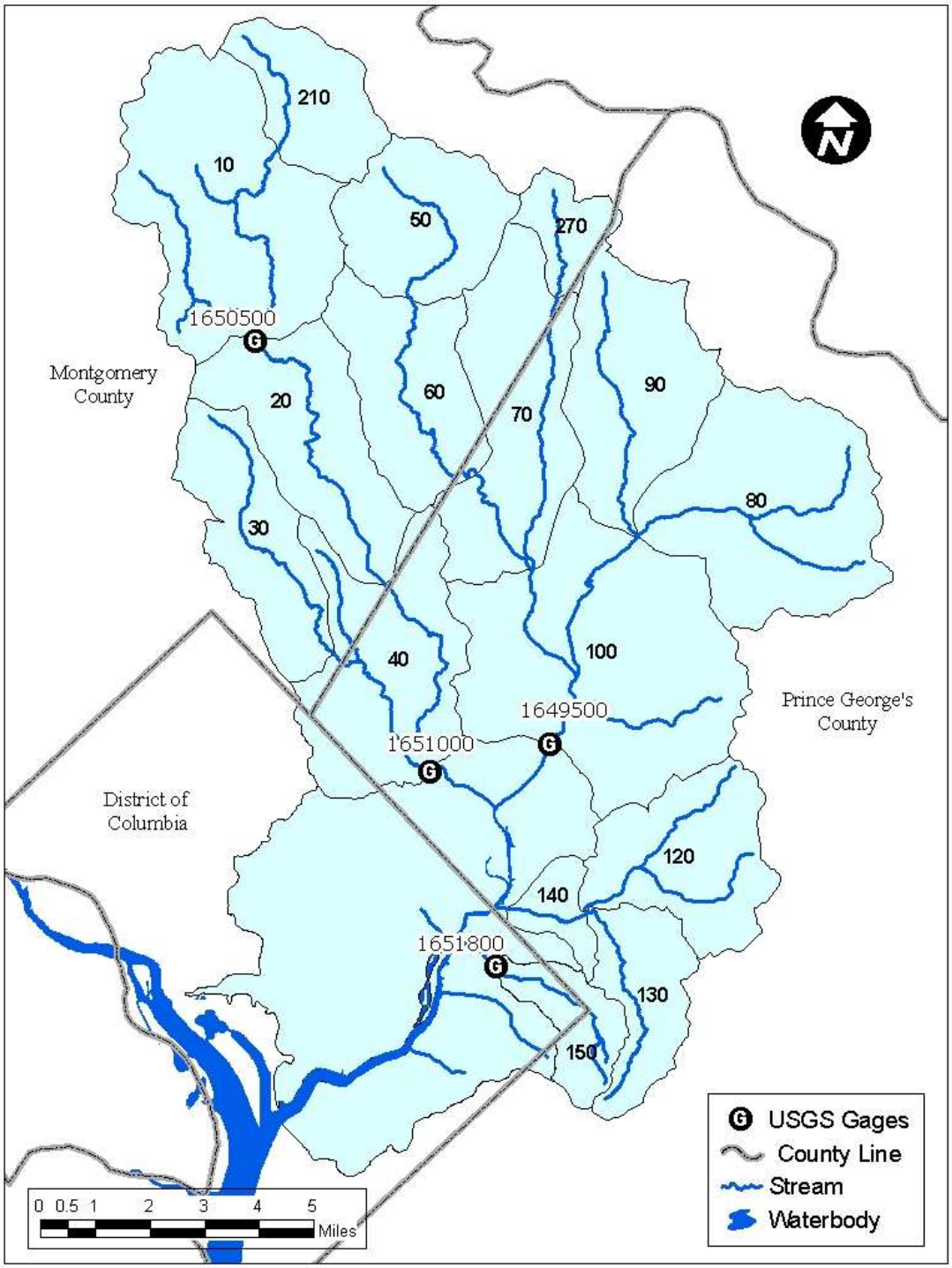

Figure 2.3.1. HSPF Model Segmentation

The following nine land uses are represented in the HSPF model:

Developed Land:
- Low Density Residential
- Medium Density Residential
- High Density Residential
- Commercial
- Industrial

Undeveloped Land:
- Forest
- Pasture
- Crops
- Hay

The developed land uses were further subdivided into pervious and impervious areas. Table A.1 in Appendix A gives the model land use categories and the acreage of each category by model segment.

Schultz *et al*. (2007) describe in more detail the development of the land use for the HSPF models.

2.3.3 Hydrology and Sediment Simulation Calibration

Schultz *et al*. (2007) describe the calibration of the hydrology and sediment simulations in the Anacostia HSPF models.

2.3.4 The Application of HSPF to Simulating Nutrients in Anacostia Watershed

HSPF is a modular simulation program. The user can choose how to simulate constituents by turning modules on off. Table 2.3.1 lists the relevant modules available in HSPF.

In simulating nutrients, the primary choice is between using the PQUAL module or the AGCHEM modules, NITR and PHOS. The PQUAL module simulates user-specified constituents. The concentration of the constituent in eroded sediment, interflow, and baseflow is fixed by the user. The concentration of the constituent in runoff is determined by a simple build-up, wash-off model, which can also take into account the decay of the constituent on the land surface. In the AGCHEM modules, on the other hand, the nitrogen and phosphorus species are defined in the model. The AGCHEM modules keep a mass balance of nitrogen and phosphorus. Inputs, losses, and the transformation of one species to another are all explicitly simulated.

Table 2.3.1. Description of HSPF Subroutines

Subroutine	Description
MSTLAY	Solute transport (pervious land)
PQUAL	Build-up, wash-off, decay of constituent on surface; Fixed monthly concentrations in subsurface. For PERLND (pervious land)
IQUAL	Build-up, wash-off, decay of constituent on surface. For IMPLND (impervious land)
NITR	Full mass balance: nitrification, mineralization, vegetation uptake and cycling.
PHOS	Full mass balance: sorption, mineralization, vegetation uptake and cycling.
SEDMNT	Detachment, washoff, and storage of sediment. For PERLND (pervious land).
SOLIDS	Accumulation and washoff of solids. For IMPLND (impervious land).
NUTRX	Transformation of inorganic nitrogen and phosphorus by nitrification, denitrification, sorption, deposition, and scour.
OXRX	Oxygen dynamics: reparation, BOD decay.
PLANK	Phytoplankton dynamics and organic nutrient cycling.
SEDTRN	Deposition, scour and transport of sediment.

The simulation of forest and agricultural land in the Anacostia HSPF models takes as its point of departure the simulation of these land uses in the Chesapeake Bay Program's Phase 5 Watershed Model. The Watershed Model uses AGCHEM to simulate nitrogen and phosphorus dynamics. The phosphorus simulation on forest was not implemented at the time the Anacostia models were developed, so PQUAL was use simulate phosphorus from forests. Neither BOD no organic phosphorus is explicitly simulated in the Watershed Model, but are calculated based on simulated labile organic nitrogen (LON) and refractory organic nitrogen (RON).

In the Anacostia models, PQUAL was used to simulate BOD, nitrate, TKN, and TP from developed land. IQUAL, the impervious equivalent to PQUAL, is the only choice for simulating nutrients on impervious surfaces. Full nutrient cycling of inorganic and organic nutrient species, including plankton dynamics, was simulated in river reaches. Table 2.3.2 summaries the constituents simulated and the modules used to simulate them.

There is a problem matching state variables in AGCHEM and RCHRES. As mentioned above, BOD is not explicitly simulated in AGCHEM, but BOD is a state variable in RCHRES. On the other hand, LON is a state variable in AGCHEM, but is only implicitly represented in RCHRES. It is implicit in BOD, since both inorganic nitrogen and inorganic phosphorus is released when BOD decays in RCHRES. To make matters more complicated, the BOD state variable in RCHRES is best identified as BOD ultimate, the total amount of labile organic material in units of oxygen, rather than the five-day BOD conventionally measured in the laboratory. It is therefore necessary (1) to covert EOS LON to BOD, and (2) account for the nitrogen and phosphorus content of

RCHRES BOD. Table 2.3.3 gives the nitrogen and phosphorus content of BOD. It also shows the BOD5 to BOD ultimate conversion factor used to (1) compare HSPF loads to ESTIMATOR loads and (2) convert EMC targets in BOD5 to ultimate BOD.

Table 2.3.2. HSPF Subroutines Used in the HSPF Model by Land Use and Constituent

Land Use	Ammonia	Nitrate	Organic N	Total P	BOD	DO	Chla
Crop and Hay	NITR	NITR	NITR	PHOS	NITR		
Pasture	NITR	NITR	NITR	PHOS	NITR		
Forest	NITR	NITR	NITR	PQUAL	NITR		
Pervious Developed	PQUAL	PQUAL	PQUAL	PQUAL	PQUAL		
Impervious	IQUAL	IQUAL	IQUAL	IQUAL	IQUAL		
River Reach	NUTRX	NUTRX	PLANK	NUTRX PLANK	OXRX	OXRX	PLANK

Table 2.3.3. Nitrogen, Phosphorus, and BOD Relationships

BOD5 to ultimate BOD Ratio	1.8
TN to BOD Ratio	0.0436
TP to BOD Ratio	0.006

2.3.5 Nutrient Calibration Targets

Forest and agricultural land uses. The starting point for the calibration of the forest and agricultural land uses was the CBP Phase 5 Model. Parameter values and nutrient loading rates from fertilizer, manure, and atmospheric deposition were taken from the March, 2007 version of the calibration. In the Phase 5 Model, loading rates and calibration targets are set by county. Table 2.3.4 shows the calibration targets for the land uses adopted in the Anacostia models. USEPA (2008) describes the Phase 5 Model is greater detail. Although the nutrient loading rates from the Phase 5 Model were used in the Anacostia models, the land use simulations had to be recalibrated because of the difference in the hydrology and sediment simulation between the Phase 5 Model and the Anacostia models. The land use loading rates were recalibrated so that the target loads were within two standard deviations of the simulated average annual load, taken over the simulation period 1995-2004. Forest was simulated with PQUAL, based on CBP loading rate targets.

Developed land uses. Stormwater loads from developed land were calibrated based on the stormwater EMCs discussed in section 2.1. Since HSPF represents BOD as BOD ultimate and implicitly represents labile organic nitrogen and phosphorus as BOD ultimate in RCHRES, the stormwater EMCs were corrected (1) to convert BOD5 to BOD ultimate and (2) to account for the labile nitrogen and phosphorus in BOD. Table 2.3.5

shows the corrected targets. The targets, expressed as loads, are equal to the product of the corrected EMC and the average annual runoff for the simulation period 1995-2004.

Table 2.3.4. CBP Phase 5 Calibration Targets (June, 2007) for Forest and Agricultural Land (lbs/ac/yr)

Constituent	Flow	Forest (Mont. Co.)	Forest (PG)	Pasture (Mont. Co)	Pasture (PG)	Crop (PG)	Hay (PG)
NH4	Surface	0.0235	0.0277	0.349	0.271	1.271	0.235
	Base	0.212	0.25	0.236	0.183	1.046	0.352
NO3	Surface	0.235	0.277	3.491	2.709	12.711	2.348
	Base	2.117	2.495	4.712	3.658	20.926	7.044
LON	Surface	0.0091	0.01	0.079	0.061	0.413	0.253
	Base	0.009	0.01	0.079	0.061	0.504	0.253
RON	Surface	0.091	0.1	0.794	0.613	4.133	2.535
	Base	0.091	0.1	0.794	0.613	5.041	2.535
PO4	Surface	0.093	0.093	0.687	0.521	1.052	0.575
	Base	0.005	0.005	0.036	0.027	0.079	0.03

Table 2.3.5. Corrected Stormwater Event Mean Concentration Targets (mg/l)

Region	Land Use	BODu	TKN	NO3	TP
NEB and NWB	Residential	20.84	0.67	0.91	0.20
	Commercial	36.85	1.26	0.6	0.00
	Industrial	26.62	0.24	0.98	0.06
LBC and Watts	Residential	22.6	0.89	1.54	0.4
	Commercial	33.5	1.13	0.7	0.06
	Industrial	25.2	0.73	0.6	0.09

Interflow and baseflow concentrations in the NEB and NWB were calibrated to improve the correlation between monthly HSPF loads and Monthly ESTIMATOR loads, 1995-1997, the simulation period for determining baseline loads for the TMDLs. Interflow and baseflow concentrations were set on an annual basis and were not allowed to vary monthly. Interflow and baseflow parameters for Paint Branch (Segments 50 and 60) were taken from the NEB calibration before calibrating the coastal plain segments in NEB. Interflow and baseflow parameters for LBC and Watts Branch were taken from the Coastal Plain segment parameters in the NEB.

Reach Calibration. Monthly reach loads in the NWB and NEB were calibrated against monthly ESTIMATOR loads. The monthly ESTIMATOR loads were also corrected for the presence of constituent loads associated with municipal and industrial dischargers, as described below in Section 2.5. In addition to the calibration of interflow and baseflow concentrations from developed land, the following processes were calibrated:

- BOD decay;

- Erosion and deposition of inorganic phosphorus; and
- Nitrification of ammonia to nitrate.

Generally, the calibration indicated that about 5% of EOS TKN is ammonia. Overall, EOS TN is approximately equal to the ESTIMATOR loads so there is no net gain or loss of TN, although the species composition changes through nitrification and BOD decay. About 15% of EOS BOD is lost in decay, while 14% of TP comes from streambank erosion.

2.3.6 BMPs

Table 2.3.6 shows the estimated BMP reduction efficiency for the major types of BMPs. Montgomery County provided a GIS layer with the location and classification of installed urban best management practices. Using this layer, the number of acres of each modeled land use type under each type of BMP was estimated. Table 2.3.7 shows the results. Reduction efficiencies were taken from CBP Phase 4.3 Watershed Model. BOD reduction efficiencies were assumed to equal nitrogen reduction efficiencies. The reduction in load for each land use type was calculated using the information in Table 2.3.6 and 2.3.7. Since most of the urban load comes from impervious land, BMPs were applied to impervious land only. Table 2.3.8 shows the net reduction in load by constituent, segment, and land use type used in the model.

Table 2.3.6. Urban BMP Types and Reduction Efficiencies

Structure Type	Abbreviation	TN and BOD Efficiency	TP Efficiency
Detention Structure, Dry Pond	DP	0.05	0.1
Extended Detention Structure, Dry	EDSD	0.3	0.2
Extended Detention Structure, Wet	EDSW	0.3	0.5
Infiltration Basin	IB	0.5	0.7
Oil/Grit Separator	OGS	0	0
Retention Structure, Wet Pond	WP	0.3	0.5
Sand Filter	SF	0.4	0.7
Shallow Marsh	SM	0.3	0.5
Underground Storage	UG	0.05	0.1

Table 2.3.7. BMP Acres by Segment and Land Use

Segment	Land Use	DP	EDSD	EDSW	IB	OGS	WP	SF	SM	UG
10	Commercial	14	5		2	8	10	5	2	0
	HDR	56	0	4		21	31	0	1	0
	LDR	6				0	18	0	7	
	MDR	68	0		5	10	49	1	33	
20	Commercial	3	0	1		26	12	3		9
	HDR		0		2	1	0	0		
	LDR	0		1		3	7	0		0
	MDR	27		3		2	3	0		2
30	Commercial	4		26		16	6	1	119	1
	HDR	1		11		1			33	0
	Industrial					0		3		
	LDR	2		67		3	0		138	
	MDR			6		1				
40	Commercial	0				11		1		
	HDR					1				
	LDR	3				0		1		
	MDR					0				
50	Commercial	10		0		5	5	0	4	1
	HDR	3								
	LDR	3		1		0	9		0	0
	MDR	51	9	5		1	10	1	3	0
60	Commercial	3	10	3	1	11	18	7		2
	HDR	21	0			1	9			
	Industrial	20		60		29	15	4	1	4
	LDR			1				0		0
	MDR	13	29		3	3	15	24		0
70	Commercial	58	8	27	0	3	8	2	0	1
	HDR	56	9	9		1	28			
	Industrial			5	0	4	2			
	LDR	1		4			4			
	MDR	9	40	14		1	53			
210	Commercial	4				7	0		4	0
	HDR									0
	LDR	0					8	1	2	1
	MDR							0	1	
270	Commercial	2	2	0	2	1				
	HDR	12								
	Industrial	0			0				2	
	LDR			0			0			
	MDR	4		37			6	2	0	

Table 2.3.8. Simulated BMP Load Reductions by Segment and Land Use

SEG	LDR	MDR	HDR	COM	IND
TN and BOD BMP Reductions					
10	6%	6%	6%	6%	0%
20	1%	1%	1%	2%	0%
30	14%	25%	9%	12%	13%
40	0%	0%	0%	0%	0%
50	6%	5%	4%	7%	0%
60	3%	6%	3%	4%	11%
70	16%	7%	8%	5%	4%
210	7%	1%	2%	3%	0%
270	1%	14%	3%	5%	1%
TP BMP Reductions					
10	10%	9%	10%	9%	0%
20	2%	1%	1%	4%	0%
30	23%	42%	15%	19%	24%
40	1%	0%	0%	0%	0%
50	10%	7%	8%	12%	0%
60	4%	9%	6%	6%	19%
70	27%	9%	13%	7%	6%
210	12%	1%	5%	5%	0%
270	1%	23%	5%	6%	1%

2.3.7 Calibration Results

Figures A.1 and A.2 compare the time series and scatter plot, respectively, of monthly ESTIMATOR and HSPF loads for the NWB for BOD. Figures A.3 and A.4, A.5 and A.6, A.7 and A.8, and A.9 and A.10 show the same pair of plots for TP, NH4, ON, and NO3, respectively. NWB HSPF monthly loads show a high degree correlation with their ESTIMATOR counterparts. With the exception of NH4, which has coefficient of determination (R^2) of 0.56, the R^2 values between the HSPF and ESTIMATOR monthly loads is greater than 0.7. If not for general tendency to under predict the ESTIMATOR load in January, 1996, which is the largest monthly load, the correlation between HSPF and ESTIMATOR would be even higher.

Figures A.11 through A.20 show the same series of plots for NEB. The coefficients of determination between the monthly loads from HSPF and ESTIMATOR are not as high as in NWB, but, with the exception of BOD, all remain above 0.5. The HSPF BOD simulation tends to under predict the months that have the highest ESTIMATOR loads. The other constituents tend to under predict the January 1996 ESTIMATOR load (and to

a lesser extent, the March 1997 load) but reasonably match the variation in loads for other months.

2.4 CSO Loads

CSO loads were calculated as a product of estimated flow volume and average constituent concentration. Flow volumes for individual events were simulated using the MOUSE model, developed by the Danish Institute of Hydrology. The MOUSE model of the DC combined sewer system was developed by Limno-Tech as part of DCWASA's LTCP (DCWASA, 2002). Table 2.4.1 shows total monthly CSO volumes over the baseline simulation period. Average concentrations were derived from the average EMC concentrations for Anacostia CSO outfalls taken from monitoring data collected for the LTCP. Table 2.4.2 shows the average CSO concentration by constituent.

Table 2.4.1. Simulated CSOs (MGD) for Baseline Conditions

Month	1995	1996	1997	Total
Jan	139	89	57	285
Feb	21	14	12	46
Mar	158	116	77	351
Apr	54	76	76	205
May	162	158	67	386
Jun	83	137	124	344
July	254	308	1	563
Aug	14	175	185	374
Sep	198	132	12	342
Oct	643	250	175	1,068
Nov	99	265	119	483
Dec	13	246	6	265
Total	1,837	1,965	912	4,714

Table 2.4.2. Event Mean Concentrations for Anacostia CSOs (mg/l)

Constituent	Concentration
NH3	1.21
NO23	0.74
PO4	0.21
BOD5	50.20
DO	14.00
ON	2.89
OP	0.79

2.5 Municipal and Industrial Point Sources

There are two municipal wastewater treatment plants (WWTPs) in the Anacostia River basin that discharge BOD and nutrients. Both are associated with BARC and discharge into NEB. The only industrial facility permitted to discharge BOD or nutrients in MD's portion of the Anacostia basin is for landfill leachate from the NASA's Goddard Space Flight Center. It also discharges into NEB. In DC there are three industrial dischargers permitted for BOD: Aggregated Super Concrete, PEPCO, and CTIDC. Super Concrete is located in the portion of DC that drains into NWB. PEPCO and CTIDC discharge into the upper and lower portions of the tidal Anacostia River, respectively. Table 2.5.1 gives basic information on these permitted facilities.

Table 2.5.1. Municipal and Industrial Point Source Facilities in the Anacostia Basin

Type	NPDES No.	Name	Design Flow (MGD)	Waterbody
MD Municipal	MD0020842	BARC East Side WWTP	0.62	NEB
MD Municipal	MD0020851	Beltsville USDA West WWTP	0.20	NEB
MD Industrial	MD0067482	NASA Goddard Center	Not Applicable	NEB
DC Industrial	DC0000175	Aggregate Super Concrete Industries	Not Applicable	NWB
DC Industrial	DC0000191	CTIDC	Not Applicable	Lower Tidal Anacostia
DC Industrial	DC0000098	PEPCO	0.5 MGD	Upper Tidal Anacostia

Loads from these sources were not explicitly simulated in either HSPF or the TAM/WASP model for the baseline conditions. Facilities that discharge in the NEB or NWB watersheds are included in NEB loads from ESTIMATOR that are input into the TAM/WASP model. Loads from CTIDC and Super Concrete are insignificant, since flows are intermittent and average flow, when it occurs, is less than 0.02 MGD. Loads from PEPCO are also insignificant, because although the permitted maximum flow from the facility is 0.5 MGD, discharges occur only once or twice a year.

These facilities were, however, given wasteload allocations (WLAs) in the TMDLs, and the WLAs were explicitly simulated in the TMDL Scenario. Calculation of the WLAs is described in Section 3.7.1, below. Monthly loads from the NASA and BARC facilities were estimated for the baseline calibration period, 1995-1997, to determine the point source contribution to ESTIMATOR loads under the baseline conditions. For the BARC facilities, monthly monitoring data for flows and constituent concentrations were available from the CBP Point Source Database for 1995-1997 (CBPO, 2006). Monthly loads of BOD, NH4, NO3, ON, and TP were calculated based on the reported average

monthly flow and monitored concentrations. When monthly monitoring data were not available, monthly loads were interpolated based on the loads from the preceding and subsequent months, so that a constituent load was determined for each month of the baseline simulation period. Table 2.5.2 shows the estimated monthly constituent loads from the BARC facilities, 1995-1997. It should be noted that TP concentrations at MD0020842 were as high as 4.3 mg/l during this period, resulting in significant TP loads.

Table 2.5.2. Monthly Municipal Point Source Loads (lbs/mo)

Year	Month	MD0020842			MD0020851		
		BOD5	TN	TP	BOD5	TN	TP
1995	1				735	184	416
1995	2						
1995	3	260	533	247	573	127	287
1995	4	567	316	214			
1995	5				226	88	294
1995	6	398	302	374			
1995	7	649	410	296	176	176	293
1995	8				106	106	244
1995	9	374	238	170			
1995	10				105	127	287
1995	11	277	277	72	295	140	316
1995	12						
1996	1						
1996	2						
1996	3	389	90	59	234	131	9
1996	4						
1996	5				102	149	10
1996	6	192	63	69			
1996	7	268	189	102			
1996	8	118	788	244	73	137	9
1996	9	110	563	199	41	106	7
1996	10	185	824	170	44	134	9
1996	11	231	792	190	187	223	15
1996	12	98	50	12			
1997	1				47	53	3
1997	2				28	52	3
1997	3	342	197	14	41	81	5
1997	4	33	492	107	20	61	4
1997	5	52	428	104	25	77	5
1997	6	59	514	155	31	95	6
1997	7	134	151	161	63	118	8
1997	8	65	86	148	58	122	8
1997	9	48	468	164	34	103	7
1997	10	32	280	81	36	81	5
1997	11				19	65	4
1997	12	79	540	125	23	48	3

Monitoring data for the NASA discharge was available only for 2005 -2007. BOD and NH4 were the only constituents monitored. An average daily load was calculated as the product of the average flow and the average concentration monitored for this period. The estimated average daily BOD loads was 0.34 lbs/day and the estimated NH4 load was 0.02 lbs/day.

2.6 Small Tributaries and Direct Drainage to the Tidal River

In addition to the loads from NEB, NWB, LBC, and the Watts Branch which are simulated using ESTIMATOR and the corresponding HSPF models, there are loads from smaller tributaries, MD and DC separate storm sewers, and direct drainage to the tidal Anacostia that must be accounted for in the TAM/WASP model. Loads from these sources were estimated based on EMCs and simulated flows from the Watts HSPF Model. Table 2.6.1 summaries the land use acreage draining into the tidal Anacostia. Schultz et al. (2007) describe the determination of the land use for this portion of the watershed is greater detail. Table 2.6.2 gives the average annual simulated flows by land use. EMCs for surface flows were taken from Table 2.1.1. Table 2.6.3 gives the EMCs used for baseflow, taken from Shepp *et al.* (2000), as in previous versions of the TAM/WASP model.

Table 2.6.1. Land Use in Tidal Anacostia Drainage (acres)

Section	Impervious	Developed	Forest
MD Tidal	787	1,451	106
DC Upper Anacostia	1,594	3,791	0
DC Lower Anacostia	1,152	1,972	0
Total Tidal	3,532	7,214	106

Table 2.6.2. Average Annual Flow (in/ac) By Land Use in Tidal Anacostia Drainage

Flow	Forest	Developed	Impervious
Storm	0.2	0.8	33.5
Base	12.9	12.6	0.0
Total	13.1	13.3	33.5

Table 2.6.3. EMC Baseflow Concentrations (mg/l) in Tidal Anacostia Drainage

Constituent	NH4	NO3	ON	TP	BOD
Concentration	0.018	1.5 (winter) 1.0 (spring) 0.6 (summer) 0.9 (fall)	0.4	0.055	1.2

A small section of the Anacostia watershed lies between the NEB and NWB gages and the direct drainage to the TMA/WASP model. To account for this area, two percent of the load from the NEB and NWB were added to the load from the upstream branches. The loads from this area were represented as developed land.

2.7 Summary of BOD, TN, and TP Loads

Tables 2.7.1 – 2.7.3 give the BOD, TN, and TP loads by source and watershed for the baseline period for determining the TMDLs, 1995-1997. The contribution by land use includes loads from both surface and subsurface drainage. Over 80% of the BOD load comes from developed land, 17% from CSOs, and negligible loads from other sources. About 80% of the TN load also comes from developed land, 9% from agriculture, and 7% from CSOs. For TP, developed land is again the dominant source, accounting for 67% of the load; in-stream scour accounts for 14%, CSOs account for 13%, agriculture accounts for 3%, and other sources account for 2% or less of the overall load.

Table 2.7.1. Average Annual BOD Baseline Loads, 1995-1997

Waterbody	Forest	Agriculture	Developed	Point Sources	CSOs	Total
NEB	12,654	20,556	990,390	3,597		1,027,197
NWB	3,142	5,253	585,595			593,990
LBC	2,890		305,666			308,556
Watts	403		33,124			33,528
MD Nontidal	19,089	25,809	1,914,775	3,597		1,963,270
MD Tidal	427		182,324			182,751
DC Upper			648,576		330,662	979,238
DC Lower			342,519		327,623	670,142
Total	19,516	25,809	3,088,194	3,597	658,285	3,795,400

Table 2.7.2. Average Annual Total Nitrogen Baseline Loads, 1995-1997

Waterbody	Forest	Agriculture	Developed	Point Sources	CSOs	Total
NEB	31,898	72,051	273,647	4,189		381,785
NWB	6,644	17,731	240,091			264,466
LBC	1,655		70,025			71,680
Watts	230		8,405			8,635
MD Nontidal	40,428	89,782	592,167	4,189		726,565
MD Tidal	517		28,305			28,822
DC Upper			89,043		31,894	120,936
DC Lower			41,042		31,601	72,642
Total	40,945	89,782	750,556	4,189	63,494	948,966

Table 2.7.3. Average Annual Phosphorus Baseline Loads, 1995-1997

Waterbody	Forest	Agriculture	Developed	Scour	Point Sources	CSOs	Total
NEB	957	3,187	26,836	6,841	2,164		39,984
NWB	240	207	17,857	7,757			26,061
LBC	108		8,260	369			8,737
Watts	17		1,076	24			1,117
MD Nontidal	1,322	3,394	54,030	14,990	2,164		75,899
MD Tidal	19		2,766	0			2,785
DC Upper			8,623	15		6,600	15,238
DC Lower			3,975	0		6,539	10,514
Total	1,340	3,394	69,394	15,005	2,164	13,139	104,436

Tables A.2 through A.4 in Appendix A give the average annual BOD, TN, and TP loading rates, respectively, by land use and segment for the Anacostia HSPF models.

3 VERSION 3 TAM/WASP WATER QUALITY MODELING FRAMEWORK

This chapter describes Version 3 of the TAM/WASP water quality modeling framework, a set of coupled computer programs which can simulate the loading, fate, and transport of pollutants in the tidal portion of the Anacostia River and predict daily concentrations of DO, BOD, TSS, chlorophyll *a*, nutrients, and Secchi depth. Earlier versions of TAM/WASP modeling components have been used in previous studies of the tidal Anacostia. The first version of TAM/WASP was used to simulate algal growth and sediment oxygen demand for the District of Columbia's Anacostia BOD TMDL (Mandel and Schultz, 2000), and also to evaluate management options for the District of Columbia Water and Sewer Authority (DCWASA) Long Term Control Plan (LTCP) for combined sewer overflows (DCWASA, 2002). The model's sediment transport capabilities were further developed, in TAM/WASP Version 2 (Schultz, 2003), for use by the District of Columbia and by USEPA Region 3 for the tidal Anacostia sediment TMDL (DCDOH, 2002; USEPA, 2002a; 2002b). The Version 3 Model was recently used to develop the joint MDE/DDOE sediment TMDLs (MDE and DDOE, 2007).

3.1 Overview of the Modeling Framework

TAM/WASP is a one-dimensional (1-D) modeling framework, capable of simulating hydrodynamic and water quality variations along the length of the river, but making the assumption that conditions are uniform throughout any channel transect (*i.e.* from left bank to right bank and from the water's surface to the channel bottom). The modeling framework can be divided into the following three component models:

Hydrodynamic component, based on the Tidal Anacostia Model (TAM), originally developed at MWCOG in the 1980s (Sullivan and Brown, 1988). This component simulates the changes in water level and water flow velocities throughout the river due to the influence of tides and of flows from tributaries and sewer systems discharging into the tidal river. The TAM hydrodynamic model used in this study, described in detail in Schultz (2003), incorporates side embayments to model Kingman Lake, Kenilworth Marsh, and the tidal portions of tributaries.

Sediment transport component, based on the USEPA's Water Quality Analysis Simulation Program, Version 5 (WASP-TOXI5) water quality model for solids and toxic contaminants (Ambrose *et al*., 1993). This component simulates the physical processes that transport sediment that has entered the river, and estimates daily values of TSS in each model water column segment. The TAM/WASP sediment transport model includes ICPRB enhancements to WASP-TOXI5 that simulate sediment erosion and deposition processes more realistically, basing them on hydrodynamic conditions (see Mandel and Schultz, 2000; Schultz, 2003). The TAM/WASP sediment transport model used in this project, Version 3, has been upgraded to 38 segments, and has undergone very minor adjustments to the calibration parameters used in Version 2 that govern erosion and

settling. Schultz et al. (2007) describe in detail Version 3 of the sediment transport model.

Eutrophication component, based on the USEPA's Water Quality Analysis Simulation Program, Version 5 (WASP-EUTRO5) water quality model for dissolved oxygen, nutrients, and algae (Ambrose *et al*., 1993). This component simulates the physical processes that affect dissolved oxygen levels in the river, and estimates daily concentrations of phytoplankton (algae), dissolved oxygen, and nutrients (Mandel and Schultz, 2000). The model includes an enhanced representation of sediment oxygen demand developed by Dr. Winston Lung of the University of Virginia (Lung, 2000) that incorporates the methane dynamics described by Di Toro et al. (1990). The TAM/WASP eutrophication model used in this study, Version 3, has been upgraded to 36 segments, and incorporates new modifications by ICPRB which couple it to the sediment transport model and allow it to estimate daily light extinction, Secchi depth, and water clarity conditions based on TSS and algae concentrations. This coupled model is capable of simulating the effect of potential solids load reductions on algal growth. Schultz et al. (2007) describe in detail the coupling of the sediment transport and eutrophication models and the representation of light extinction in term of TSS and algae concentrations. Only one major modification was made to the Version 3 model: the introduction of segment-specific BOD decay coefficients. This modification is described in more detail in Section 3.4.

Figure 3.1 provides a schematic diagram of the relation between the component models. Ambrose et al. (19993) describe the WASP5 model which forms the backbone of the modeling framework.

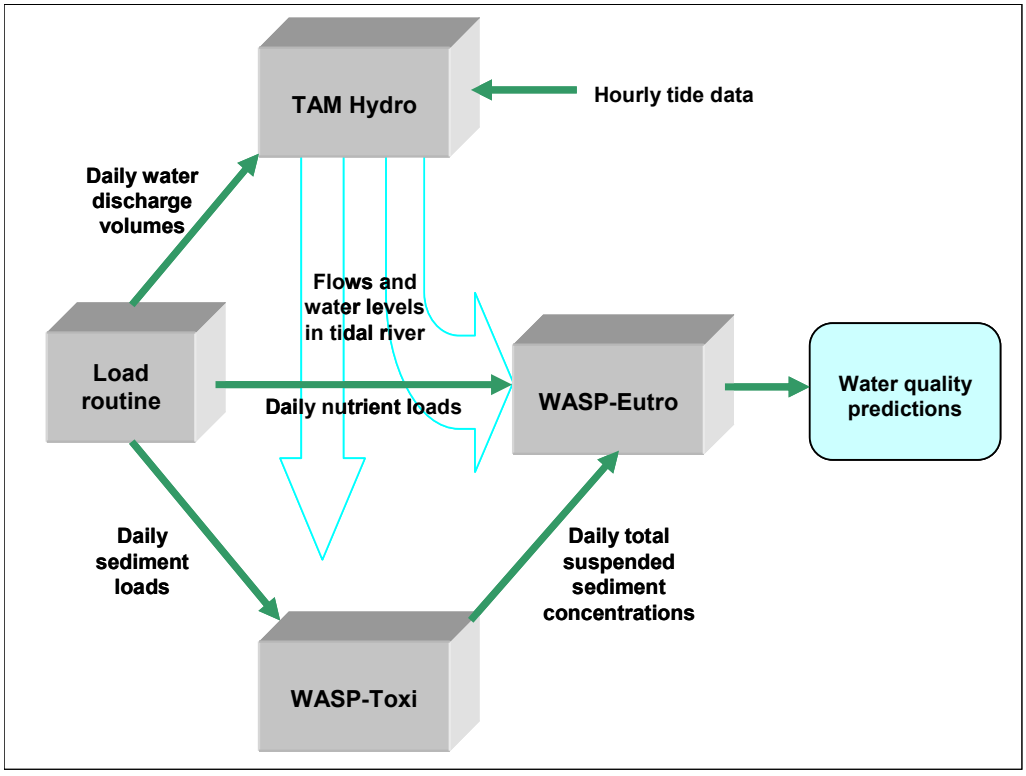

Figure 3.1. The TAM/WASP Modeling Framework

3.2 Model Segmentation

Schultz et al. (2007) describe the hydrodynamic and sediment components of Version 3 of the TAM/WASP modeling framework, inflows, tidal heights, sediment loads, and sediment model calibration. The development of constituent loads for the eutrophication model and the calibration of the eutrophication model are, of course, superseded by the current document.

As noted above, the sediment model has 38 segments while the eutrophication model has 36. The eutrophication model does not have the two segments added in Version 3 to represent the tidal portions of NEB and NWB below their USGS gages. The simulation of low tide occasionally resulted in dewatering in these segments, which, while posing no significant problems for the sediment transport model, made the full 38 segment model inappropriate for simulating nutrients and DO. The segmentation of the Version 3 eutrophication model is thus identical to the Version 2 sediment model (Schultz, 2003). Figure 3.2.1 shows the model segmentation. Table 3.2.1 gives model geometry.

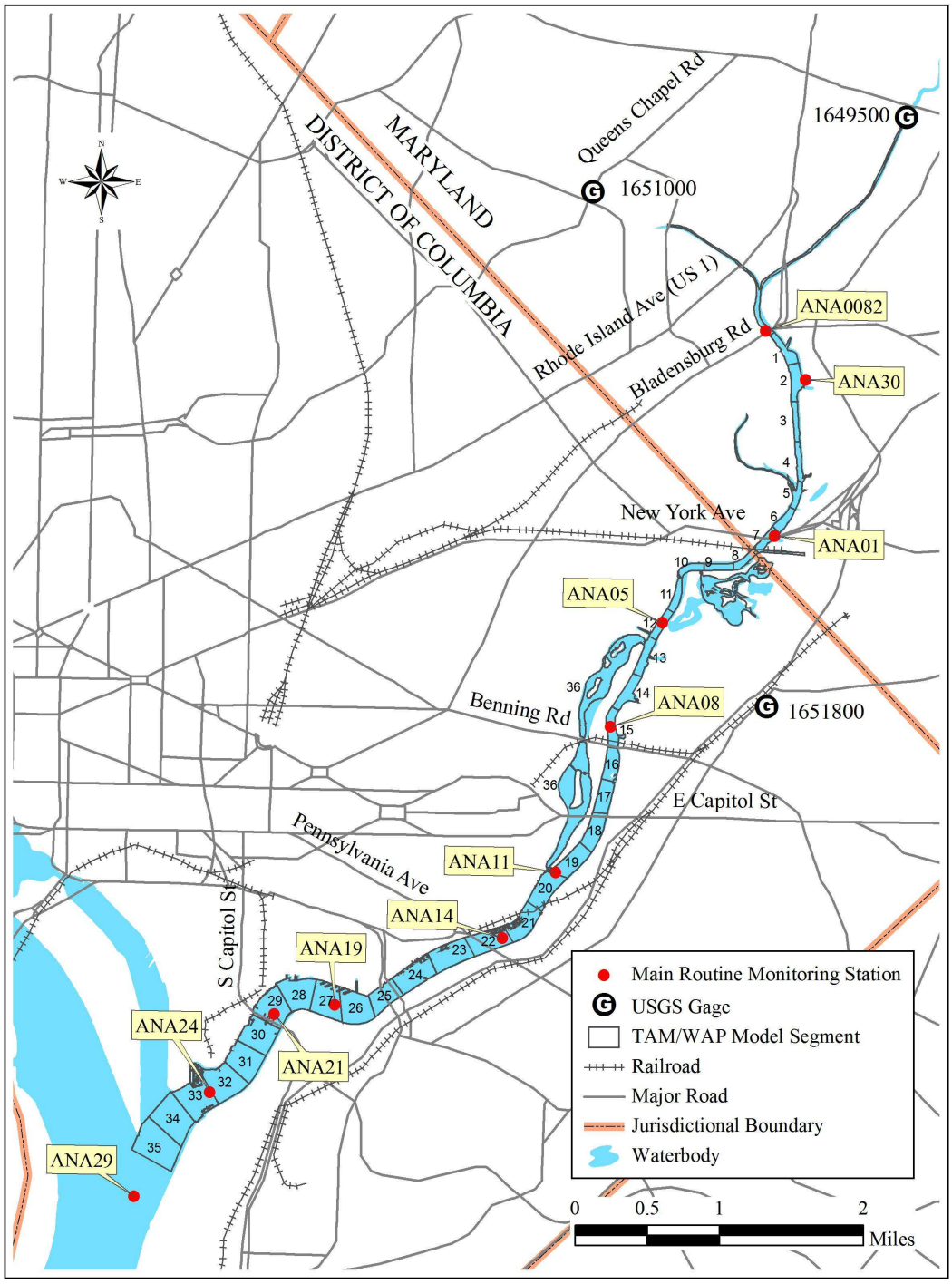

Figure 3.2.1. TAM/WASP Model Segmentation

Table 3.2.1. Sediment Transport Model Geometry

Adjacent Embayment	WASP Segment Number	River Km[1]	Segment Length (m)	Segment Width (m)	Segment Depth (m from MSL)	Main Channel Area (m^2)	Total Segment Area (m^2)	Total Segment Volume (m^3)	Transect Convey Area (m^2)	Transect Depth (m)	Mannings Roughness
	1	0.48	414	98.5	1.50	40,898	150,397	225,595	46	1.00	0.01
	2	1.17	425	119.1	1.16	50,636	50,636	58,974	103	1.08	0.01
	4	1.61	450	58.0	2.21	26,090	26,090	57,634	149	1.69	0.01
	4	2.06	442	63.3	2.17	27,993	27,993	60,790	133	2.19	0.01
Dueling Cr	5	2.43	312	93.0	1.90	29,031	56,638	107,672	159	2.04	0.01
	6	2.74	305	92.6	1.86	28,246	28,246	52,621	175	1.88	0.01
LBD Cr	7	3.05	320	90.3	1.83	28,910	38,969	71,399	169	1.85	0.01
	8	3.37	315	74.4	2.06	23,424	23,424	48,159	160	1.94	0.01
	9	3.69	330	74.2	2.08	24,485	24,485	50,841	153	2.07	0.01
Kenilworth	10	4.01	312	77.4	2.02	24,163	212,343	429,707	155	2.05	0.01
	11	4.37	405	73.1	2.12	29,605	29,605	62,862	156	2.07	0.01
Hickey Run	12	4.76	370	86.0	1.78	31,814	33,630	59,946	155	1.95	0.01
Watts Br	13	5.17	445	96.7	1.50	43,021	44,126	66,311	150	1.64	0.01
	14	5.61	445	113.7	1.33	50,606	50,606	67,539	149	1.42	0.01
	15	6.06	453	105.3	1.92	47,681	47,681	91,427	178	1.63	0.01
	16	6.48	375	146.1	1.84	54,799	54,799	100,967	236	1.88	0.02
	17	6.85	375	157.5	1.50	59,057	59,057	88,644	254	1.67	0.02
	18	7.25	425	164.3	1.30	69,840	69,840	91,030	226	1.40	0.02
Kingman	19	7.68	435	185.0	1.33	80,459	80,459	107,235	230	1.32	0.02
	20	8.12	440	205.4	1.92	90,378	90,378	173,920	318	1.63	0.02
	21	8.56	440	199.4	1.97	87,758	87,758	173,103	394	1.95	0.03
	22	9.01	455	218.8	1.98	99,535	99,535	197,156	413	1.98	0.03
	23	9.46	460	242.5	2.05	111,543	111,543	228,666	465	2.02	0.03
	24	9.92	460	235.8	3.43	108,481	108,481	371,704	655	2.74	0.03
	25	10.34	365	218.3	4.31	79,676	79,676	343,557	879	3.87	0.03
	26	10.69	353	340.3	4.58	120,140	120,140	550,303	1242	4.45	0.06
	27	11.03	323	353.4	5.10	114,137	114,137	582,039	1679	4.84	0.06
	28	11.36	335	348.3	5.28	116,693	116,693	616,495	1821	5.19	0.06
	29	11.70	335	347.4	5.10	116,383	116,383	593,380	1806	5.19	0.06
	30	12.03	335	351.2	5.61	117,642	117,642	660,057	1870	5.35	0.06
	31	12.36	320	368.2	5.36	117,829	117,829	631,411	1973	5.48	0.06
	32	12.70	355	376.8	4.81	133,762	133,762	642,905	1893	5.08	0.06
	33	13.06	365	415.2	4.25	151,554	151,554	644,722	1794	4.53	0.06
	34	13.41	340	447.0	4.25	151,978	151,978	645,249	1832	4.25	0.06
	35	13.75	350	507.9	4.25	177,761	177,761	756,277	2029	4.25	0.06
Kingman	36				1.33	250,000	250,000	333,197	2161	4.25	0.06

[1]River Km = distance at midpoint from confluence

3.3 Water Quality Monitoring Data

Maryland Department of Natural Resources (DNR) conducts water quality monitoring in the tidal Anacostia River at Station ANA0082, located at Bladensburg Road. Figure 3.2.1 shows the location of ANA0082. Table 3.3.1 shows which constituents are reported at ANA0082. DDOE has maintained as many as 30 water quality monitoring stations in the tidal Anacostia River. At six stations—ANA01, ANA08, ANA14, ANA21, ANA29, and ANA30—DDOE collects nutrient data on a monthly basis. Figure 7 shows the location of these stations. Table 3.3.1 shows which constituents are analyzed from those stations. At five other stations—ANA01, ANA05, ANA11, ANA19, and ANA24—DDOE also analyzes water quality samples for DO, water temperature, and pH. Figure

3.2.1 also shows the location of these stations. Between 1995 and 1997, approximately 10 samples per year were collected at 20 other stations and analyzed for DO, water temperature, and pH.

Table 3.3.1. Constituents Reported By Program, Tidal Anacostia River

Constituent	MDDNR	DDOE
5-day Total BOD	X	X
Active Chlorophyll a	X	X
Dissolved Oxygen	X	X
Dissolved Inorganic Nitrogen	X	X
Dissolved Ammonia Nitrogen	X	X
Dissolved Nitrite-Nitrate Nitrogen	X	X
Total Organic Nitrogen	X	
Total Kjeldahl Nitrogen	X	
Total Nitrogen	X	
Dissolved Phosphate Phosphorus		X
Total Inorganic Phosphorus	X	
Total Organic Phosphorus	X	
Total Phosphorus	X	

3.3.1 Applicable Water Quality Criteria

The Chesapeake Bay Program Office (CBPO) has developed a framework for assessing the water quality impacts of nutrients and sediment in the Chesapeake Bay and its tidal tributaries, such as the Anacostia (CBPO 2003). This framework develops guidance for setting nutrient and sediment enrichment criteria in terms of dissolved oxygen, water clarity, and chlorophyll *a*. CBPO identified five essential habitats, which, when protected by the DO, water clarity, and Chla criteria specific to it, "…will ensure the protection of the living resources of the Chesapeake Bay and tidal tributaries (CBPO 2003, p. x)." These five habitats, delineated in both space and time, form the basis for recommended designated uses for the bay and its tidal tributaries. Three of these designated uses are relevant to the Anacostia: (1) migratory fish spawning and nursery designated use, which protects migratory and resident fish during the spawning season, February 1 through May 31; (2) the shallow-water bay grass designated use, which protects the submerged aquatic vegetation (SAV) essential to shallow water habitats during the growing season, April 1 through October 31; and (3) the open-water fish and shellfish designated use, which protects menhaden, striped bass, and other fish in surface water habitats. The open-water designated use provides the DO criteria for the spawning use and shallow-water use outside of the spawning season.

Both MD and DC have incorporated the recommendations of CBPO (2003) into their water quality regulations, The District of Columbia Municipal Regulations (DCMR), Chapter 11, Section 1101.2, classifies both segments of the tidal Anacostia River as Class C: Protection and Propagation of Fish, Shellfish, and Wildlife. The Maryland Water

Quality Standards Stream Segment Designation for the tidal Anacostia River is Use II: Tidal Waters: Support of Estuarine and Marine Aquatic Life and Shellfish Harvesting [COMAR 26.08.02.08O(2)]. Designated uses present in the tidal Anacostia River include (1) Migratory Spawning and Nursery Use, (2) Open Water Fish and Shellfish Use, and (3) Seasonal Shallow Water Submerged Aquatic Vegetation Use.

Table 3.3.2 shows the DO criteria associated with each designated use. Distinct numerical criteria are used for Seasonal Migratory Fish Spawning and Nursery Use, which is in effect February 1 through May 31. During this period DO concentrations can be no less than 5.0 mg/l. During the rest of the year, the instantaneous minimum DO concentration can be no less than 3.2 mg/l. As Table 3.3.2 shows, the criteria also specify minimum seven-day average DO concentrations of 6.0 mg/l and 4.0 mg/l for the spawning season and the remainder of the year, respectively. The minimum 30-day average concentration of 5.5 mg/l holds year-round.

DC has numerical chlorophyll a criteria applicable to Class C waters. The DCMR (1104.8) specifies that the average Chla concentration in a segment, July 1 through September 30, is not to exceed 25 µg/l. MD has not adopted numerical criteria for nutrients or Chla, but MD has adopted a narrative criterion for Chla in tidal waters, which states "Concentrations of chlorophyll a in free-flowing microscopic aquatic plants (algae) shall not exceed levels that result in ecologically undesirable consequences that would render tidal waters unsuitable for designated uses." [COMAR 26.08.02.03-3 C (10)]

Table 3.3.2. DO Criteria for Designated Uses in the Tidal Anacostia River

Designated Use	Period Applicable	DO Critiera
MD Use II: Migratory Fish Spawning and Nursery Subcategory	2/1 – 5/31	≥ 5.0 mg/l (instantaneous) ≥ 6.0 mg/l (7-day average)
MD Use II: Open Water Fish and Shellfish Subcategory	6/1 – 1/31	≥ 3.2 mg/l (instantaneous) ≥ 4.0 mg/l (7-day average) ≥ 5.5 mg/l (30-day average)* ≥ 4.3 mg/l (instantaneous for water temperature > 29 ^{0}C for protection of Shortnose Sturgeon)
DC Class C	2/1 – 5/31	≥ 5.0 mg/l (instantaneous) ≥ 6.0 mg/l (7-day average)
	6/1 – 1/31	≥ 3.2 mg/l (instantaneous) ≥ 4.0 mg/l (7-day average) ≥ 5.5 mg/l (30-day average) ≥ 4.3 mg/l (instantaneous for water temperature > 29 ^{0}C for protection of Shortnose Sturgeon)

Both MD and DC have adopted water quality criteria for water clarity in tidal waters, based on CBP guidance. In DC, the average Secchi depth in a segment should be no less than 0.8 meters over the growing season, April 1 through October 31. In MD, the average Secchi depth should not be less than 0.4 meters, May 1 through October 31, averaged over a three-year period, in waters less than 0.5 meters deep.

EPA (2007b) has approved joint MD-DC sediment TMDLs (2007) that address MD's and DC's water clarity standards. Those TMDLs implicitly assumed that algal concentrations, as represented by Chla concentrations, would not increase under sediment TMDL loading rates. The nutrient TMDLs for the tidal Anacostia will have to confirm that water clarity standards are met under nutrient allocations, assuming the sediment TMDL allocations determined in the previous sediment TMDLs.

3.3.3 Dissolved Oxygen

CBPO (2003) recommends that the instantaneous minimum DO criterion be set at 5.0 mg/l to protect spawning and migratory fish and 3.2 mg/l to protect the open-water designated use. Figure B.1 in Appendix B shows the cumulative distribution of observed DO concentrations by waterbody for the spawning period, February through May, 1995-2005. Figure B.2 shows the same information for June through January, the period of the year that the open-water designated use is in effect in the tidal Anacostia. As the figures show, DO concentrations below the CBPO recommendations occur in both periods. In MD, only one sample in the spawning season and one sample outside it had DO concentrations below the recommended instantaneous minimum. In DC, the percent below the recommended concentration are 15% and 9% for the upper Anacostia and 11% and 4% for the lower Anacostia, respectively, for the spawning season and open water season. Figure B.3 in Appendix B shows the distribution of DO concentrations by station for the primary monitoring stations. As Figure B.3 shows, DO concentrations tend to be higher near the head of tide and at the Anacostia's confluence with the Potomac, and drop off between ANA08 and ANA21, which is approximately between Benning Road and South Capitol Street in the District.

Table 3.3.3 gives summary statistics for observed DO concentrations by waterbody.

Table 3.3.3. Summary Statistics for DO in Tidal Anacostia River, 1995-2005

Statistic	February - May			June - January		
	MD	DC1	DC2	MD	DC1	DC2
Min	4.5	1.4	2.1	2.2	1.4	1.7
1st Q	10.4	6.4	7.3	7.3	4.5	6.0
Median	11.6	8.7	9.3	9.0	6.2	7.3
3rd Q	12.3	10.5	10.7	11.3	8.2	8.8
Max	19.2	17.4	16.8	16.7	16.8	16.4
Average	11.2	8.4	9.1	9.3	6.6	7.6
Std. Dev.	2.0	2.9	2.9	2.6	2.9	2.7
# Samples	82	339	278	170	652	521

DDOE, MWCOG, and MDDNR had deployed equipment for continuous monitoring of DO, temperature, and pH at several stations in the tidal Anacostia River. Table 3.3.4 shows the location of these stations and the years for which some continuous monitoring data were available. Figure B.4 in Appendix B shows the daily minimum, daily maximum, and daily average DO concentrations at station PO4. Excess primarily production by algae is a major cause of diurnal DO cycle.

Hintz (2007) analyzed the available continuous monitoring data to determine the relation between the observed daily average DO and daily minimum DO concentrations. Hintz determined that the median difference between the daily average and the daily minimum DO concentration was 0.81 mg/l, February through May, 1.28 mg/l, June through January, and 1.12 mg/l overall.

Table 3.3.4. Available DO Continuous Monitoring Data in the Anacostia River

Station	Location	Agency	Years Available
PO4	Benning Road	MWCOG	1996-2000; 2002
PO7	Seafarer's Marina	MWCOG	1996-2000; 2002
ANA0082	Rt. 1 Bridge	MDDNR	2002
ANA01	New York Avenue Bridge	DDOE	2000-2002
ANA13	Conrail Bridge	DDOE	2000-2001
ANA21	S. Capitol Street Bridge	DDOE	1998-2002

3.3.4 Chlorophyll *a*

DDOE restarted monitoring for Chla in 1999. Figure B.5 in Appendix B shows the distribution of Chla concentrations by monitoring station. The average and median concentrations tend to be around 20 µg/l or lower, but concentrations can range above

100 µg/l. Concentrations tend to be lower near head of tide and near the confluence with the Potomac. Table 3.3.5 gives summary statistics for observed Chla by waterbody.

Figures B.6–B.8 in Appendix B show the average monthly observed Chla concentration by year for MD Tidal, DC Upper Anacostia, and DC Lower Anacostia, respectively. There is considerable inter-annual variability in Chla concentrations, but there is also a fairly consistent seasonal pattern, in which the highest concentrations tend to occur primarily in July and August, with a second peak sometimes occurring in November.

Table 3.3.5. Summary Statistics for Chla (µg/l) in Tidal Anacostia River, 1999-2002

Statistic	Annual			July - September		
	MD	DC1	DC2	MD	DC1	DC2
Min	0.3	0.3	0.4	1.4	2.0	1.0
1st Q	1.7	4.9	4.0	3.0	13.2	16.0
Median	3.0	11.0	10.0	4.9	25.0	28.0
3rd Q	5.6	25.0	26.3	8.4	49.4	41.8
Max	80.0	103.0	65.0	68.0	103.0	65.0
Average	5.7	18.2	16.6	8.2	32.2	30.0
Std. Dev.	9.9	19.7	15.7	11.7	24.3	17.6
# Samples	171	161	103	45	55	33

3.3.5 Secchi Depth

Figure B.9 in Appendix B shows the distribution of Secchi depths by monitoring station during the growing season. Median Secchi depths range from 0.4 m at ANA01 and ANA08 in the DC Upper Anacostia to 0.8 m at ANA29 at the confluence with the Potomac. On average the lowest observed Secchi depths tend to occur mid-river. Table 3.3.6 gives summary statistics for observed Secchi depth by waterbody. Additional analysis of observed Secchi depths can be found in Schultz et al. (2007).

Table 3.3.6. Summary Statistics for Secchi Depth (m) in Tidal Anacostia River, 1995-2005

Statistic	Annual			May - October	April - October	
	MD	DC1	DC2	MD	DC1	DC2
Min	0.0	0.0	0.0	0.1	0.1	0.0
1st Q	0.4	0.3	0.4	0.4	0.3	0.5
Median	0.6	0.4	0.6	0.6	0.4	0.6
3rd Q	0.8	0.5	0.8	0.7	0.5	0.8
Max	1.8	1.8	2.2	1.2	1.0	2.1
Average	0.7	0.4	0.6	0.5	0.4	0.6
Std. Dev.	0.3	0.2	0.3	0.2	0.1	0.3
# Samples	118	755	568	63	516	388

3.3.6 BOD

Figure B.10 in Appendix B shows the distribution of BOD concentrations by monitoring station. With the exception of ANA0082, where concentrations are higher, the 75th percentile concentration tends to be below 3.0 mg/l, with median concentrations around 2.0 mg/l. Concentrations tend to drop off from mid-river to the Potomac confluence. Concentrations tend to be highest near head of tide. The longitudinal pattern of BOD concentrations could reflect either a drop in concentration with residence time, as BOD is consumed, or a significant solid-phase BOD component which deposits downstream of head of tide. Table 3.3.7 gives summary statistics for observed BOD concentration by waterbody.

Table 3.3.7. Summary Statistics for BOD (mg/l) in Tidal Anacostia River, 1995-2005

Statistic	February - May			June - January		
	MD	DC1	DC2	MD	DC1	DC2
Min	0.7	0.9	0.6	0.2	0.3	0.2
1st Q	1.9	1.7	1.3	1.9	1.8	1.1
Median	2.0	2.1	1.8	2.1	2.3	1.6
3rd Q	2.9	2.6	2.3	3.2	3.1	2.4
Max	8.2	6.9	3.9	10.7	10.0	4.0
Average	2.6	2.2	1.8	2.8	2.5	1.8
Std. Dev.	1.4	0.8	0.7	1.8	1.3	0.9
# Samples	75	114	78	165	247	168
# BDL	20	1	4	25	0	2
% BDL	26.7	0.9	5.1	15.2	0.0	1.2

3.3.7 Nutrients

DDOE only analyzes water quality samples for dissolved inorganic nitrogen and phosphorus species—ammonia, nitrate, and phosphate. It is not possible, therefore, to give an analysis of total nitrogen, total phosphorus, or the organic forms of nutrients.

Figures B.11–B.13 in Appendix B show the distribution of ammonia, nitrate, and phosphate by monitoring station, respectively. Ammonia concentrations tend to be highest in mid-river, while nitrate concentrations show the opposite longitudinal trend. Phosphate concentrations, on the other hand, tend to show no longitudinal trend. Tables 3.3.8 -3.3.10 give summary statistics by waterbody for ammonia, nitrate, and phosphate, respectively.

Table 3.3.8. Summary Statistics for Ammonia-N (mg/l) in Tidal Anacostia River, 1995-2005

Statistic	Annual			July - September		
	MD	DC1	DC2	MD	DC1	DC2
Min	0.004	0.004	0.004	0.004	0.040	0.009
1st Q	0.034	0.121	0.060	0.032	0.139	0.048
Median	0.063	0.218	0.134	0.057	0.208	0.086
3rd Q	0.120	0.316	0.239	0.121	0.271	0.158
Max	0.520	1.760	0.997	0.405	0.495	0.997
Average	0.093	0.244	0.172	0.092	0.210	0.132
Std. Dev.	0.090	0.168	0.139	0.091	0.108	0.149
# Samples	253	450	284	64	49	79
# BDL	6	0	2	1	0	0
% BDL	2.4	0.0	0.7	1.6	0.0	0.0

Table 3.3.9. Summary Statistics for Nitrite-Nitrate-N (mg/l) in Tidal Anacostia River, 1995-2003

Statistic	Annual			July - September		
	MD	DC1	DC2	MD	DC1	DC2
Min	0.020	0.042	0.052	0.020	0.042	0.220
1st Q	0.681	0.468	0.663	0.501	0.318	0.486
Median	0.865	0.629	0.890	0.785	0.467	0.760
3rd Q	1.115	0.835	1.230	0.888	0.609	1.093
Max	3.200	2.180	3.760	1.890	2.170	3.060
Average	0.920	0.692	1.007	0.719	0.494	0.879
Std. Dev.	0.420	0.361	0.537	0.326	0.287	0.560
# Samples	184	339	231	47	102	62
# BDL	1	0	2	1	0	0
% BDL	0.5	0.0	0.9	2.1	0.0	0.0

Table 3.3.10. Summary Statistics for Dissolved Inorganic Phosphorus (mg/l) in Tidal Anacostia River, 1995-2002

Statistic	Annual			July - September		
	MD	DC1	DC2	MD	DC1	DC2
Min	0.001	0.001	0.001	0.001	0.001	0.001
1st Q	0.006	0.006	0.007	0.005	0.004	0.004
Median	0.012	0.014	0.013	0.010	0.010	0.010
3rd Q	0.015	0.022	0.029	0.026	0.022	0.021
Max	0.057	0.301	0.260	0.043	0.051	0.091
Average	0.014	0.017	0.020	0.015	0.015	0.017
Std. Dev.	0.012	0.020	0.023	0.014	0.013	0.018
# Samples	57	369	268	15	102	71
# BDL	1	2	2	1	0	1
% BDL	1.8	0.5	0.7	6.7	0.0	1.4

3.3.8 Sediment Oxygen Demand and Sediment Nutrient Fluxes

Two recent studies have attempted to quantify sediment oxygen demand and nutrient fluxes between sediment and the water column. As part of the LTCP, MWCOG and Naval Research Laboratory made two sets of measurements of SOD at nine sites in the Anacostia in September and December, 1999 (MWCOG 2000). The September measurements were made under "hypoxic" conditions in the water column; DO concentrations ranged as low as 3.4 mg/l. Estimated SOD rates were all less than 1.0

$g/m^2/d$, possibly due to the low DO water column concentrations. In the second set of measurements taken in December, SOD rates ranged from 0.39 to 3.45 $g/m^2/d$. The study also attempted to quantify the fate of gaseous methane released from anaerobic diagenesis in the sediments, without obtaining consistent results.

Bailey et al. (2003) measured SOD and nutrient fluxes at five locations in the tidal Anacostia in June, July, August, and September 2002. DO concentrations in the water column were generally above 5.0 mg/l with only a few observations 3.0 mg/l or less in the upper reaches of the tidal Anacostia River in June. Measured SOD ranged from 1.37 to 3.6 $g/m^2/d$ and averaged 2.3 $g/m^2/d$. Measurements of nutrient fluxes yielded the following conclusions:

- Ammonia fluxes from the sediments are high (> 500 μmols-$N/m^2/h$) in the Anacostia, particularly in the upper reaches of the tidal river;
- The nitrate flux from the water column to the sediment is extremely high (~100 μmols-$N/m^2/h$), compared with other sites in the Chesapeake Bay region; and
- Phosphate fluxes were directed from the sediments to the water column but were very small (~ 3 μmols-$P/m^2/h$).

It is unclear, however, what effect the extremely dry conditions in the summer of 2002 had on these observations.

3.4 Overview of the Calibration of the Eutrophication Model

The primary role of a computer simulation model in TMDLs is to determine the relation between constituent loads and the water quality response. That means, in this case, that the role of the TAM/WASP model is to determine the relation between BOD, nitrogen, and phosphorus loads, on the one hand, and DO, Chla, and Secchi depth in the tidal Anacostia River, on the other. The latter three water quality constituents, of course, define the water quality standards which are not currently met in the tidal Anacostia and which the nutrient and BOD TMDLs are designed to address.

In the sediment TMDL (MDE and DDOE, 2007; Schultz et al., 2007), the TAM/WASP model was calibrated to represent Secchi depth as a function of sediment loads and simulated Chla concentrations at their observed levels. Although algae, as measured by Chla concentrations, contribute to light extinction, Secchi depth is predominately a function of sediment concentrations, at least under baseline conditions in the Anacostia. Any calibration of the eutrophication model that uses the simulated sediment baseline concentrations and successfully reproduces observed Chla concentrations will preserve the Secchi depth calibration. Secchi depth was therefore not a focus of the calibration of Version 3 of the eutrophication model and the sediment TMDL parameterization of light extinction in terms of sediment and Chla concentration was adopted for the current calibration for the sake of consistency with the sediment TMDL.

The relation between the best estimate of current nutrient loads, described in Chapter 2, and Chla concentration was not calibrated for the sediment TMDL. This is one of the

two primary goals the recalibration of the eutrophication model for the BOD and nutrient TMDLs. The second goal is to calibrate the relation between BOD loads and DO, taking into account the impacts of primary production and nitrification on DO concentrations.

3.4.1 State Variables and Boundary Conditions

The eutrophication model has eight state variables representing constituents: ammonia-nitrogen (NH4), nitrate-nitrogen (NO3), inorganic phosphorus (PO4), algal carbon, BOD ultimate, DO, organic nitrogen (ON), and organic phosphorus (OP). There is a single state variable representing both dissolved and particulate forms of the constituents. The fraction of dissolved form is a user-input variable and varies by segment but not in time. This makes it difficult to capture the fate and transport of storm-driven particulates, since under storm conditions, the particulate fraction of a constituent can be expected to rise above ambient conditions. This problem is discussed in greater detail in Section 3.5.

Neither Chla nor Secchi depth is a state variable. Although Chla is not a state variable, both input loads and boundary conditions are calculated in terms of Chla. Simulated Chla concentrations are determined in the eutrophication model on the basis of algal carbon using the Smith light extinction formulation which makes the carbon:Chla ratio a variable function of light extinction. Ambrose et al. (1993) describes the Smith formulation, as implemented in WASP, in detail. Secchi depth is calculated on the basis of simulated Chla, non-algal solids, and background light extinction. Non-algal solids for each segment are input on a daily basis into the eutrophication model from the sediment transport model. Schultz et al. (2007) describe the development of the sediment transport model and the calibration of Secchi depths used in the joint MD-DC sediment TMDL and adopted for the nutrient TMDLs.

Input loads for the state variables were discussed in the pervious chapter. Time series representing downstream boundary conditions were constructed directly from available routine monitoring data at station ANA29, located near the Potomac confluence, for the calibration period, 1995 through 2002. Because no data were available for ON, PO4, or OP during the calibration time period, time series for these constituents were constructed using quarterly averages of ON and total phosphorus data from the period, 1984-1992. Similarly, for the years 1995 – 1998, in which no chlorophyll *a* data were available, quarterly averages of available data were used.

3.4.2 Simulation Period

The simulation period for the calibration of the eutrophication model was 1995-2002. The TMDL simulation period is 1995-1997. This period was chosen for two related reasons: (1) because 1995 was a relatively dry year, 1996 a wet year, and 1997 an average year, the TMDL period encompasses a variety of hydrological conditions and helps meet the requirement that the TMDLs take into account variations in hydrology; and (2) hydrological conditions 1995-1997 are very similar to the CSO LTCP design period of 1998-1990 and thus provide a fair test of the design of the LTCP. Baseline loads for the TMDL are also calculated for the period 1995-1997. No Chla data were

collected in the Anacostia 1995-1997 so the eutrophication model could not be exclusively calibrated against data from those years. For this reason, the calibration period was extended to 2002 to include the years 1999-2002 when Chla monitoring data were available.

3.4.3 Other Input Time Series

TAM/WASP requires daily time series of air temperature, water temperature, solar radiation, daylight hours, and wind speed. These were computed according to the methods used in earlier versions of the TAM/WASP Model (Mandel and Schultz, 2000). Table 3.4.1 summaries data sources for these time series.

Table 3.4.1 Daily Time Series Used in TAM/WASP Model

Time Series	Source
Air Temperature	Reagan National Airport (NCDC 448906)
Water Temperature	Interpolation from DDOE Ambient Monitoring Stations
Solar Radiation	Reagan National Airport (NCDC 448906)
Fraction of Daylight Hours	Monthly mean daylight hours, Mills *et al*. (1985)
Wind Speed	Reagan National Airport (NCDC 448906)

3.4.4 Overall Calibration Results

Final values of global calibration parameters are given in Table C.1 in Appendix C. Table C.2 gives the values of key calibration parameters that vary by segment. Table C.3 in Appendix C gives overall summary statistics comparing observed and simulated concentrations of DO, BOD, Chla, Secchi Depth, NH4, NO3, and DIP at the major ambient monitoring stations: ANA0082, ANA30, ANA01, ANA07, ANA14, and ANA21. Section 3.5 gives a more detailed discussion of the DO calibration, and Section 3.6 gives a more details discussion of the Chla and nutrient calibrations.

3.5 DO and BOD Calibration

As is well-known, DO concentrations show a strong seasonal pattern with higher concentrations in the winter and lower concentrations in the summer. The seasonal pattern is first of all a function of water temperature and the negative correlation between temperature and solubility. Summer DO concentrations in the tidal Anacostia, however, dip well below maximum saturation concentrations. Concentrations routinely drop to 2 mg/l and periodically reach anoxic conditions.

The goal of the DO calibration was to match the annual minimum DO concentration observed in the primary monitoring stations: ANA0082, ANA30, ANA01, ANA07, ANA14, and ANA21. Preliminary optimization analysis using PEST, the parameter optimization software, suggested that (1) period of low DO concentrations are sustained

by SOD; (2) the diagenic material consumed in periods of low DO can originate during wet weather periods in the winter and spring; and (3) episodic excursions toward anoxic conditions can be triggered by storm events. In other words, diagenic material is deposited in the winter and spring, then consumed in the summer, when influxes of fresh BOD cause low DO concentrations to drop even more sharply. The seasonal pattern of DO concentrations is the product of temperature-dependent oxygen solubility and the temperature dependent consumption of organic material.

Developing a calibration strategy that follows the outline above runs into two limitations of WASP5. First, there is only one BOD state variable, so WASP cannot explicitly capture the heterogeneity of types of organic material that may have quite different decay rates. Observed BOD5, for example, could be a single material with a uniform decay rate or two materials, one with a fast decay rate and one with a slower rate. Moreover, the problem is compounded in WASP because the state variable is ultimate BOD, not BOD5. Therefore, the total oxygen content of the organic material is fixed regardless of the decay rate.

The second limitation, as was mentioned earlier, is that WASP does not have separate state variables for particulate and dissolved forms of BOD. Rather the fraction of dissolved BOD (or any other WASP constituent) is a fixed segment property. This means on average, WASP will probably underestimate the concentration of particulate constituents under storm events and overestimate settling under dry conditions. In effect, under dry conditions, as the particulate fraction settles, additional dissolved material is converted to particulate form to maintain the constant fraction for that segment.

One aspect of the first limitation was addressed by making the base BOD decay rates in both the water column and sediment vary by segment. This enables the WASP model to take into account that the dominant sources of BOD and their associated decay rates may differ from head of tide to the confluence with the Potomac, if only because the travel times or residence times of the organic material is most likely differs spatially. BOD at the head of tide represents the contribution of the entire upstream watershed; BOD at the Potomac confluence may represent in part transit through an even larger watershed. It is to be expected that, all other things equal, decay rates would be lower for the materials from these sources than from Lower Beaverdam Creek, Watts Branch, or the small tributaries that drain into the tidal Anacostia in DC.

Incorporating this modification, the following overall strategy was used to calibrate the simulation of DO and BOD:

- The tidal river was divided into zones roughly corresponding to the major ambient monitoring stations;
- Winter (October through May) and summer (June through September) BOD settling rates were determined each year for each zone with the initial presumption that (1) the winter settling rate would be greater than the summer rate, and (2) settling in wet years (1996, 1998) would be greater than dry years;

- Settling rates and sediment BOD decay rates were adjusted until the general summer DO sag was captured each year at each major ambient monitoring station; and
- Water column decay rates were adjusted until simulated DO concentrations were no greater than minimum observed DO concentrations at each major ambient monitoring station on an annual basis.

Simulated daily rearation rates were calculated internally to WASP on a segment based on wind speed and water velocity. No calibration parameters are involved in the simulation.

Table C.1 in Appendix C gives the overall calibration parameters values for DO and BOD. Table C.2 gives the values of spatially varying parameters. Summer settling rates had to be increased for dry years like 1999 or 2002; otherwise, the calibration strategy was successfully implemented. Typical SOD rates averaged about 2 $g/m^2/d$ and fell within the range reported by Bailey *et al*. (2003). Table C.3 gives the summary statistics comparing observed and simulated DO. Figures C.1 through C.6 compare the observed and simulated DO concentrations at stations ANA0082, ANA30, ANA01, ANA07, ANA14, and ANA21, respectively. As the figures show, the calibration met its objective of matching the annual minimum DO concentration by station.

Table C.3 shows summary statistics comparing observed and simulated BOD concentrations. Figures C.7 through C.12 compare the observed and simulated BOD concentrations at stations ANA0082, ANA30, ANA01, ANA07, ANA14, and ANA21, respectively. The calibrated model undersimulates water column BOD. Underestimation of water column BOD was a feature of the first version of the TAM/WASP model; Mandel and Schultz (2000) discuss its causes and remedies. This is probably due to the fact that both dissolved and particulate BOD are represented by the same state variable, even though they have different decay rates and thus should have different BOD ultimate conversion rates associated with them. In other words, the ultimate DO demand of settling BOD is probably underestimated, so that in compensation more water column BOD must settle and is perhaps decayed at a higher rate. Recommendations for addressing this problem are discussed in Section 7.2.

3.6 Calibration of Chlorophyll *a*, Secchi Depth, and Nutrients

The goal of the Chla calibration was to match the annual maximum Chla concentration observed in the primary monitoring stations: ANA0082, ANA30, ANA01, ANA07, ANA14, and ANA21. Chla monitoring data exist only for 1999-2002 during the simulation period. Since there is no Chla data for the TMDL Scenario simulation period 1995-1997, unlike the DO calibration, the Chla calibration was constrained to use time-invariable parameters. Since Chla concentrations depend to a large extent on nitrogen and phosphorus concentrations, this constraint applies to the calibration of nutrients as well.

The calibration of nutrients and Chla takes as its starting point the calibration of these constituents performed for the sediment TMDL (Schultz et al, 2007). That calibration employed the Smith formulation of the relation between algal growth rates and light availability. That formulation recognizes that the ratio of algal biomass to Chla concentrations varies with light availability: the greater the limitation light poses to growth, the greater the Chla production by algae attempting to compensate for the lack of light. Thus the Smith formulation is marked by a variable Carbon:Chla ratio in algal stoichiometry, which increases with increasing light availability. The Smith formulation recognizes that there is an optimum light intensity for algal growth and above that intensity the growth rate diminishes. See Ambrose et al. (1993) for more details on the Smith formulation.

3.6.1 Chlorophyll *a* Calibration

The maximum photosynthetic yield (PHIMAX) characterizes the maximum rate at which algae can utilize light. It is the only adjustable parameter used in the Smith formulation and at least under the conditions simulated in the Anacostia, did not have a large effect on the calibration over the accepted range of values. In effect, the sensitivity of the model to light was set by the Smith formulation so the Chla calibration focused on the algal growth rate and its relation to nutrients.

After the calibration of the general levels of bio-available nutrients—ammonia, nitrate, and dissolved phosphate—the Chla base growth rate, temperature correction factor, and nitrogen and phosphorus half-saturation coefficients were adjusted to meet the calibration objectives. Table C.1 in Appendix C shows the final calibration parameter values. The temperature correction factor was used to seasonally-bound algal growth as a surrogate for zooplankton and other forms of predation that were not explicitly represented in the model. WASP uses Michaelis-Menten dynamics to represent the nutrient limitation of algal growth. The nutrient limitation is calculated separately for nitrogen and phosphorus, and the minimum of the two is used to represent overall nutrient limitation. The half-saturation coefficient, which represents the concentration at which nutrients limit growth to half its base value, was set in the range of observed values.

Table C.3 shows summary statistics comparing observed and simulated Chla concentrations. Figures C.13 to C.18 compare observed and simulated Chla concentrations at stations ANA0082, ANA30, ANA01, ANA07, ANA14, and ANA21, respectively. As the figures show, the calibration met its objective of matching the annual maximum Chla concentration by station.

3.6.2 Secchi Depth

The relation between non-algal solids, Chla concentrations, and background color was calibrated for the sediment TMDL (Schultz *et al*, 2007). Under baseline conditions, Secchi depth is primarily a function of non-algal solids. Roughly the same simulated Chla concentrations occur in the sediment and nutrient TMDLs, because they both were calibrated to the same observed data. Therefore, as planned, there was no need to adjust

the calibration of Secchi depth for the nutrient TMDL. Table C.3 shows summary statistics comparing observed and simulated Secchi depths. Figures C.19 to C.24 compare observed and simulated Secchi depths at stations ANA0082, ANA30, ANA01, ANA07, ANA14, and ANA21, respectively.

3.6.3 Phosphorus Calibration

TP is monitored at ANA0082; otherwise, only DIP data is available in the tidal Anacostia. This means it is not possible to determine (1) the total phosphorus concentration, (2) how it is split between organic and inorganic phosphorus, or (3) how phosphorus species are divided into solid and dissolved phases.

In the face of these uncertainties, the overall calibration strategy was to approximate the DIP concentration by adjusting the settling rate and dissolved fraction of inorganic phosphorus. The limitations of WASP's representation of solid-phase dynamics again come into play, for although inorganic phosphorus can be assigned a distinct settling rate from organic species, the dissolved fraction of inorganic phosphorus is a fixed characteristic of each modeling segment. In addition, necessity of avoiding time-variable parameters, as discussed in Section 3.6.1, prevents adjusting settling rates over time.

The TAM/WASP model's diagenesis component does not simulate the release of phosphate from the sediments. A fixed sediment release rate of 1.5 $mg/m^2/d$ was applied during the summer months, based on the observations reported by Bailey *et al* (2003).

Table C.1 in Appendix C gives the inorganic phosphorus settling rate and organic phosphorus decay rates used in the calibration. Table C.2 gives the values of inorganic and organic phosphorus dissolved fractions by segment. OP settling rates are identical to the BOD settling rates shown in Table C.2 Figure C.25 compares observed and simulated TP concentrations at Station ANA0082. Figures C.26 to C.30 compare observed and simulated DIP concentrations at stations ANA30, ANA01, ANA07, ANA14, and ANA21, respectively. The range of simulated DIP concentrations tends to be higher than observed, because simulated DIP includes storm events with artificially higher DIP concentrations due to the fixed dissolved fraction of inorganic phosphorus.

3.6.4 Nitrogen Calibration

Like phosphorus, the nitrogen calibration is constrained by the limited number of species monitored in the tidal Anacostia. Samples from Stations ANA30, ANA01, ANA08, ANA14, and ANA21 are only analyzed for ammonia and nitrate nitrogen. It is not possible, therefore, to calibrate total nitrogen or organic nitrogen. This is problematic because, after input loads, the primary determinant of the concentration of nitrogen species is the interaction between the water column and sediments, which in turn is driven by deposition organic nitrogen and its subsequent decay.

Observed nitrate concentrations in the water column show a seasonal pattern: concentrations tend to be lower in the summer than the winter, primarily because of

denitrification of nitrate in the sediments. NH4 concentrations, on the other hand, do not exhibit a strong seasonal pattern. The following calibration strategy was adopted to capture (1) the seasonal pattern of water column NO3 concentrations; (2) the average water column NO3 concentrations; and (3) average water column NH4 concentrations:

- Adjust sediment denitrification rates to capture the seasonal NO3 concentrations;
- Adjust organic nitrogen deposition rates and decay rates to adjust NH4 and NO3 water column concentrations; and
- Adjust water column nitrification rate to balance NH4 and NO3 concentrations.

Table C.1 in Appendix C gives the key parameters in the calibration of nitrogen species. The organic nitrogen deposition rate is a function of both the dissolved fraction of organic nitrogen in the water column and the solid fraction settling rate. The latter, however, is fixed by the calibration of the BOD settling rate, since one settling rate applies to all organic material; BOD, ON, and OP. The ON deposition rate was therefore calibrated by setting the dissolved fraction of ON by segment. Table C.2 gives the ON dissolved fraction and the ON settling rate by segment.

Figures C.31 to C.36 compare observed and simulated NH4 concentrations at stations ANA0082, ANA30, ANA01, ANA07, ANA14, and ANA21, respectively. The model captures the central tendency of the observed concentrations but has a smaller variance, underpredicting higher concentrations and overpredicting the lower concentrations.

Figures C.37 to C.42 compare observed and simulated NO3 concentrations at stations ANA0082, ANA30, ANA01, ANA07, ANA14, and ANA21, respectively. The model captures the seasonal trend in observed NO3 concentrations as well as the central tendency of the concentrations, but underpredicts higher concentrations. As many of the graphs show, concentrations 1995-1997 trend higher than the later years of the simulation period. An explanation for this trend is not apparent, and it is not capture in the model.

Table C.3 gives summary statistics comparing observed and simulated concentrations for both NH4 and NO3.

3.7 TMDL Scenario

The purpose of the redevelopment of the TAM/WASP eutrophication model is to determine the BOD, TN, and TP loads to the tidal Anacostia River that are compatible with the water quality standards discussed in Section 3.3.1. This section describes three technical aspects of the TMDL scenario: (1) input loads, (2) boundary conditions, and (3) initial conditions. A brief interpretation of the TMDL Scenario results is also provided.

3.7.1 Input Loads

Generally speaking, the TMDL Scenario consists in an across-the-board reduction in BOD, NH4, NO3, TP, TON, and TOP loads for all sources except municipal and industrial point sources and CSOs.

For CSOs, simulated flows were based on simulated flows of CSOs under the LTCP. The MOUSE model was used to determine the LTCP flows for this period. Table 3.7.1 gives the total CSO flow by month over the simulation period as determined by the MOUSE model. The average EMC concentrations shown in Table 2 were also used to calculate CSO loads in the TMDL Scenario.

Table 3.7.1. Simulated CSOs (MGD) under WASA Long-Term Control Plan

Month	1995	1996	1997	Total
Jan	0	0	0	0
Feb	0	0	0	0
Mar	12	0	0	12
Apr	0	0	0	0
May	0	0	140	140
Jun	0	0	0	0
July	42	0	0	42
Aug	0	0	102	102
Sep	0	16	0	16
Oct	308	4	0	311
Nov	0	160	0	160
Dec	0	0	0	0
Total	361	179	242	783

As described in Chapter 2, there are two municipal wastewater treatment plants (WWTPs) contributing BOD, TN, and TP loads to the Anacostia river: The Beltsville Agricultural Research Center (BARC) East Side and Beltsville U.S. Department of Agriculture (USDA) West WWTPs. BOD loads were calculated based on the permitted flow and maximum weekly average concentrations. The permits contain values for two seasons for BOD, which were incorporated into the calculations based on the permit-defined seasons. TN and TP loads were calculated based on permitted flow and concentrations. There are no permit-defined seasons for TN and TP. Table 3.7.2 shows the design flows and permitted concentrations. It should be noted that the use of the maximum weekly average concentration is a conservative assumption. The waste load allocations for these facilities were determined using the maximum monthly average permitted concentrations.

In addition to these two municipal WWTPs, there is one industrial point sources in MD and three industrial point sources contributing to BOD loads to the Anacostia River. There are no permit limits on nutrients for any of the four industrial point sources. Table 3.7.2 shows the maximum reported flows and permit conditions on BOD and nutrient concentrations. For the NASA facility, the BOD loads were calculated from the maximum reported flow of 0.080 MGD, 2005 through 2007, and the monthly average permitted BOD concentration of 45 mg/l. For Aggregated Super Concrete and CTIDC, in the absence of explicit permit limits on BOD concentrations, the maximum reported flow was multiplied by a BOD concentration of 30 mg/l. The PEPCO hydrostatic testing

facility has a permitted maximum daily average concentration of 30 mg/l and a maximum permitted discharge of 0.5 MGD. It discharges, however, at most once or twice a year. It was assigned a WLA assuming it would overflow no more than four times a year. A sensitivity analysis using the calibrated TAM/WASP model showed that water quality standards would be met even if the average weekly BOD discharged from the plant was equal to its annual WLA.

For nutrient and BOD loads from Lower Beaverdam Creek, Watts Branch, small tributaries, and direct drainage to the tidal river, nutrient and BOD loads were simply reduced by a fixed reduction rate on a daily basis. NEB and NWB load from ESTIMATOR implicitly include loads from the three point source facilities described above. Under the TMDL Scenario, however, the loads from these sources are explicitly added to the NEB and NWB loads. To account for the explicit representation of point sources, the ESTIMATOR loads were adjusted to account for the point source contribution to baseline loads. The percent of the baseline load from point sources was calculated on a monthly basis, and the ESTIMATOR load was reduced on a daily basis by this percentage. Nutrient and BOD reductions were taken from these adjusted ESTIMATOR loads for NEB and NWB.

Table 3.7.2. Maximum Permitted Concentrations and Flows for Calculation of Municipal and Industrial Waste Load Allocations

NPDES No	Name	Maximum Permitted Concentration (mg/L)			Flow (MGD)	
		BOD5	TN	TP	Design Flow	Maximum Observed Flow
MD0020842	BARC East Side WWTP	26 (4/1-9/30) 45 (10/1-3/31) Weekly average	4.0	0.3	0.6	
MD0020851	Beltsville USDA West WWTP	30 (4/1-10/31) 45 (11/1-3/31) Weekly average	4.0	0.3	0.22	
MD0067482	NASA Goddard Center	45 Daily max	Report NH4-N	NA		0.08
DC0000175	Aggregate Super Concrete Industries	Report	NA	NA		0.013
DC0000191	CTIDC	Report	NA	NA		0.011
DC0000098	PEPCO	30 mg/l Daily average	NA	NA		0.5

3.7.2 Initial Concentrations

The concentrations of state variables used to initialize the WASP eutrophication model have only transient effects, except for BOD and, to a lesser extent, ON in the sediments. The initial values of sediment BOD and ON concentrations were reduced by approximately the percent reduction of BOD and TN, respectively, in the TMDL Scenario.

3.7.3 Boundary Conditions

Boundary conditions used in the calibration were taken primarily from station ANA29 at the confluence of the Anacostia and the Potomac Rivers. Figure 3.7.1 shows the location of this station. Constituent concentrations from this station are the product of water quality in both the Anacostia and the Potomac, and therefore are not likely to represent boundary conditions under the significant nutrient and BOD reductions needed to meet water quality standards.

Under the TMDL Scenario, the boundary conditions for DO, Chla, BOD, NH4, and NO3 were taken from Potomac stations PMS01, PMS10, and PMS21 “upstream” of the confluence with the Anacostia. These stations are also shown in Figure 3.7.1. The Potomac is still tidal at these station locations and therefore influenced to some extent by conditions downstream of the stations, including current water quality in the Anacostia. The monthly median concentrations for these stations for the period 1995-2004 were used as monthly boundary conditions. These are shown in Table 3.7.3. These boundary conditions represent typical seasonal Potomac River concentrations of these constituents and do not assume any nutrient or BOD reductions are made to the Potomac.

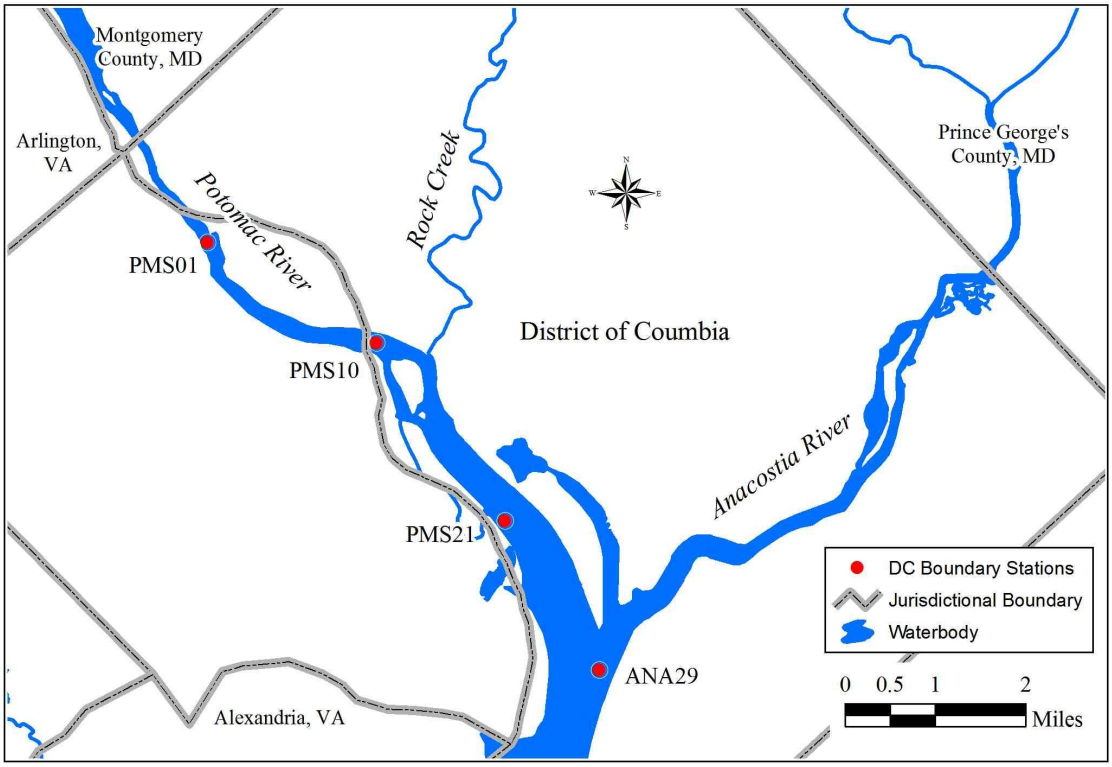

Figure 3.7.1. Potomac River Monitoring Stations Used for TMDL Boundary Conditions

Monitoring data was not available for TIP, TOP, or TON so the boundary conditions for these constituents were left unchanged from the calibration.

Table 3.7.3. TMDL Boundary Conditions

Month	NH4	NO3	CHLA	DO
Jan	0.034	1.34	1.5	13.9
Feb	0.046	1.58	3.7	13.1
Mar	0.04	1.26	4.6	12
Aprl	0.051	1.19	3	10.2
May	0.053	0.87	2.6	8.4
Jun	0.032	0.85	4.3	7.9
July	0.032	0.54	8.2	7.6
Aug	0.044	0.53	6.8	7.2
Sep	0.049	0.66	2.7	7.7
Oct	0.028	0.99	0.8	9.4
Nov	0.015	1.06	1	12.1
Dec	0.016	0.96	1.4	12.5

3.7.4 TMDL Scenario Results

Under the TMDL Scenario, it was determined that, to meet water quality standards, sources other than CSOs, WWTPs, and industrial dischargers would have to reduce their BOD loads by 58% and both their TN and TP loads by 80%. TMDL Scenario results for DO are discussed in the main TMDL report and Appendix C to that report (MDE and DDOE, 2008). Nutrient reductions and their relation to the water clarity standard and DC's numeric Chla standard are also discussed, but what is not explained is why such large nutrient reductions are necessary to meet water quality standards.

The reason lies in the fact that the TMDL Scenario assumes the load reductions called for in the sediment TMDL and is run with the sediment concentrations from the TMDL Scenario for the sediment TMDL. To meet the water quality standards for water clarity, dramatic reductions in sediment concentrations were necessary. Improved water clarity *ceteris paribus*, diminishes any light limitations to algal growth, leading to greater growth and greater Chla concentrations. Figure 3.7.2 shows the impact of greater water clarity on algae growth. It shows simulated Chla concentrations for (1) calibration, (2) TMDL Scenario, and (3) simulation with baseline nutrients but TMDL sediment concentrations. Reducing sediment concentrations with reducing nutrients nearly doubles Chla concentrations. Simulated peak concentrations rise to nearly 200 ug/l. This occurs even though the Smith algal growth formulation used in TAM/WASP (a) increases the C:Chla ratio as light limitation diminishes and (b) recognizes that algal growth can become light inhibited if light intensity is above a threshold value. Nutrient reductions of 80% are necessary to bring the very high simulated Chla concentrations caused by the improvement in water clarity down to levels required by DC's numerical criterion for Chla.

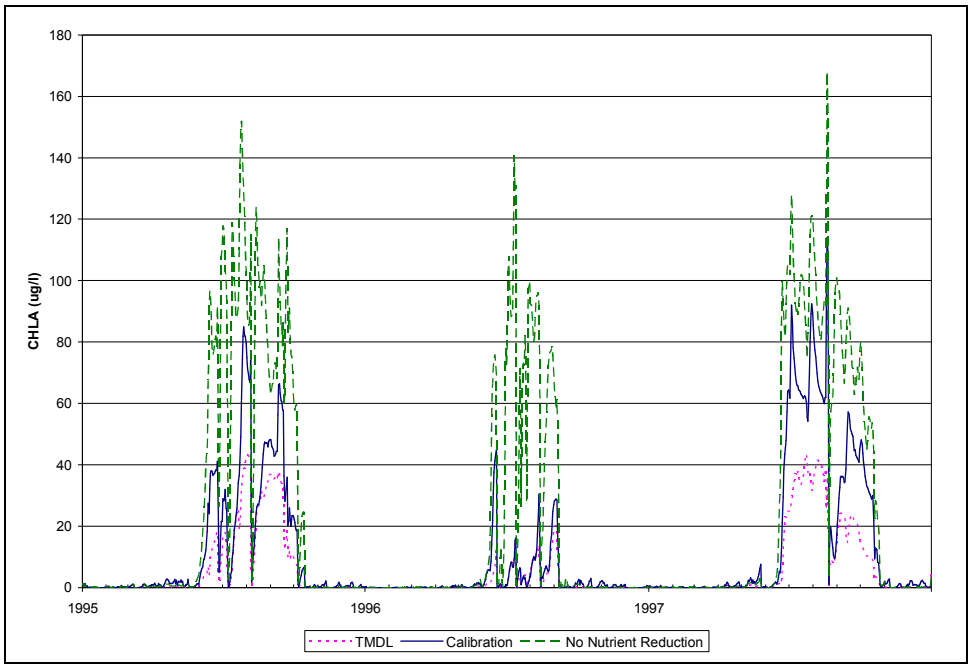

Figure 3.7.2. Simulated Chla under Baseline Calibration, TMDL Scenario, and TMDL Sediment Loads with Baseline Nutrient Loads at ANA08

4 SUMMARY AND RECOMMENDATIONS

4.1 Summary

The TAM/WASP modeling framework has been successfully updated to develop BOD, TN, and TP TMDLs for the tidal Anacostia River. The updated framework includes revised loads from NEB, NWB, LBC, and Watts Branch, as well as smaller tributaries, direct drainage to the tidal river, CSOs, and municipal and industrial point sources. The USGS software ESTIMATOR was used to determine total nutrient and BOD loads from NE and NWB. A revised HSPF model of the NEB and NWB was used to quantify the sources of these loads. Revised HSPF models of LBC and Watts Branch were used both to determine overall loads to the Anacostia from these tributaries, as well as to quantify the sources of these loads. CSO loads were determined based on information developed for WASA's LTCP, included simulated flows from the LTCP's MOUSE model.

The eutrophication component of the TAM/WASP model was recalibrated for the period 1995-2002. This period encompasses both the TMDL simulation period (1995-1997) and a period (1999-2002) in which Chla monitoring data was collected in the Anacostia. The calibration successfully met its two objectives: (1) the minimum simulated DO should be no greater than the minimum DO observed at the major ambient monitoring stations on an annual basis, and (2) the maximum simulated Chla should be no less than the maximum Chla observed at the major ambient monitoring stations. After meeting these two objectives, the recalibrated model was used to demonstrate that water quality standards for DO, Chla, and water clarity could be met in the Anacostia if BOD loads were reduced by 58% and both TN and TP loads reduced by 80%.

4.2 Recommendations

The performance of the recalibrated TAM/WASP model is more than sufficient to fulfill its fundamental role in TMDL development: to provide the link between nutrient and BOD loading rates, on the one hand, and water quality response, on the other. There is one feature of the calibration, the underprediction of water column BOD, which has been a persistent problem of the TAM/WASP model since the continuous simulation of sediment diagenesis was implemented in the TAM/WASP modeling framework. It might appear erroneously that either (1) the input BOD loads to the model are underestimated or (2) too much BOD is settling from the water column to the sediments. Both of these hypotheses can be shown to be incorrect. ESTIMATOR provides the most sophisticated statistical determination of BOD loads in the perhaps too-long history of modeling the tidal Anacostia. Simulated SOD is in the range observed by field studies. In another sense, however, both hypotheses point in the direction of the most probably explanation: the use of a single variable to represent both water column and sediment BOD (if not other species of BOD).

BOD ultimate, the total amount of potential oxygen demand, is the WASP state variable. Monitoring programs measure 5-day BOD. The current version of TAM/WASP model uses a conversion factor of 1.8. This value has been used in past models and is safely

within the range of literature values. The "true" conversion factor, however, is a function of the decay rate of the material. The sediment decay rate is, to the first approximation, an order of magnitude smaller than the water column decay rate, and therefore should have associated with it a larger conversion factor from 5-day BOD to BOD ultimate. That is, if material decays at a slower rate, the rate of how much potentially decays to how much decays after 5 days should be larger than that for a material which decays faster. In a sense the model is (1) underestimating the input of BOD ultimate (not BOD5, in terms of which the TMDL is expressed) and depositing proportionately too much water column BOD to sediment BOD, to make up for the underestimation of sediment BOD ultimate.

It is not necessary to address this problem to have an adequate TMDL, because the model replicates oxygen demand in the Anacostia, given BOD5 input loads. Addressing the problem would require a monitoring component and modeling component, both of which are discussed below.

4.2.1 Recommendation for Improving Computer Simulation of the Tidal Anacostia

The simulation of all constituents, not just BOD, could be improved if there were separate state variables for particulate and solid phases. This would allow the possibility of independent estimates of the relation of BOD5 to BOD ultimate for particulate and dissolved BOD. Some models, like CE-QUAL-W2, permit multiple BOD species, each with their own decay rates and settling rates. Other models, like ICM which forms the basis of the CBP Water Quality Model, have the capability of representing multiple species of carbon. Separate simulation of particulate and dissolved inorganic phosphorus could also improve the simulation of phosphorus in the Anacostia.

A second direction for model improvement is in the representation of the diel oxygen cycle. A good deal of continuous monitoring data has been collected in the Anacostia, but it is difficult to integrate this into the modeling framework because WASP, although it is driven hydrologically by the tidal cycle, represents algal growth and therefore oxygen dynamics on a daily average basis. A true diel model would require not only a reformulation of the representation of algal and DO kinetics but hourly inputs of solar radiation, air temperature, and other variables. Water temperature, which is currently a model input, may need to be calculated within the model on an hourly basis to capture diel effects. Rather than modify WASP to accommodate diel dynamics, it may be more cost effective to adopt a different model such as CE-QUAL-W2, which is designed to simulate diel effects.

4.2.2 Recommendations for Additional Water Quality Monitoring

To implement the changes in the model outline above would require the collection of additional monitoring data. The calibration of even the current model could be improved if organic nitrogen or organic phosphorus, or total nitrogen or total phosphorus, were routinely monitored in the tidal Anacostia. If there were separate state variables for dissolved and particulate forms of constituents, it would be necessary to have monitoring

data to help calibrate the fate and transport of the phase of constituents. In particular, it would be helpful to have estimates of dissolved and particulate BOD5 from a variety of sources: NWB and NEB; LBC and Watts Branch; CSOs and DC storm sewers.

To better interpret the diurnal variation of DO in continuous monitoring data, it would be helpful if other variables were collected on a continuous basis, in particular Chla. MDDNR collects Chla and several nutrient species in their continuous monitoring program. This information would help to determine whether diel variations of DO are caused by primary production of algae or has another source.

REFERENCES

Ambrose, R.B. Jr., T.A. Wool, and J.L. Martin. 1993. The Water Quality Analysis Simulation Program, WASP5. U.S. Environmental Protection Agency Research Laboratory. Athens, GA.

Bailey, E. K. M., R. M. Stankelis, P. W. Smail, S. Greene, F. M. Rohland, and W. R. Boynton. 2003. Dissolved Oxygen and Nutrient Flux Estimation from Sediments in the Anacostia River. University of Maryland Center for Environmental Science, Chesapeake Bay Laboratory. Solomons, MD.

Bicknell, B.R., J.C. Imhoff, J.L. Kittle, Jr., and A.S. Donigian, Jr. 2000. Hydrological Simulation Program - Fortran (HSPF): User's Manual for Release 12.

CBPO (Chesapeake Bay Program Office). 2003. Ambient Water Quality Criteria for Dissolved Oxygen, Water Clarity and Chlorophyll a for the Chesapeake Bay and its Tidal Tributaries. U.S. Environmental Protection Agency. EPA 903-R-03-002, April 2003.

CBPO (Chesapeake Bay Program Office). 2006. CBP Watershed Model Scenario Output Database, Phase 4.3. http://www.chesapeakebay.net/data/index.htm

Cohn, T. A. , L. L. Delong, E. J. Gilroy, R. M. Hirsch, and D. Wells. 1989. Estimating Constituent Loads. Water Resources Research 28. pp.937-942.

Cohn, T. A., D. L. Caulder, E. J. Gilroy, L. D. Zynjuk, and R. M. Summers. 1992. The Validity of a Simple Log-linear Model for Estimating Fluvial Constituent Loads. Water Resources Research 28. pp. 2353-2364.

COMAR (Code of Maryland Regulations). 2006. 26.08.02, 26.08.02.08 O, 26.08.02.03B(2). Website http://www.dsd.state.md.us/comar, last visited 06/08/06.

DCMR (District of Columbia Municipal Regulations). Title 21. Chapter 11.

DiToro, D.M., P. R. Paquin, K. Subburamu, and D. A. Gruber. 1990. Sediment Oxygen Demand Model: Methane and Ammonia Oxidation. Journal of Environmental Engineering (116). Pp. 945-986.

DCDOH. 2001. Total Maximum Daily Loads Upper Anacostia River Lower Anacostia River District of Columbia Biochemical Oxygen Demand. District of Columbia Department of Health, Environmental Health Administration, Bureau of Environmental Quality, Water Quality Division, Water Quality Control Branch, May 2001.

DCDOH. 2002. Total Maximum Daily Loads Upper Anacostia River Lower Anacostia River District of Columbia Total Suspended Solids. District of Columbia Department of Health, Environmental Health Administration, Bureau of Environmental Quality, Water Quality Division, Water Quality Control Branch, Draft - January 4, 2002.

DCWASA. 2002. Combined Sewer System Long Term Control Plan – Final Report. District of Columbia Water and Sewer Authority, Washington, DC, July 2002.
Doherty, J. 2001. PEST: Model independent parameter estimation - User's Manual. Watermark Numerical Computing.

Katz, C.N., A.R. Carlson, and D.B. Chadwick. 2000. Anacostia River water quality assessment – draft report to the Anacostia Watershed Toxics Alliance, SPAWAR Systems Center, Marine Environmental Quality Branch, San Diego, CA, December 2000.

Langland, M.J., S. W. Phillips, J. P. Raffensperger, and D. L. Moyer. 2005. Changes in streamflow and water quality in selected nontidal sites in the Chesapeake Bay Basin, 1985-2003: U.S. Geological Survey Scientific Investigations Report 2004-5259.

Lung, W. 2000. Incorporating a Sediment Model into the WASP/EUTRO Model. Appendix A in Mandel, R. and C.L. Schultz. 2000. *The TAM/WASP model: a modeling framework for the Total Maximum Daily Load Allocation in the tidal Anacostia River – Final Report*. Interstate Commission on the Potomac River Basin, Rockville, MD. ICPRB Report No. 00-07. www.potomacriver.org/info_center/publications.htm.

Mandel, R. and C.L. Schultz. 2000. The TAM/WASP Model: a modeling framework for the Total Maximum Daily Load allocation in the tidal Anacostia River – Final Report. Prepared by the Interstate Commission on the Potomac River Basin for the District of Columbia, Department of Health, Environmental Health Administration. Washington, DC.

Manchester, M. and R. Mandel. 2001. Technical Memo: A Preliminary Calibration of the Simulation of Hydrology, Sediment Transport, and Nutrient Dynamics in the HSPF Model of the Non-Tidal Anacostia River. Draft. The Interstate Commission on the Potomac River Basin. Rockville, MD.

Mandel, R., R. Shi, and D. Vann. 2003. The Development of an HSPF Model of the Non-tidal Anascostia River Watershed, PhaseII. The Interstate Commission on the Potomac River Basin. Rockville, MD.

Maryland Department of the Environment and the District of Columbia Department of the Environment. 2007. Total Maximum Daily Loads of Sediment/Total Suspended Solids for the Anacostia River Basin, Montgomery and Prince George's Counties, Maryland, and the District of Columbia.

Maryland Department of the Environment and the District of Columbia Department of the Environment. 2008. Total Maximum Daily Loads of Nutrients/Biochemical Oxygen Demand for the Anacostia River Basin, Montgomery and Prince George's Counties, Maryland, and the District of Columbia.

Mills, W. B. , D. B. Porcella, M. J. Ungs, S. A. Gherini, K. V. Summers, L. Mok, G. L.

Rupp, G. L. Bowie, D. A. Haith. 1985. Water Quality Assessment: A Screening Procedure for Toxic and Conventional Pollutants in Surface and Ground Water. EPA 600/6-85/002. U. S. Environmental Protection Agency. Athens, GA.

MWCOG (Metropolitan Washington Council of Governments). 2002. Sediment Oxygen Demand and Nutrient Flux in the Tidal Anacostia River. Washington, DC.

Runkel, R. L., C. G. Crawford, and T. A. Cohn. 2004. Load Estimator (LOADEST): A FORTRAN Program for Estimating Constituent Loads in Streams and Rivers. Techniques and Methods Book 4, Chapter A5. U. S. Geological Survey. Reston, VA.

Schultz, C.L. 2003. Calibration of the TAM/WASP sediment transport model – Final Report. Interstate Commission on the Potomac River Basin, Rockville, Maryland, October 2001, Revised April 2003, ICPRB Report No. 03-01.

Schultz, C.L., and D.V. Velinsky. 2001. Collection of Field Data for the Transport of Sediments in the Anacostia River - Draft Report. Prepared for the District of Columbia, Department of Health, Environmental Health Administration by the Interstate Commission on the Potomac River Basin, Rockville, Maryland, May 3, 2001.

Schultz, C. L., R., S. Kim, R. Mandel, and A. Nagel. 2007. *Anacostia sediment models: Phase 3 Anacostia HSPF watershed model and Version 3 TAM/WASP water clarity model.* Interstate Commission on the Potomac River Basin, Rockville, MD.

Shepp, D.L., C. Clarkson, and T.J. Murphy. 2000. Estimation of Nonpoint Source Loads to the Anacostia River in the District of Columbia for the Total Maximum Daily Load Process. Prepared by the Metropolitan Washington Council of Governments for the District of Columbia Department of Health, Environmental Health Administration, Water Quality Management Division, March 2000.

Sullivan, M.P. and W.E. Brown. 1988. The Tidal Anacostia Model. Metropolitan Washington Council of Governments. Washington, DC.

USEPA. 2002a. Total Maximum Daily Loads Upper Anacostia River Lower Anacostia River District of Columbia Total Suspended Solids. U.S. Environmental Protection Agency Region 3, Philadelphia, PA. March 1, 2002.

USEPA. 2002b. Decision Rationale Total Maximum Daily Loads Total Suspended Solids Upper Anacostia River Lower Anacostia River District of Columbia, U.S. Environmental Protection Agency Region 3, Philadelphia, PA. March 1, 2002.

U.S. EPA. 2008. Chesapeake Bay Phase 5 Community Watershed Model In preparation EPA XXX-X-XX-008 Chesapeake Bay Program Office, Annapolis MD. January 2008

Warner, A., D. Shepp, K. Corish, and J. Galli. 1997. An existing source assessment of pollutants to the Anacostia watershed. Prepared for the DC Department of Consumer and

Regulatory Affairs, Environmental Regulation Administration, by the Metropolitan Washington Council of Governments, Washington, DC.

APPENDIX A

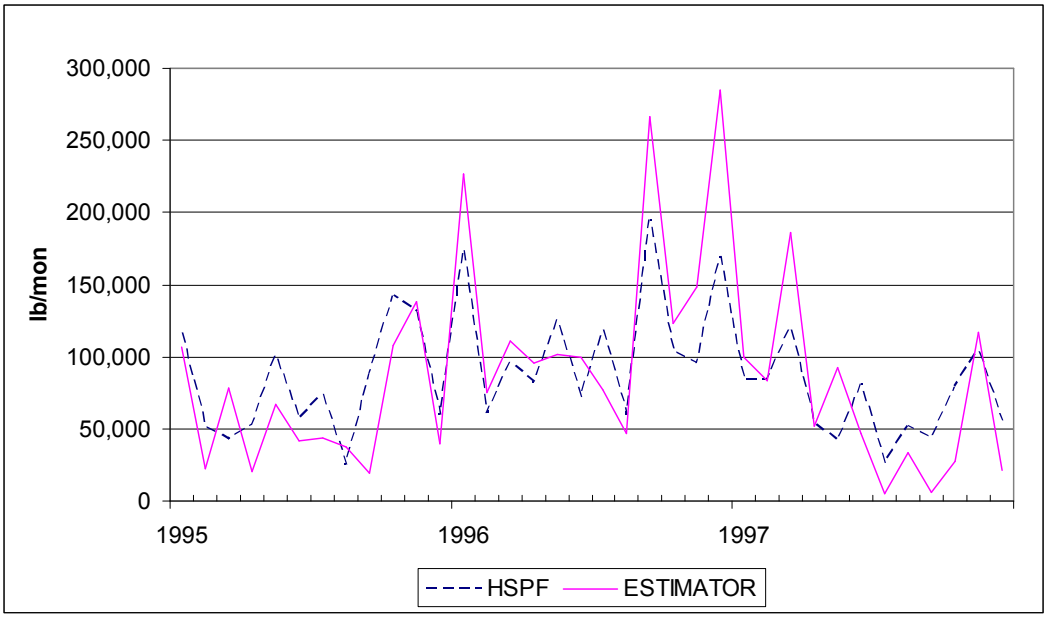

Figure A.1. Time Series of Monthly ESTIMATOR and HSPF BODu Loads, NWB

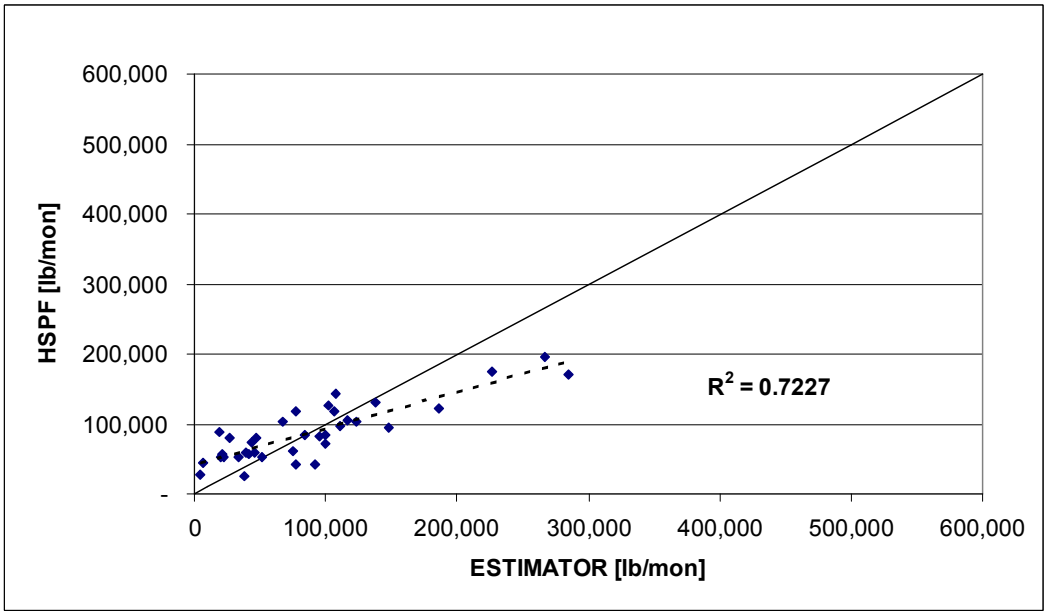

Figure A.2. Scatter Plot of Monthly ESTIMATOR and HSPF BODu Loads, NWB

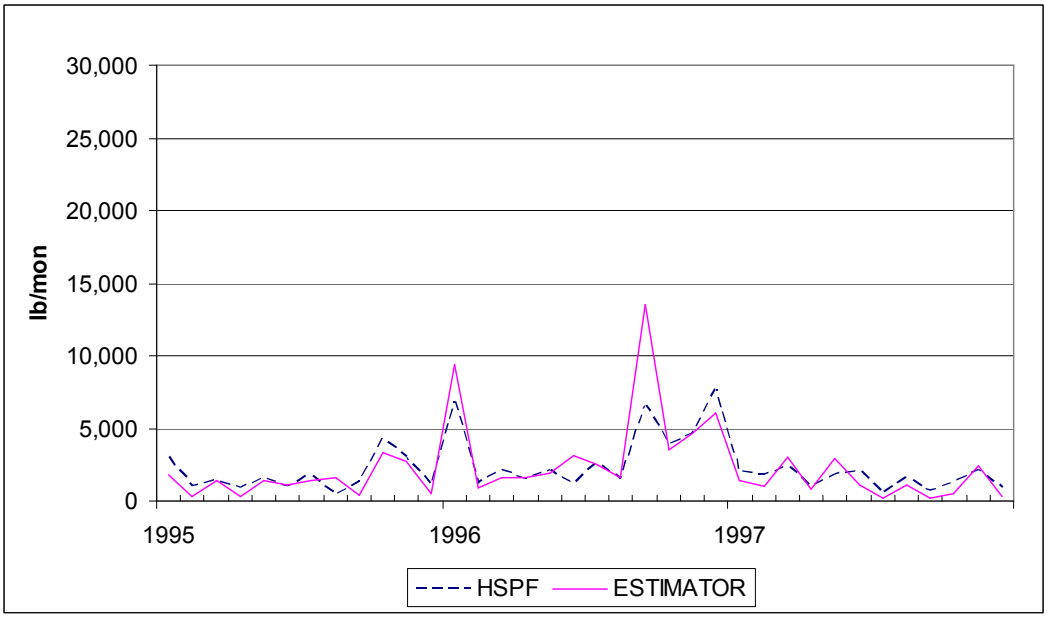

Figure A.3. Time Series of Monthly ESTIMATOR and HSPF TP Loads, NWB

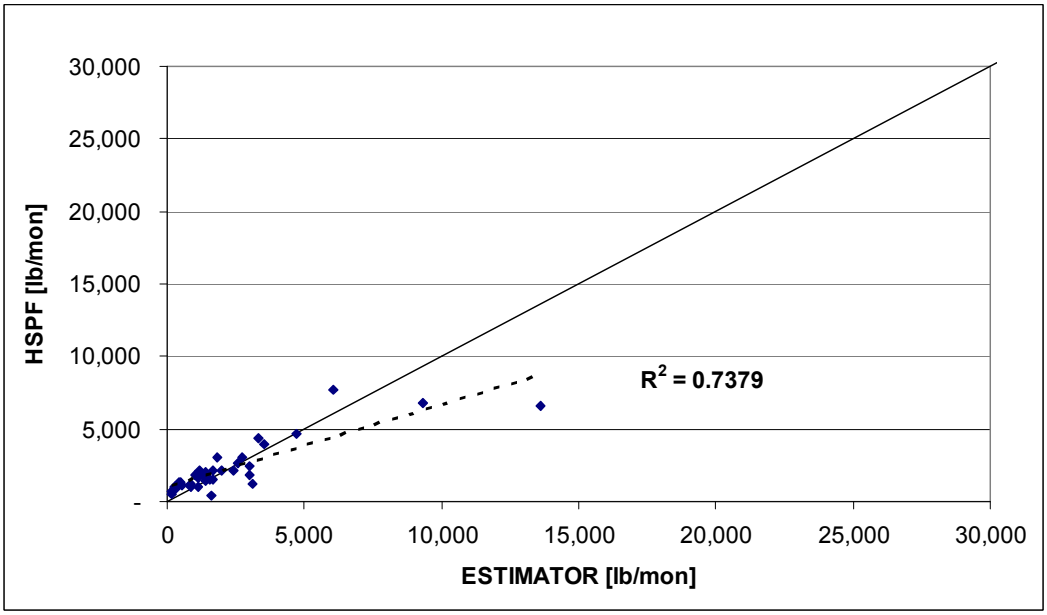

Figure A.4. Scatter Plot of Monthly ESTIMATOR and HSPF TP Loads, NWB

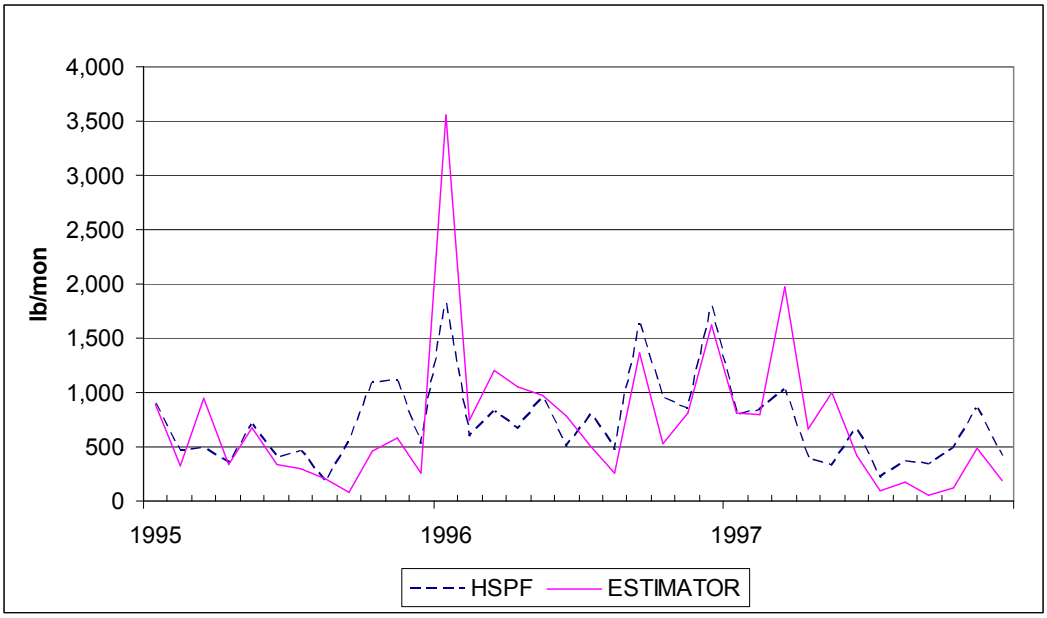

Figure A.5. Time Series of Monthly ESTIMATOR and HSPF NH4 Loads, NWB

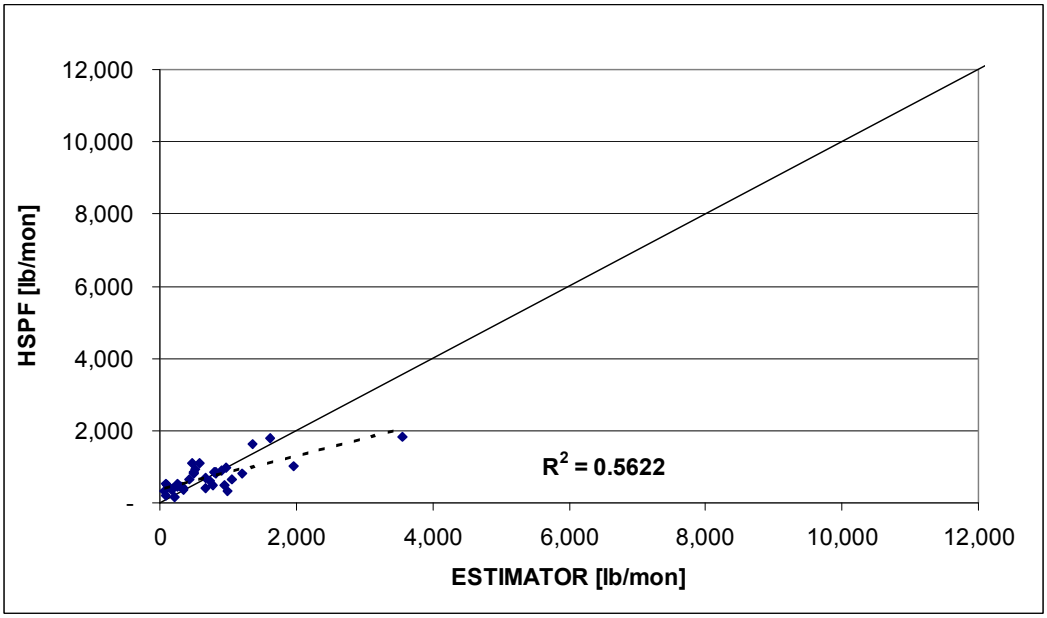

Figure A.6. Scatter Plot of Monthly ESTIMATOR and HSPF NH4 Loads, NWB

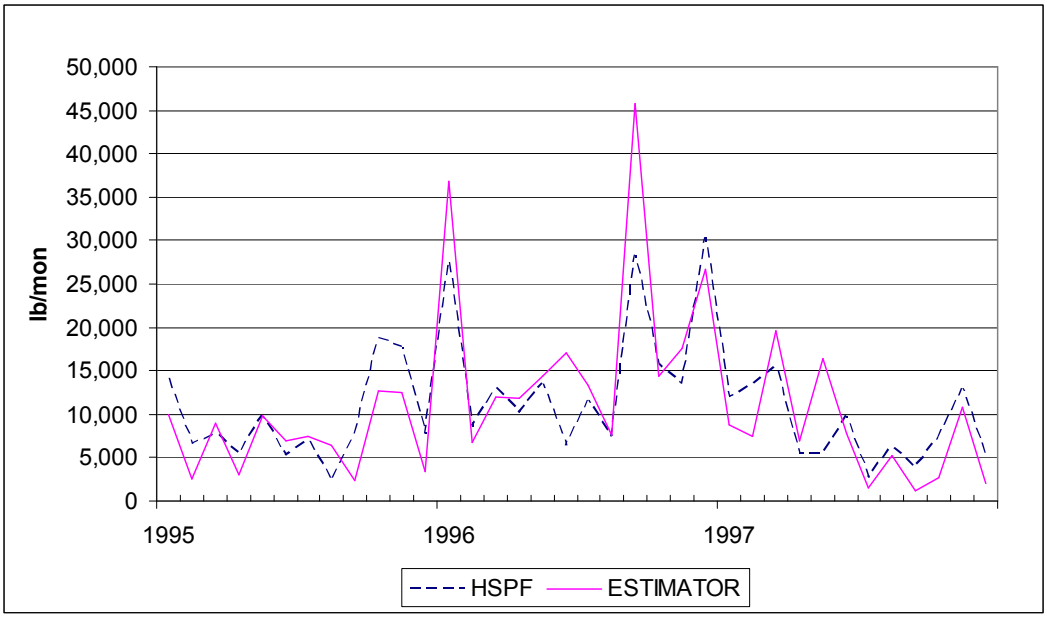

Figure A.7. Time Series of Monthly ESTIMATOR and HSPF ON Loads, NWB

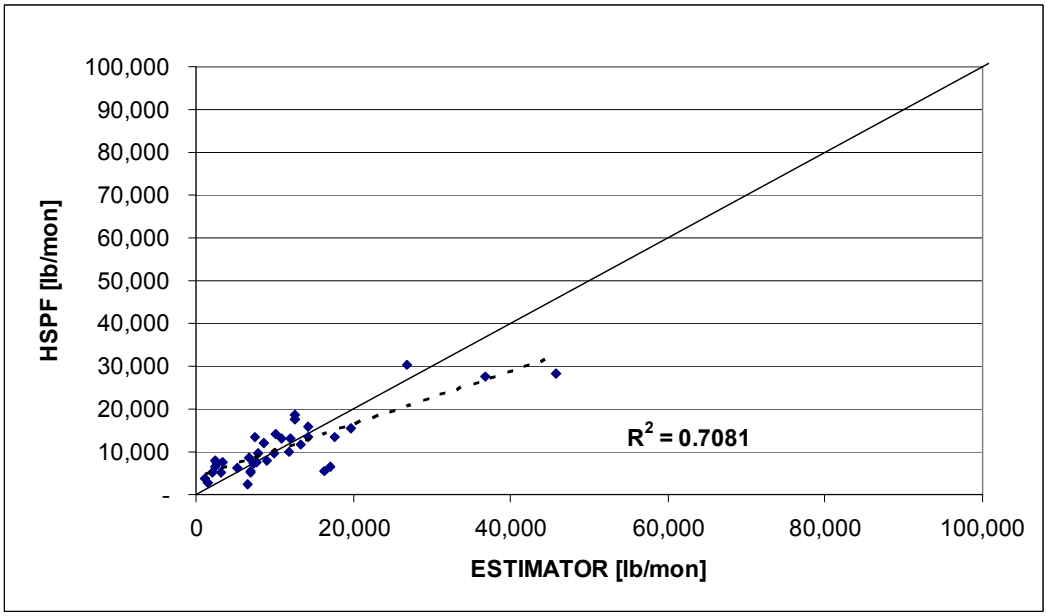

Figure A.8. Scatter Plot of Monthly ESTIMATOR and HSPF ON Loads, NWB

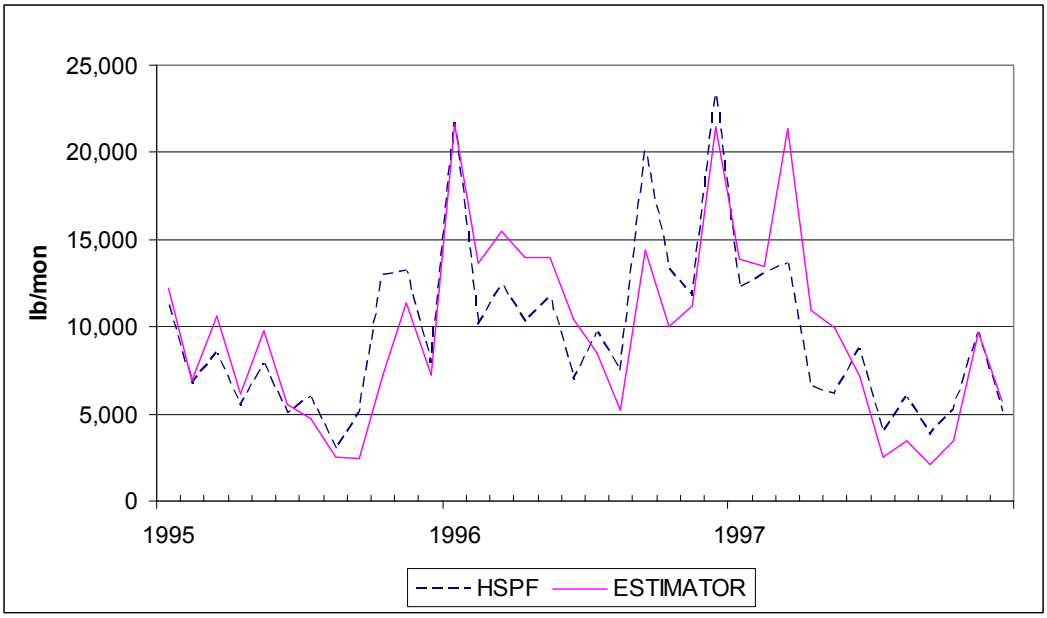

Figure A.9. Time Series of Monthly ESTIMATOR and HSPF NO3 Loads, NWB

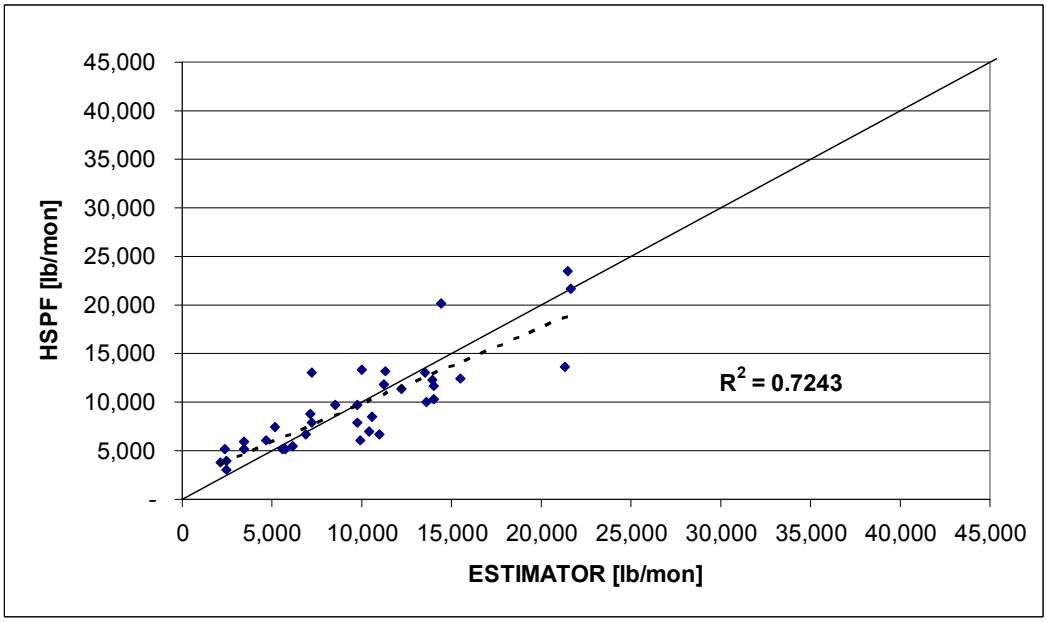

Figure A.10. Scatter Plot of Monthly ESTIMATOR and HSPF NO3 Loads, NWB

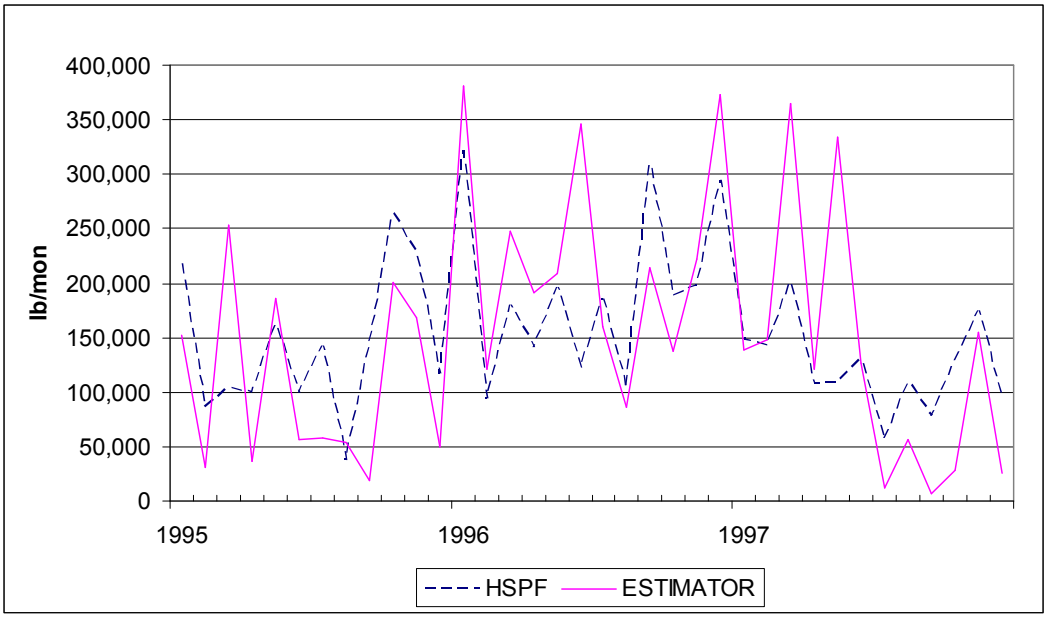

Figure A.11. Time Series of Monthly ESTIMATOR and HSPF BODu Loads, NEB

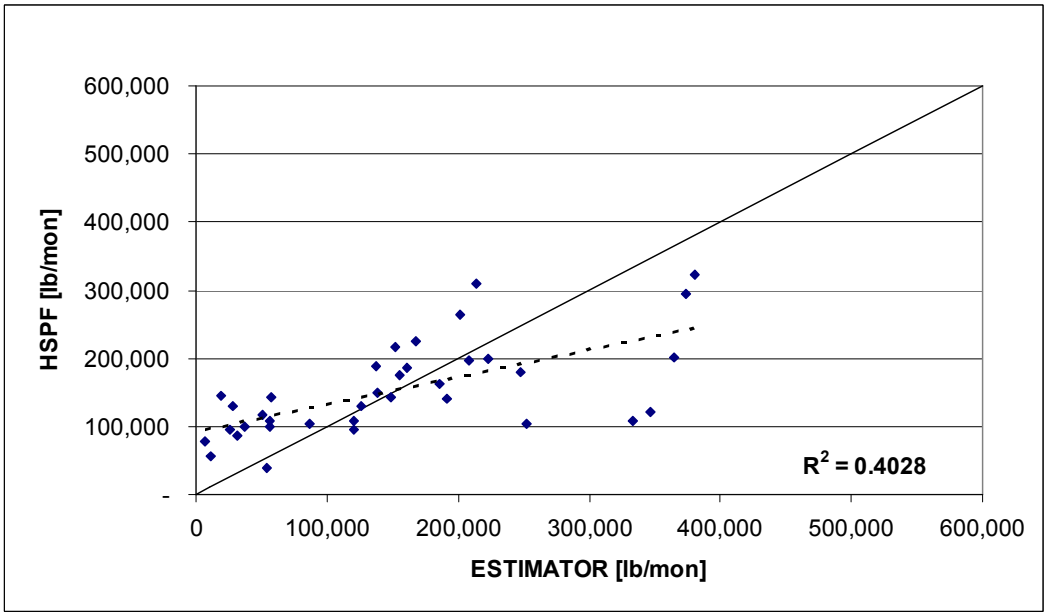

Figure A.12. Scatter Plot of Monthly ESTIMATOR and HSPF BODu Loads, NEB

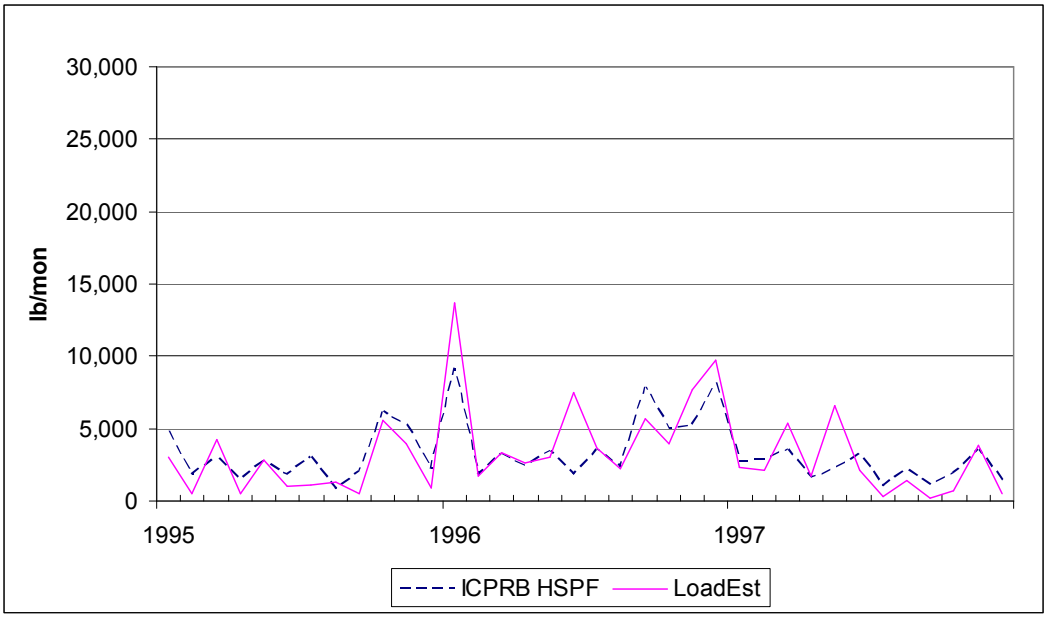

Figure A.13. Time Series of Monthly ESTIMATOR and HSPF TP Loads, NEB

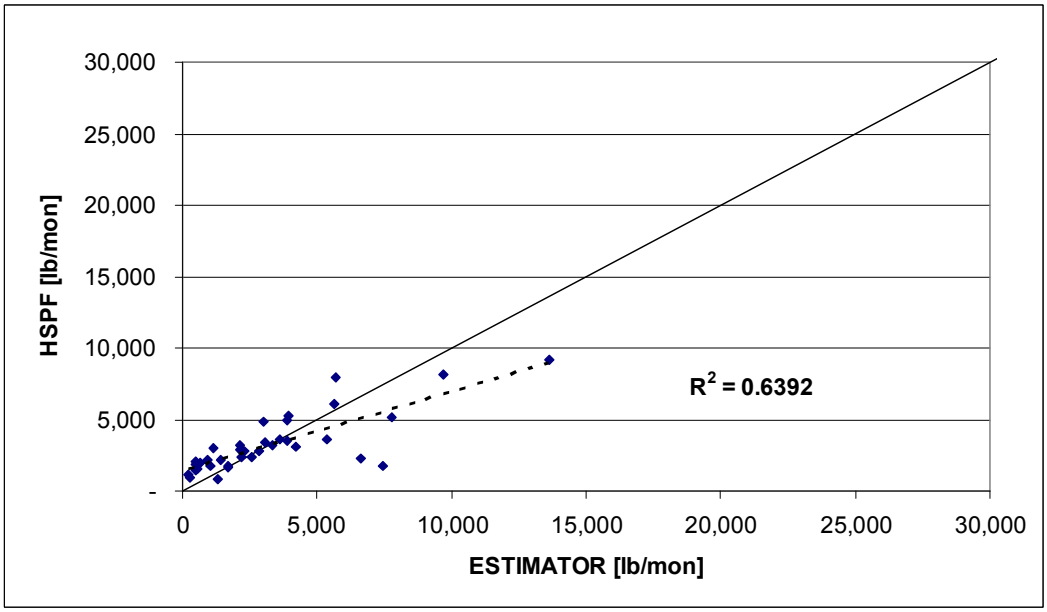

Figure A.14. Scatter Plot of Monthly ESTIMATOR and HSPF TP Loads, NEB

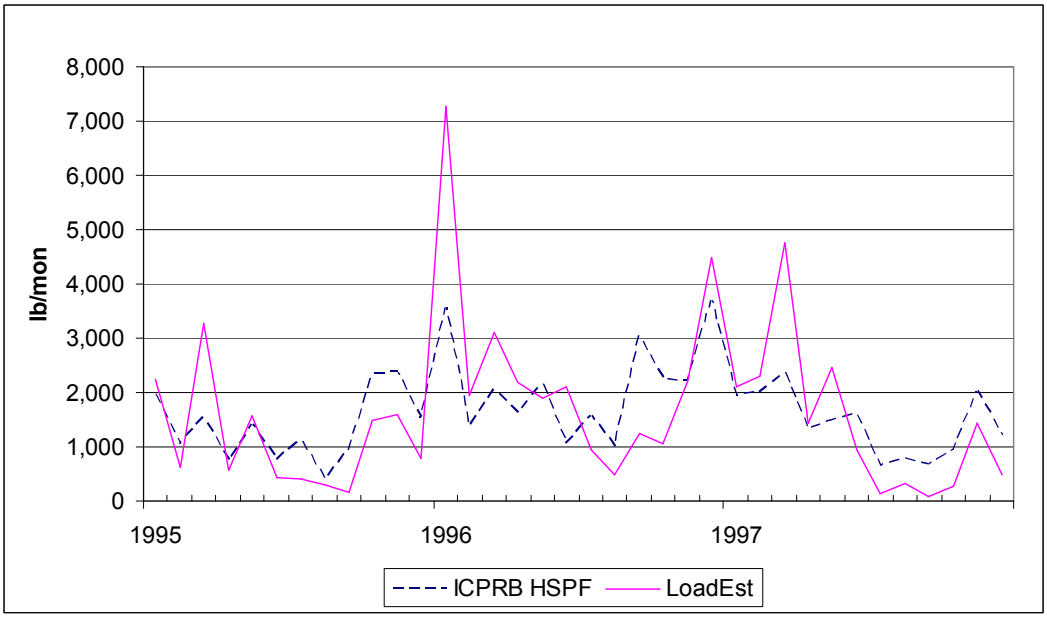

Figure A.15. Time Series of Monthly ESTIMATOR and HSPF NH4 Loads, NEB

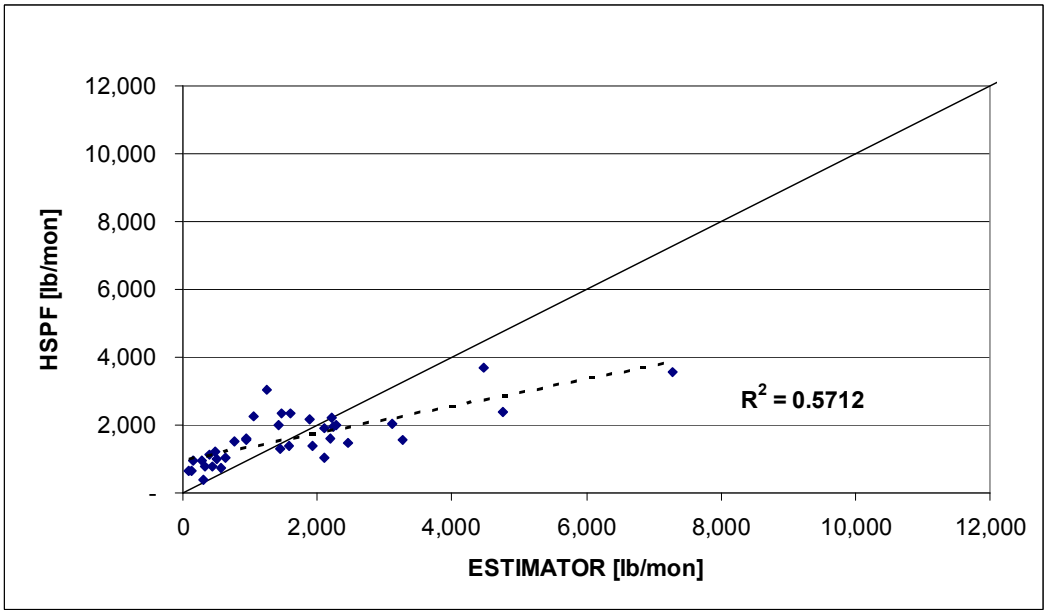

Figure A.16. Scatter Plot of Monthly ESTIMATOR and HSPF NH4 Loads, NEB

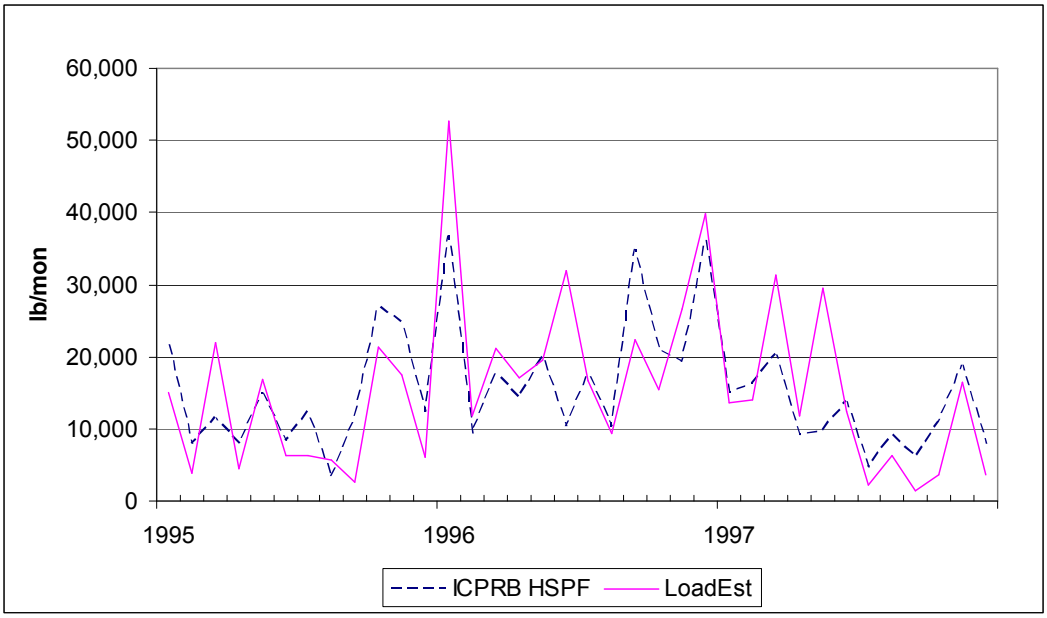

Figure A.17. Time Series of Monthly ESTIMATOR and HSPF ON Loads, NEB

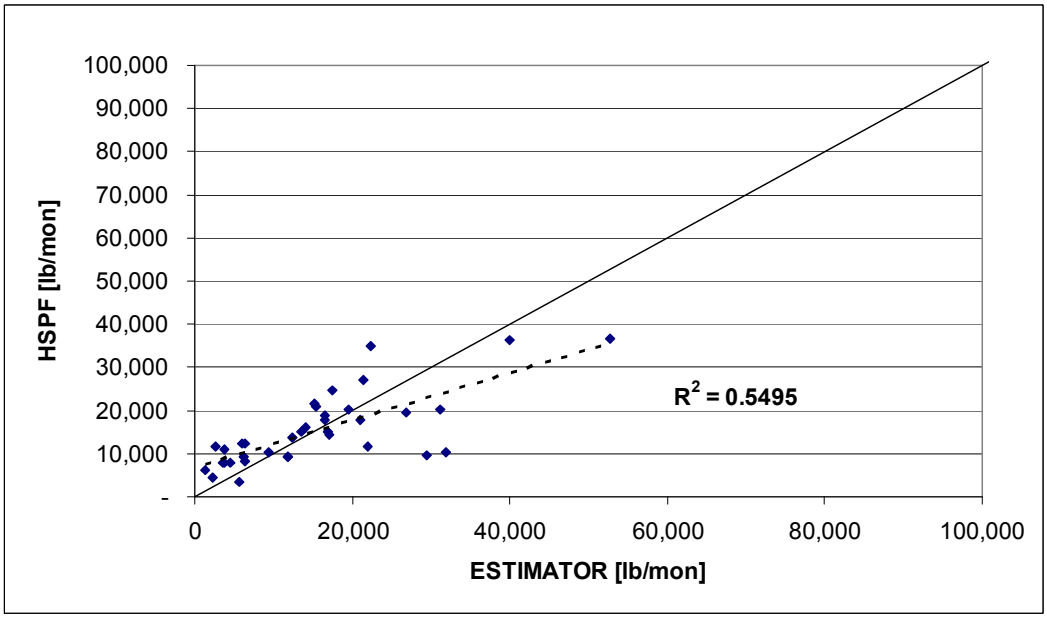

Figure A.18. Scatter Plot of Monthly ESTIMATOR and HSPF ON Loads, NEB

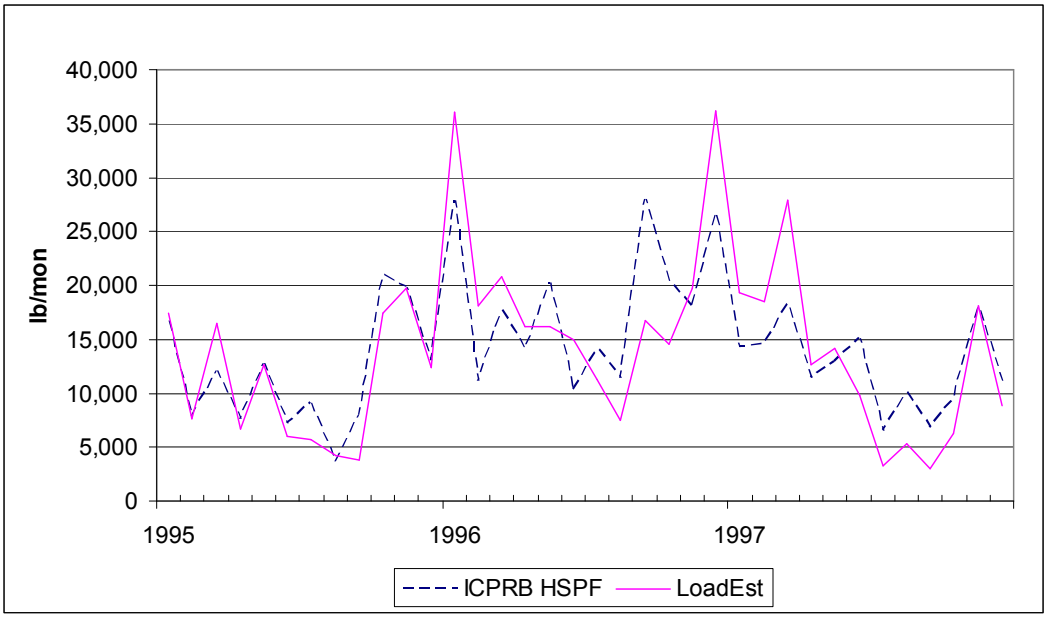

Figure A.19. Time Series of Monthly ESTIMATOR and HSPF NO3 Loads, NEB

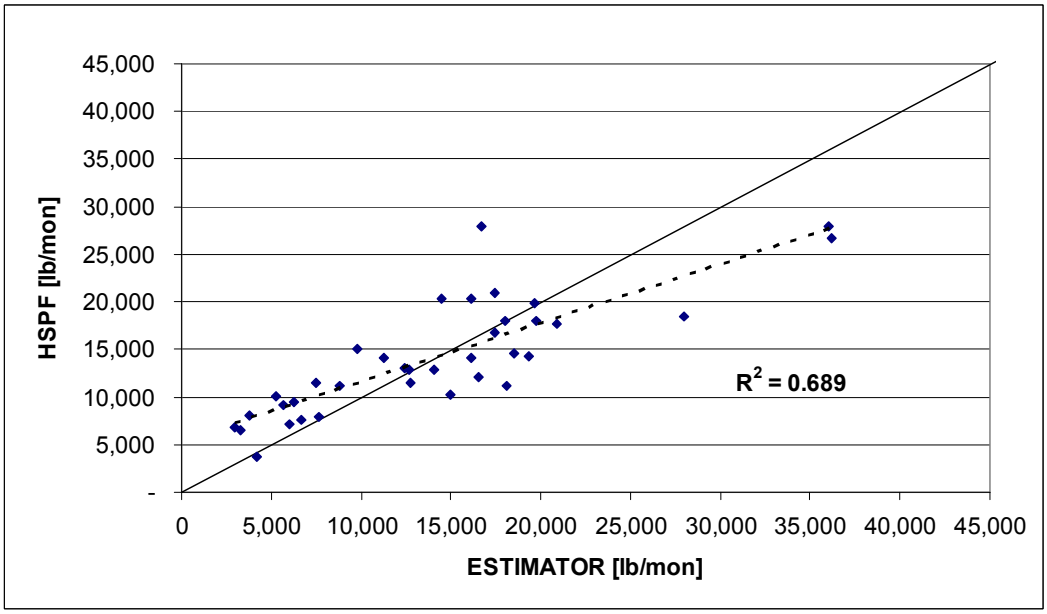

Figure A.20. Scatter Plot of Monthly ESTIMATOR and HSPF NO3 Loads, NEB

Table A.1. HSPF Model Use Acreage by Segment (acres)

Segment	Pervious Low Density Residential	Impervious Low Density Residential	Pervious Medium Density Residential	Impervious Medium Density Residential	Pervious High Density Residential	Impervious High Density Residential	Pervious Commercial	Impervious Commercial	Pervious Industrial	Impervious Industrial	Forest	Pasture	Crop	Hay	Total
10	2,009	136	2,506	552	338	245	1,541	150	0	0	2,107	541	0	0	10,123
20	1,607	192	1,430	430	133	92	852	226	0	0	889	17	0	0	5,868
30	2,535	450	14	7	188	152	494	396	22	10	417	0	0	0	4,686
40	653	106	2,018	636	747	462	1,046	648	38	58	778	45	0	0	7,233
50	1,228	56	1,258	242	13	4	241	45	0	0	1,284	362	0	0	4,732
60	102	9	1,696	391	159	115	1,102	307	407	226	596	41	0	0	5,150
70	213	14	1,793	497	315	203	851	351	45	54	1,817	644	217	262	7,059
80	169	9	242	33	237	90	922	205	3	0	5,458	1,030	504	607	9,006
90	205	7	577	113	102	36	316	122	600	1,568	1,859	272	297	358	6,135
100	200	12	2,839	894	1,211	547	2,471	1,263	115	64	2,884	151	0	0	12,651
120	39	1	970	311	559	303	901	433	341	514	895	20	0	0	5,286
130	79	3	493	128	514	175	393	116	253	223	755	53	0	0	3,184
140	0	0	259	79	39	15	117	58	109	157	316	12	0	0	1,162
150	80	2	646	335	315	115	207	99	16	7	269	28	0	0	2,119
210	1,096	44	328	27	2	1	271	52	0	0	1,086	499	0	0	3,404
270	90	5	309	101	43	22	441	29	101	77	310	30	0	0	1,558
NW	7,900	927	6,297	1,651	1,408	951	4,204	1,471	60	68	5,276	1,102	0	0	31,314
NE	2,207	112	8,714	2,271	2,081	1,016	6,345	2,322	1,270	1,990	14,210	2,530	801	164	46,353
LBC	118	4	1,722	517	1,111	492	1,410	608	704	893	1,966	85	0	0	9,631
Watts	80	2	646	335	315	115	207	99	16	7	269	28	0	0	2,119

Table A.2. Average Annual BOD Edge-of-Stream Load (lbs/acre)

SEG	Forest	Pasture	Crop	Hay	Impervious					Pervious				
					COM	IND	LDR	MDR	HDR	COM	IND	LDR	MDR	HDR
10	1	5			147	113	82	82	82	8	6	6	6	6
20	1	5			153	113	86	86	86	7	6	5	5	5
30	1	5			137	99	75	65	79	7	6	5	5	5
40	1	5			156	113	87	87	87	7	6	5	5	5
50	1	4			121	97	62	63	63	8	7	6	6	6
60	1	4			125	87	64	62	64	8	7	6	6	6
70	1	3	14	9	174	96	87	97	96	17	16	15	15	15
80	1	3	14	9	184	100	104	104	104	17	15	15	15	15
90	1	3	14	9	184	132	104	104	104	17	15	15	15	15
100	1	3			184	100	104	104	104	17	15	15	15	15
120	2				137	102	91	91	91	12	11	10	10	10
130	2				137	102	91	91	91	12	11	10	10	10
140	2				137	102	91	91	91	12	11	10	10	10
150	2				137	102	91	91	91	12	11	10	10	10
210	1	5			151	113	81	86	85	7	6	5	5	5
270	1	3			174	99	103	89	101	17	16	15	15	15

Table A.3. Average Annual TN Edge-of-Stream Load (lbs/acre)

					Impervious					Pervious				
SEG	**Forest**	**Pasture**	**Crop**	**Hay**	**COM**	**IND**	**LDR**	**MDR**	**HDR**	**COM**	**IND**	**LDR**	**MDR**	**HDR**
10	1.3	16.0			24.8	18.1	17.7	17.7	17.7	6.8	6.6	6.6	6.6	6.6
20	1.3	16.0			25.9	18.1	18.6	18.6	18.6	6.8	6.6	6.6	6.6	6.6
30	1.3	16.0			23.3	15.8	16.2	14.1	17.1	6.8	6.6	6.6	6.6	6.6
40	1.2	15.8			26.4	18.1	18.8	18.8	18.8	6.6	6.4	6.4	6.4	6.4
50	1.3	6.7			22.6	16.5	15.9	16.1	16.2	6.9	6.7	6.7	6.7	6.7
60	1.3	6.6			23.4	14.7	16.4	15.9	16.4	6.8	6.6	6.6	6.6	6.6
70	2.4	8.2	48.6	16.1	29.5	18.3	18.7	20.7	20.5	4.2	3.9	4.0	4.0	4.0
80	2.4	8.1	47.6	15.8	31.1	19.1	22.3	22.3	22.3	4.1	3.9	3.9	3.9	3.9
90	2.4	8.1	47.5	15.8	31.1	21.2	22.3	22.3	22.3	4.1	3.9	3.9	3.9	3.9
100	2.4	8.1			31.1	19.1	22.3	22.3	22.3	4.1	3.9	3.9	3.9	3.9
120	0.8				24.0	17.7	25.0	25.0	25.0	2.8	2.7	2.9	2.9	2.9
130	0.8				24.0	17.7	25.0	25.0	25.0	2.8	2.7	2.9	2.9	2.9
140	0.9				24.0	17.7	25.0	25.0	25.0	2.6	2.7	3.2	2.9	2.9
150	0.8				24.0	17.7	25.0	25.0	25.0	2.8	2.7	2.9	2.9	2.9
210	1.2	15.9			25.6	18.1	17.5	18.6	18.4	6.8	6.6	6.6	6.6	6.6
270	2.5	8.2			29.5	18.9	22.0	19.1	21.6	4.2	3.9	4.0	4.0	4.0

Table A.4. Average Annual Edge-of-Stream TP Load (lbs/acre)

						Impervious					Pervious				
SEG	**Forest**	**Pasture**	**Crop**	**Hay**	**Scour**	**COM**	**IND**	**LDR**	**MDR**	**HDR**	**COM**	**IND**	**LDR**	**MDR**	**HDR**
10	0.05	0.27			2,131	2.96	1.67	2.29	2.31	2.29	0.35	0.35	0.37	0.37	0.37
20	0.05	0.25			896	3.11	1.67	2.46	2.48	2.48	0.35	0.35	0.37	0.37	0.37
30	0.05	0.26			99	2.71	1.40	2.01	1.61	2.19	0.35	0.35	0.37	0.37	0.37
40	0.04	0.25			4,937	3.20	1.66	2.48	2.50	2.50	0.34	0.34	0.36	0.36	0.36
50	0.06	0.26			602	1.31	1.49	2.09	2.14	2.13	0.43	0.43	0.45	0.45	0.45
60	0.06	0.26			1,953	1.35	1.29	2.20	2.10	2.17	0.36	0.36	0.38	0.38	0.38
70	0.06	0.78	1.07	0.60	385	1.88	1.54	2.28	2.71	2.63	0.43	0.47	0.49	0.49	0.49
80	0.06	0.77	1.04	0.59	95	1.98	1.62	2.95	2.95	2.95	0.42	0.42	0.45	0.45	0.45
90	0.06	0.77	1.06	0.61	161	1.98	1.96	2.95	2.95	2.95	0.42	0.42	0.45	0.45	0.45
100	0.06	0.97			2,932	1.98	1.62	2.95	2.95	2.95	0.42	0.42	0.45	0.45	0.45
120	0.06				137	1.91	1.76	3.94	3.94	3.94	0.27	0.27	0.34	0.34	0.34
130	0.05				56	1.91	1.76	3.94	3.94	3.94	0.27	0.27	0.34	0.34	0.34
140	0.05				174	1.91	1.76	3.94	3.94	3.94	0.26	0.25	0.24	0.24	0.24
150	0.06				39	1.91	1.76	3.94	3.94	3.94	0.27	0.27	0.34	0.34	0.34
210	0.05	0.16			111	3.07	1.67	2.25	2.48	2.41	0.35	0.35	0.37	0.37	0.37
270	0.07	0.76			22	1.88	1.60	2.92	2.37	2.83	0.43	0.43	0.46	0.46	0.46

APPENDIX B

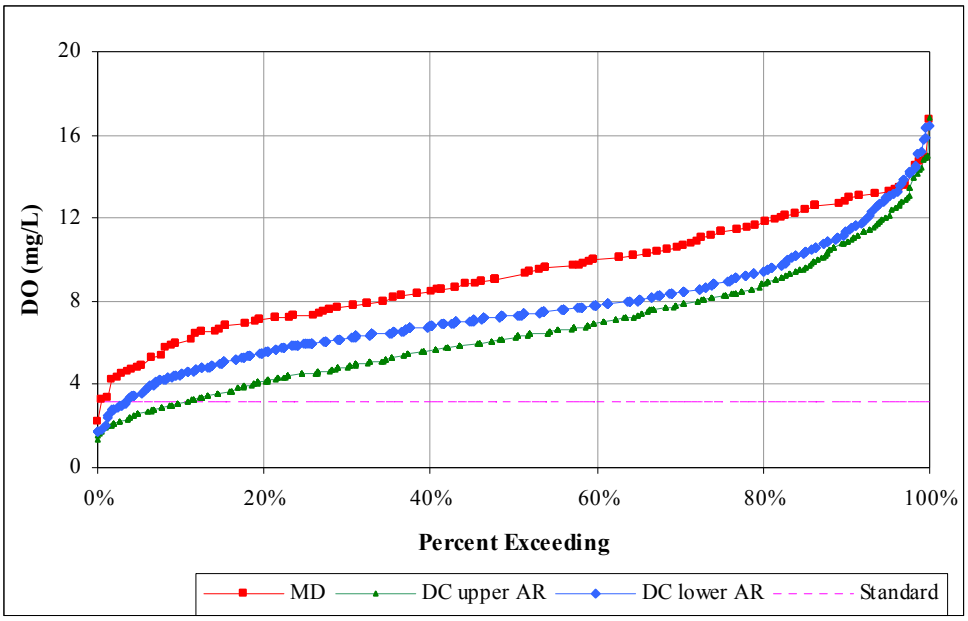

Figure B.1. Cumulative Distribution of DO Concentrations, February – May, Tidal Anacostia River

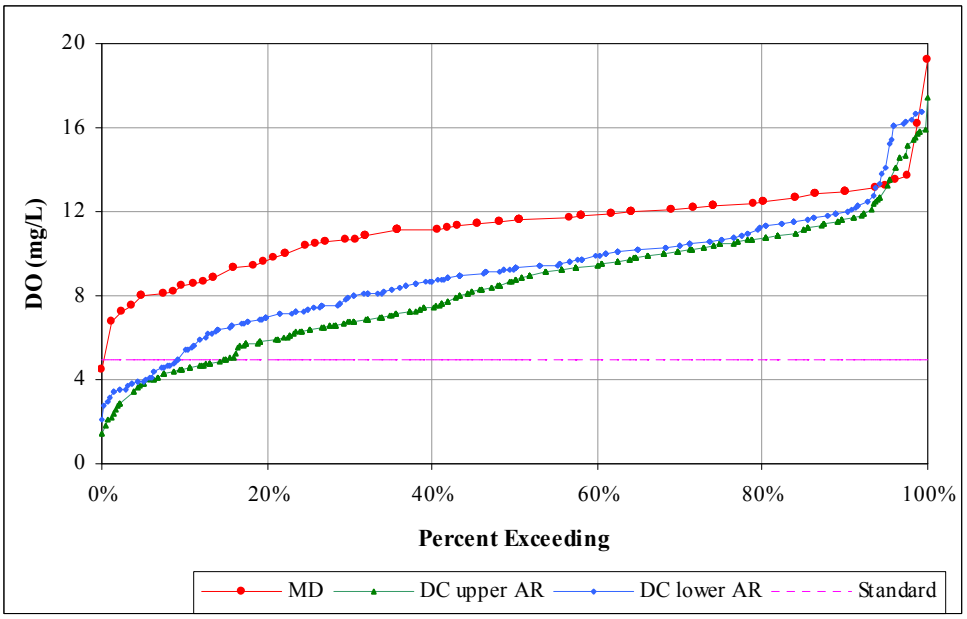

Figure B.2. Cumulative Distribution of DO Concentrations, June – January, Tidal Anacostia River

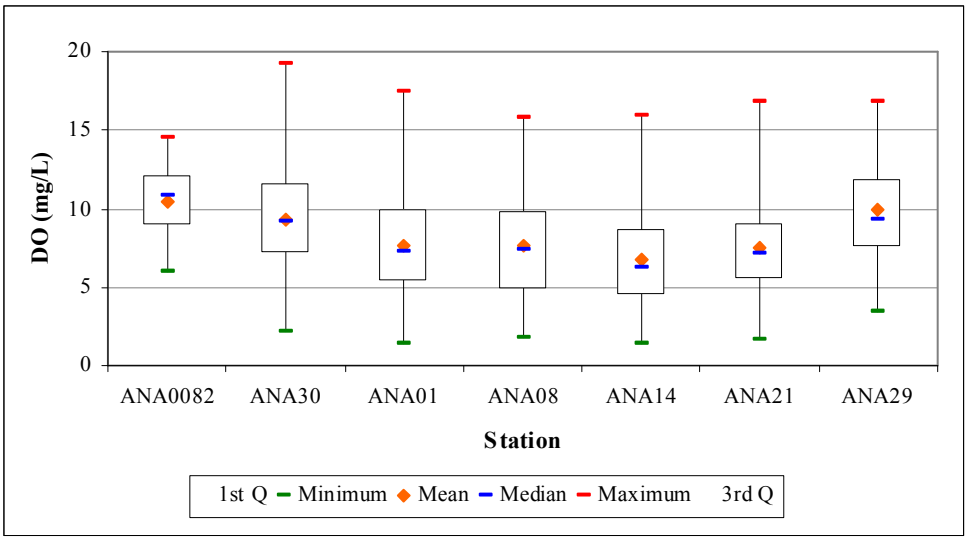

Figure B.3. Distribution of DO Concentrations by Station, Tidal Anacostia River

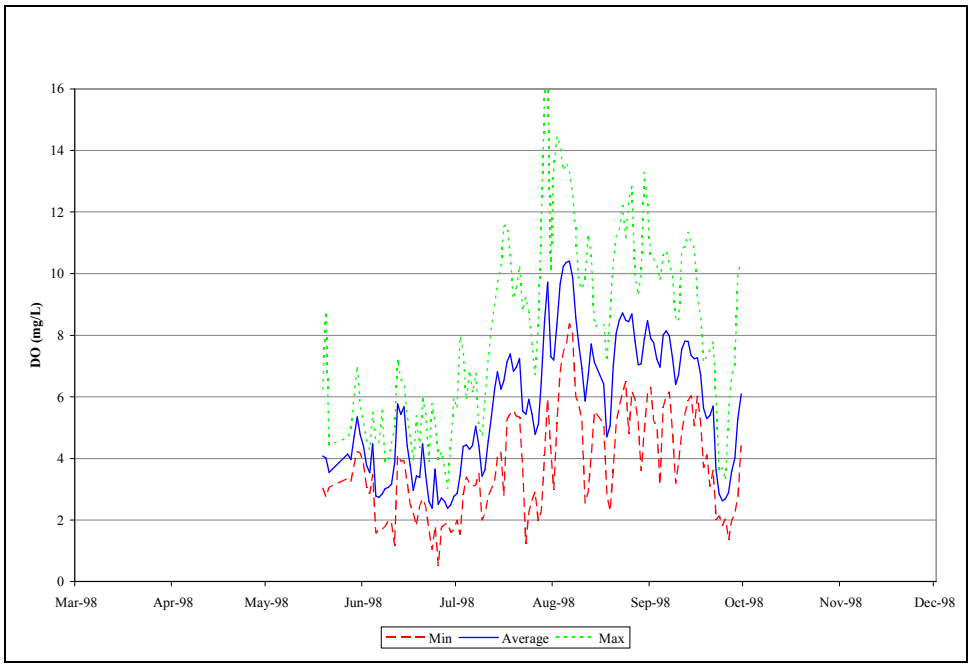

Figure B.4. Observed Daily Minimum, Average, and Maximum DO Concentrations, Station PO4 at Benning Road Bridge, 1998

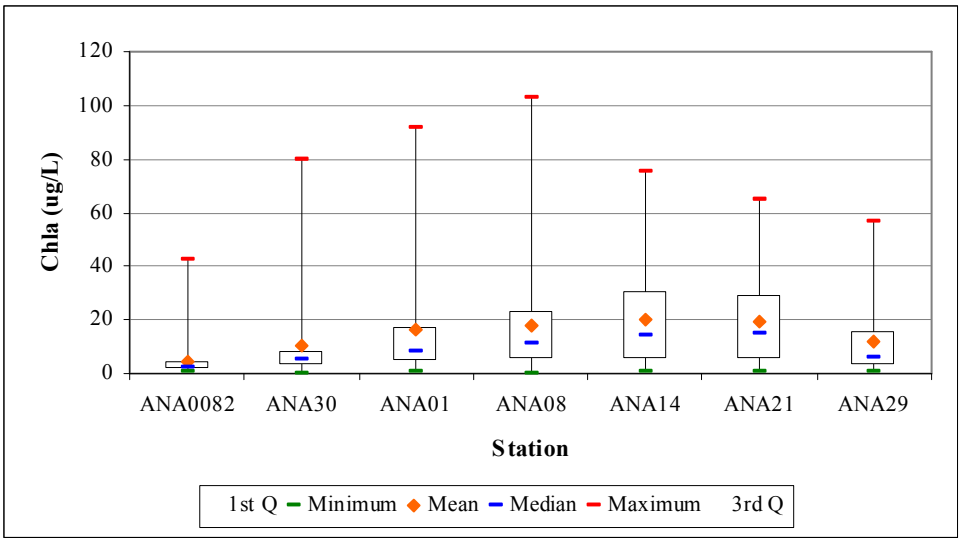

Figure B.5. Annual Distribution of Chla Concentrations by Station, Tidal Anacostia River

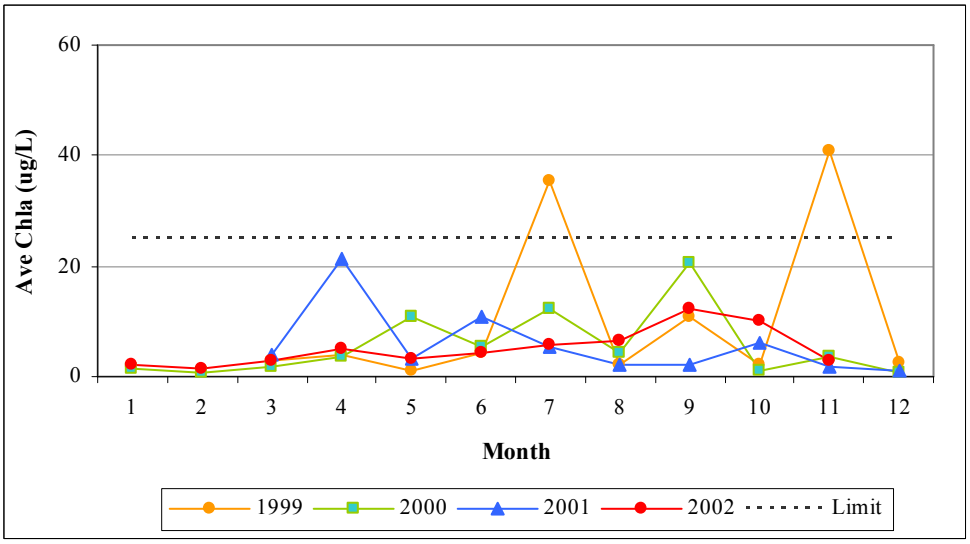

Figure B.6. Monthly Average Chla Concentrations in MD Portion of Tidal Anacostia River

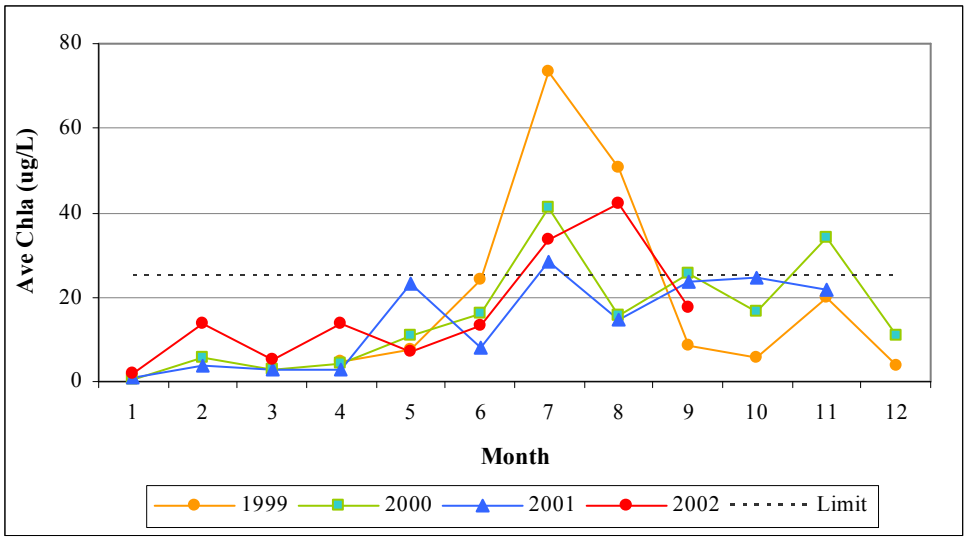

Figure B.7. Monthly Average Chla Concentrations in DC Upper Tidal Anacostia River

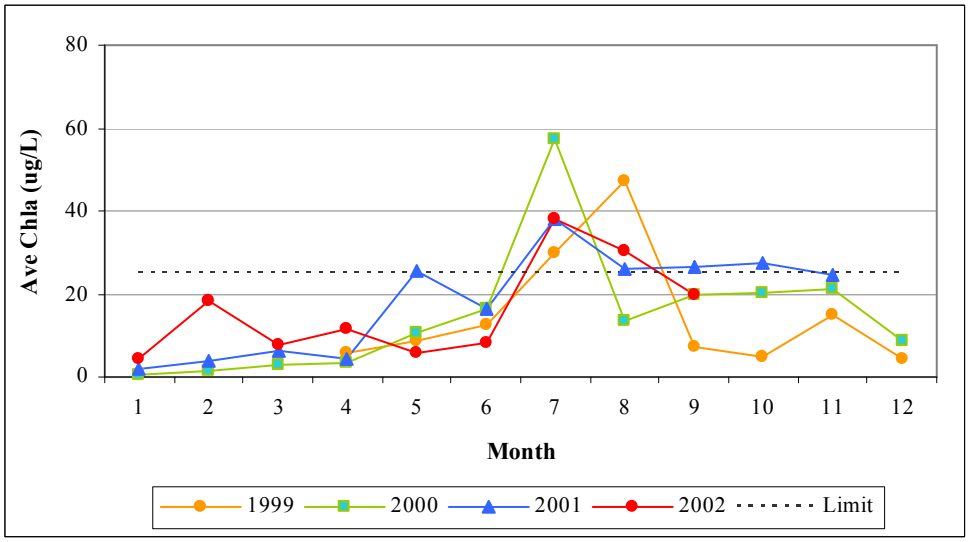

Figure B.8. Monthly Average Chla Concentrations in DC Lower Tidal Anacostia River

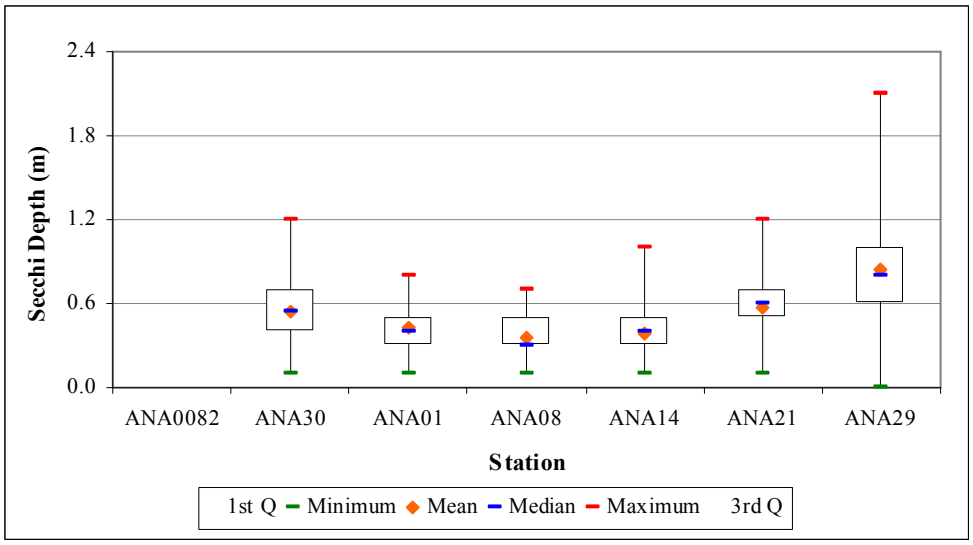

Figure B.9. Distribution of Growing Season Secchi Depths by Station, Tidal Anacostia River

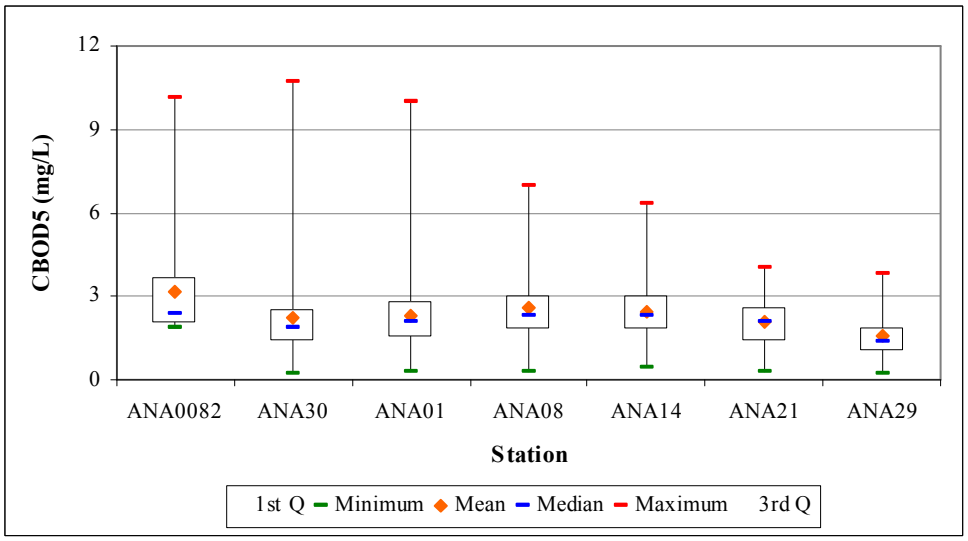

Figure B.10. Distribution of BOD5 Concentrations By Station, Tidal Anacostia River

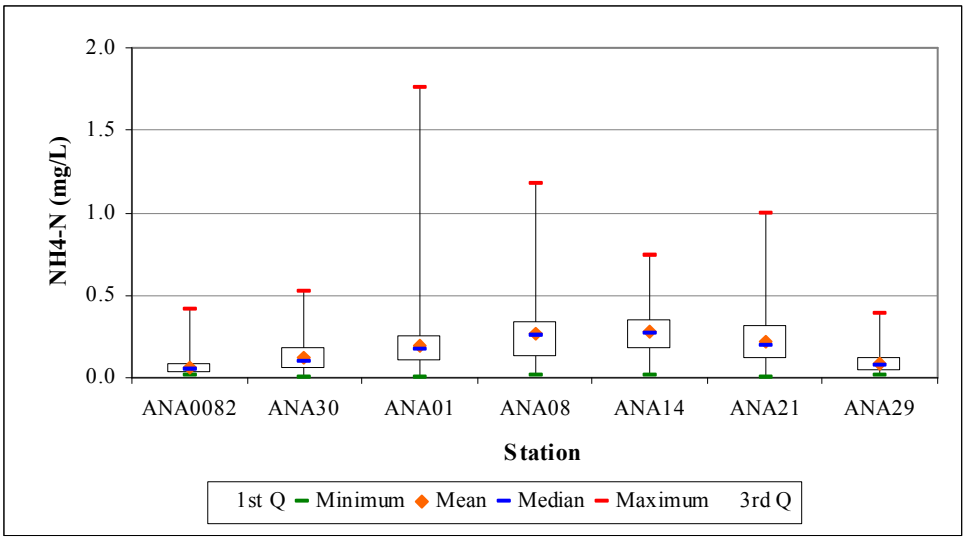

Figure B.11. Distribution of NH4-N Concentrations By Station, Tidal Anacostia River

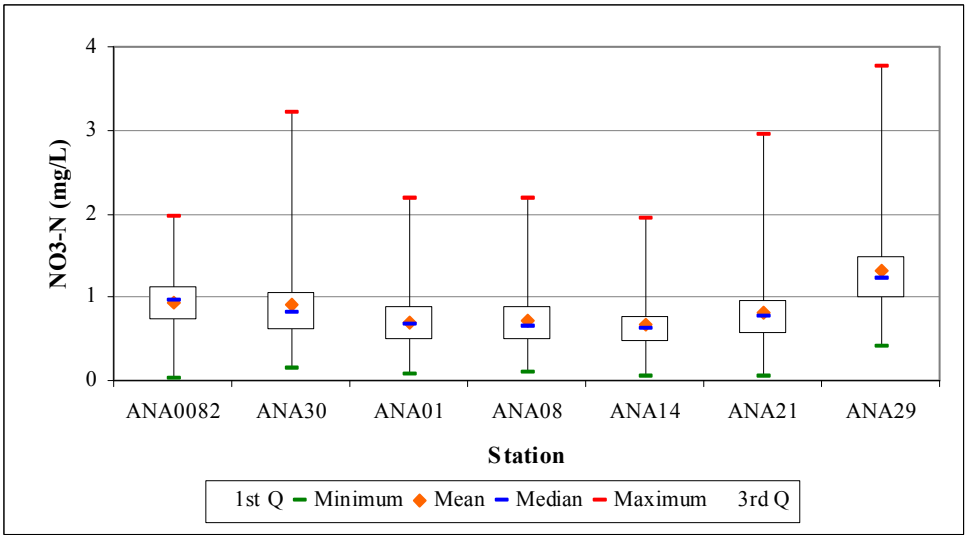

Figure B.12. Distribution of NO3-N Concentrations By Station, Tidal Anacostia River

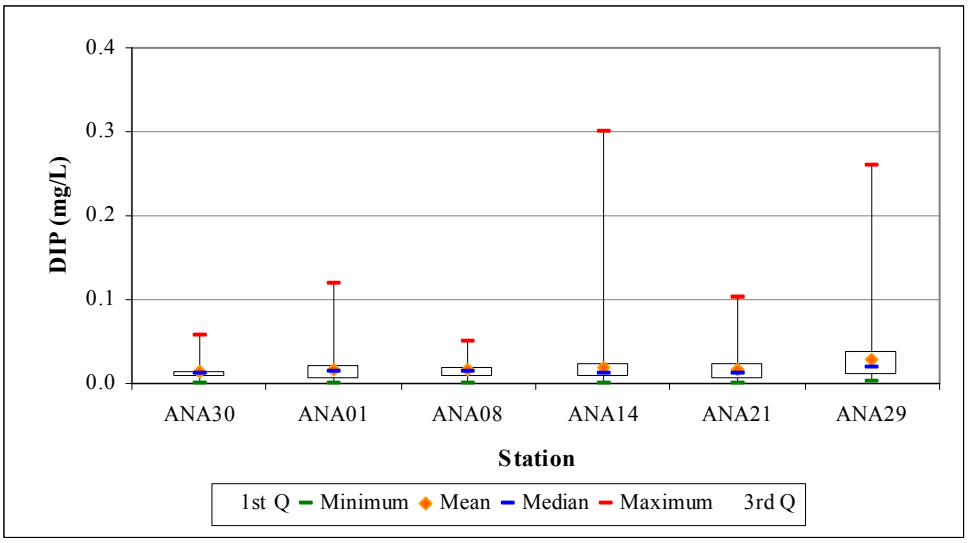

Figure B.13. Distribution of DIP Concentrations By Station, Tidal Anacostia River

APPENDIX C

Table C.1. Global Calibration Parameters

Parameter	Description	Value	Units
K122C	Nitrification rate	0.16	/d
K12T	Nitrification temperature coefficient	1.05	
KNIT	Nitrification half-saturation constant	1.00	
K20C	Denitrification rate	0.15	/d
K20T	Denitrification temperature coefficient	1.07	
KNO3	Denitrification half-saturation constant	0.2	
KF20	Sediment denitrification rate	0.15	
NFT	Sediment denitrification temperature coefficient	1.08	
K1C	Algal base growth rate	2.475	/d
K1T	Growth temperature coefficient	1.15	
PHIMX	Maximum quantum yield	720	mg C/mole
XKC	Chla extinction coefficient	0.017	$(mg/m^3)^{-1}/m$
KMNG1	N Chla half-saturation constant	0.125	
KMPG1	P Chla half-saturation constant	0.008	
KIRC	Phytoplankton respiration rate	0.12	/d
KIRT	Respiration temperature coefficient	1.045	
K1D	Phytoplankton death rate	0.02	/d
PCRB	Phytoplankton P:C ratio	0.025	
NCRB	Phytoplankton N:C ratio	0.125	
KDT	Temperature coefficient	1.04	
KDST	Sediment deoxygenation temperature coefficient	1.30	
GFRAC	Methane gas oxidation fraction	0.985	
KD	Methane diffusion mass transfer coefficient	0.003	m/d
KC20	Methane oxidation reaction velocity	2.00	m/d
KN20	Ammonia oxidation reaction velocity	0.16	m/d
KCT	Methane oxidation temperature coefficient	1.4	
KNT	Ammonia oxidation temperature coefficient	1.08	
CLE1	Light extinction color constant	0.5	m^{-1}
CLE2	Light extinction non-algal solids coefficient	0.13	$(m*mg/l)^{-1}$
OCRB	Phytoplankton O:C ratio	2.67	
K71C	N mineralization rate	0.08	/d
K71T	N mineral. temperature coefficient	1.05	
KONDC	Sediment N mineralization rate	0.02	/d
KONDT	Sediment N mineralization temperature coefficient	1.08	
K83C	P mineralization rate	0.08	/d
KOPDC	P mineral. temperature coefficient	1.05	
FON	ON Phytoplankton fraction	0.5	
FOP	OP Phytoplankton fraction	0.5	
	Inorganic P settling rate	0.01	m/d

Table C.2. Spatially Varying Calibration Parameters

Segment	Water Column BOD Decay Rate, /day	Sediment BOD Decay Rate, /day	Average Winter BOD* Settling Rate, m/d	Average Summer BOD* Settling Rate, m/d	BOD Dissolved Fraction	PO4 Dissolved Fraction	ON/OP Dissolved Fraction
1	0.1	0.005	0.0	0.0	1.0	0.5	0.9
2	0.01	0.007	3.56	0.25	0.65	0.5	0.9
3	0.01	0.007	3.56	0.25	0.65	0.5	0.9
4	0.01	0.007	3.56	0.25	0.65	0.5	0.9
5	0.01	0.007	3.56	0.25	0.65	0.5	0.9
6	0.01	0.007	3.56	0.25	0.65	0.5	0.9
7	0.05	0.005	1.72	1.06	0.85	0.5	0.9
8	0.05	0.005	1.72	1.06	0.85	0.5	0.9
9	0.05	0.005	1.72	1.06	0.85	0.5	0.9
10	0.05	0.005	1.72	1.06	0.85	0.5	0.9
11	0.05	0.005	1.72	1.06	0.85	0.5	0.9
12	0.05	0.005	1.72	1.06	0.85	0.5	0.9
13	0.05	0.005	4.28	3.31	0.85	0.5	0.85
14	0.05	0.005	4.28	3.31	0.85	0.5	0.85
15	0.05	0.005	4.28	3.31	0.85	0.5	0.85
16	0.05	0.005	4.28	3.31	0.85	0.5	0.85
17	0.05	0.005	4.28	3.31	0.85	0.5	0.85
18	0.05	0.005	4.28	3.31	0.85	0.5	0.85
19	0.05	0.005	4.28	3.31	0.85	0.5	0.85
20	0.05	0.005	4.28	3.31	0.85	0.5	0.85
21	0.05	0.005	4.28	3.31	0.85	0.5	0.85
22	0.05	0.005	4.28	3.31	0.85	0.5	0.85
23	0.05	0.005	1.84	0.81	0.85	0.5	0.85
24	0.05	0.005	1.84	0.81	0.85	0.5	0.85
25	0.05	0.005	1.84	0.81	0.85	0.5	0.8
26	0.05	0.005	1.84	0.81	0.85	0.2	0.8
27	0.05	0.005	1.84	0.81	0.85	0.2	0.8
28	0.05	0.005	1.84	0.81	0.85	0.2	0.8
29	0.05	0.005	1.84	0.81	0.85	0.2	0.8
30	0.05	0.005	1.84	0.81	0.85	0.2	0.8
31	0.001	0.001	6.0	6.0	0.85	0.1	0.8
32	0.001	0.001	6.0	6.0	0.85	0.1	0.8
33	0.001	0.001	6.0	6.0	0.85	0.1	0.8
34	0.001	0.001	6.0	6.0	0.85	0.1	0.8
35	0.001	0.001	6.0	6.0	0.85	0.1	0.8
36	0.05	0.005	6.0	6.0	0.85	0.2	0.8

* Identical settling rates applied for ON and OP.

Table C.3. Calibration Summary Statistics

Statistic	DO		BOD		CHLA		SECCHI		NH3		NO3		DIP	
	SIM	OBS	SIM	OBS	SIM	OBS	SIM	OBS	SIM	OBS	SIM	OBS	SIM	OBS
ANA0082														
Min	3.73	6.00	0.10	1.90	0.00	0.00	0.00		0.01	0.01	0.00	0.02		
Median	10.30	10.75	1.84	2.30	0.01	2.39	0.79		0.10	0.04	0.81	0.87		
Max	14.90	14.50	12.40	10.10	80.00	41.12	1.26		0.50	0.42	1.25	1.97		
Ave.	10.33	10.49	2.21	3.16	7.45	3.88	0.79		0.10	0.07	0.73	0.91		
S.D.	2.29	2.08	1.78	1.76	16.75	5.38	0.38		0.04	0.07	0.34	0.37		
ANA30														
Min	0.93	2.20	0.08	0.20	0.00	0.27	0.00	0.00	0.01	0.00	0.00	0.15	0.00	0.00
Median	10.00	8.61	1.84	1.90	0.02	4.90	0.78	0.60	0.11	0.11	0.79	0.76	0.02	0.01
Max	14.60	16.70	11.30	7.10	84.00	80.00	1.26	1.80	0.50	0.52	1.24	3.20	0.50	0.06
Ave.	10.01	8.81	2.18	2.06	8.19	10.51	0.77	0.66	0.12	0.14	0.70	0.87	0.03	0.01
S.D.	2.64	2.94	1.75	1.23	18.01	17.52	0.38	0.35	0.05	0.11	0.34	0.52	0.03	0.01
ANA01														
Min	0.26	1.40	0.08	0.00	0.00	0.67	0.00	0.10	0.02	0.00	0.00	0.06	0.00	0.00
Median	9.67	6.90	1.96	2.00	0.19	8.55	0.56	0.40	0.16	0.20	0.70	0.61	0.02	0.01
Max	16.50	17.40	12.20	10.00	95.70	92.00	1.26	1.80	0.57	1.76	1.41	2.17	0.50	0.12
Ave	9.53	7.19	2.46	2.23	10.07	16.27	0.55	0.46	0.18	0.22	0.63	0.68	0.03	0.02
S.D.	2.92	2.88	2.05	1.37	20.27	20.08	0.31	0.21	0.08	0.19	0.31	0.37	0.04	0.02
ANA08														
Min	0.78	1.73	0.07	0.30	0.00	0.27	0.00	0.00	0.04	0.01	0.00	0.09	0.00	0.00
Median	9.37	6.98	1.86	2.35	1.01	11.05	0.39	0.40	0.23	0.27	0.68	0.62	0.02	0.01
Max	17.80	15.50	14.00	7.00	106.00	103.00	1.24	0.70	0.73	1.18	1.53	2.18	0.50	0.05
Ave	9.10	7.01	2.38	2.55	12.31	17.71	0.38	0.37	0.26	0.30	0.62	0.72	0.03	0.02
S.D.	3.20	3.02	2.05	1.29	21.40	20.42	0.20	0.15	0.11	0.19	0.29	0.43	0.04	0.01
ANA14														
Min	0.16	1.37	0.10	0.00	0.00	1.00	0.01	0.00	0.09	0.01	0.00	0.04	0.00	0.00
Median	9.01	6.40	1.77	2.30	2.34	14.00	0.44	0.40	0.25	0.28	0.74	0.60	0.02	0.01
Max	15.90	15.90	12.80	6.30	116.00	75.00	1.23	1.00	0.78	0.74	2.00	1.95	0.50	0.30
Ave.	8.72	6.46	2.26	2.37	13.56	20.24	0.43	0.39	0.28	0.29	0.71	0.65	0.03	0.02
S.D.	3.38	2.72	1.96	1.09	20.70	18.97	0.22	0.15	0.11	0.15	0.29	0.35	0.03	0.03
ANA21														
Min	0.11	2.12	0.32	0.00	0.00	0.40	0.01	0.00	0.10	0.00	0.17	0.05	0.01	0.00
Median	8.62	7.00	1.78	2.05	5.35	14.65	0.68	0.60	0.24	0.22	0.90	0.70	0.02	0.01
Max	15.10	16.20	12.50	4.00	87.90	65.00	1.26	1.20	0.69	1.00	2.83	2.95	0.50	0.10
Ave.	8.49	7.14	2.19	2.01	13.18	19.32	0.65	0.57	0.25	0.23	0.98	0.80	0.03	0.02
S.D.	3.19	2.50	1.55	0.88	15.69	16.51	0.30	0.22	0.08	0.16	0.41	0.40	0.03	0.02

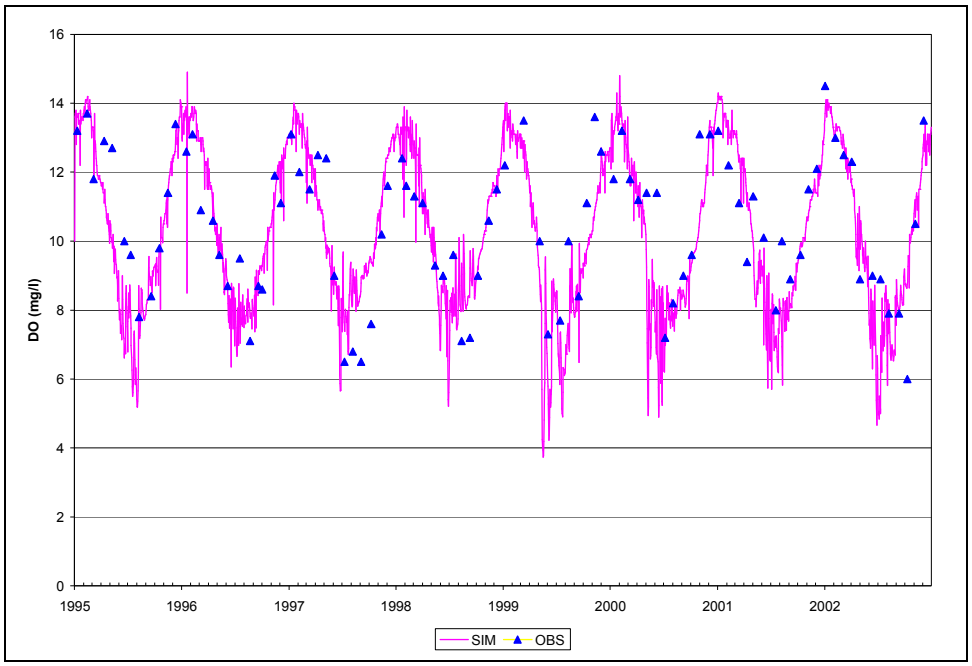

Figure C.1. Time Series of Observed and Simulated DO, Calibration Scenario, ANA0082

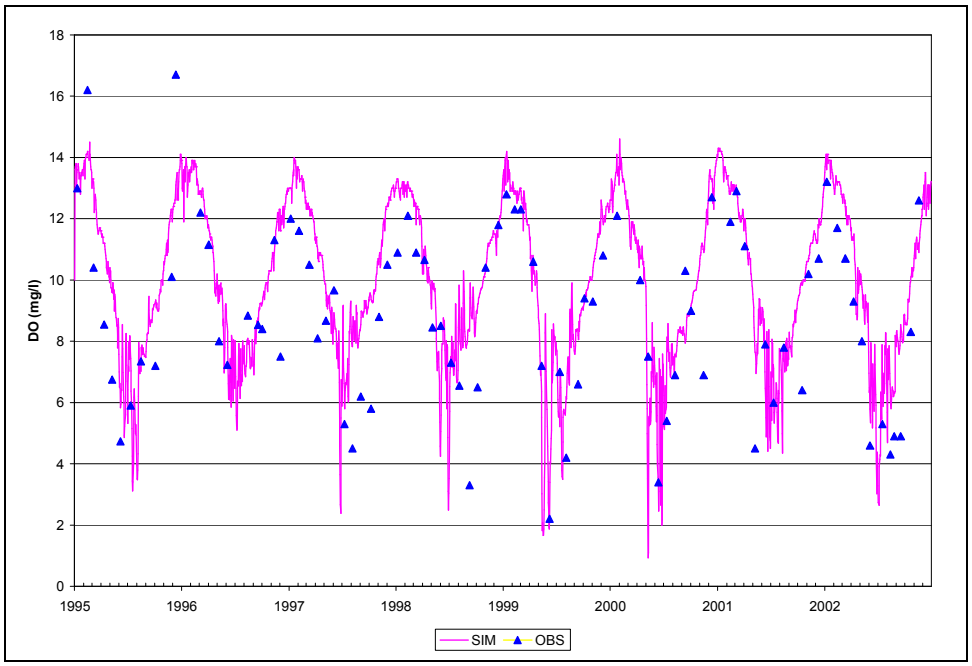

Figure C.2. Time Series of Observed and Simulated DO, Calibration Scenario, ANA30

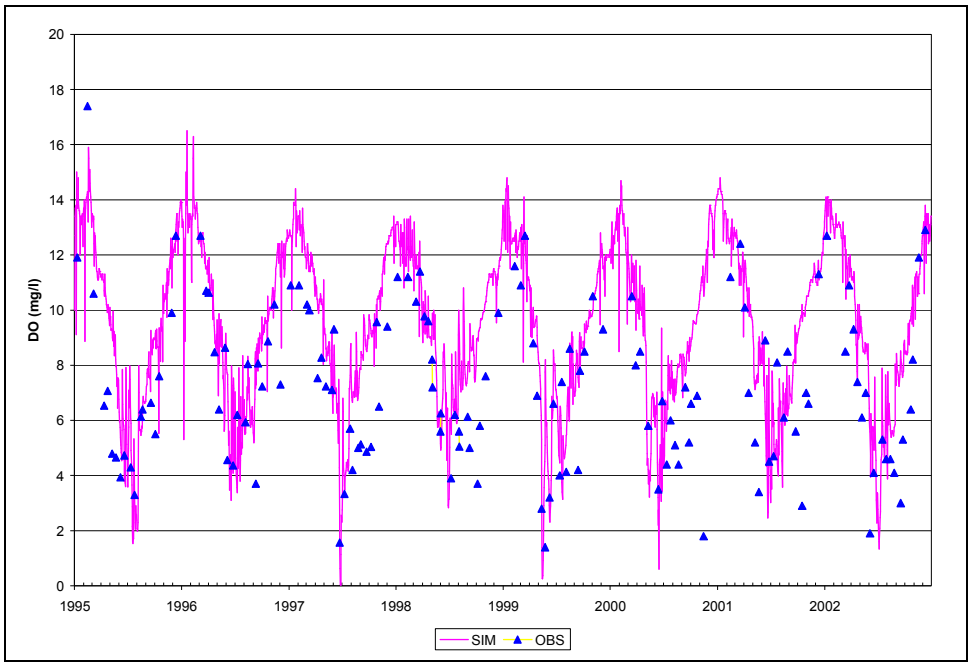

Figure C.3. Time Series of Observed and Simulated DO, Calibration Scenario, ANA01

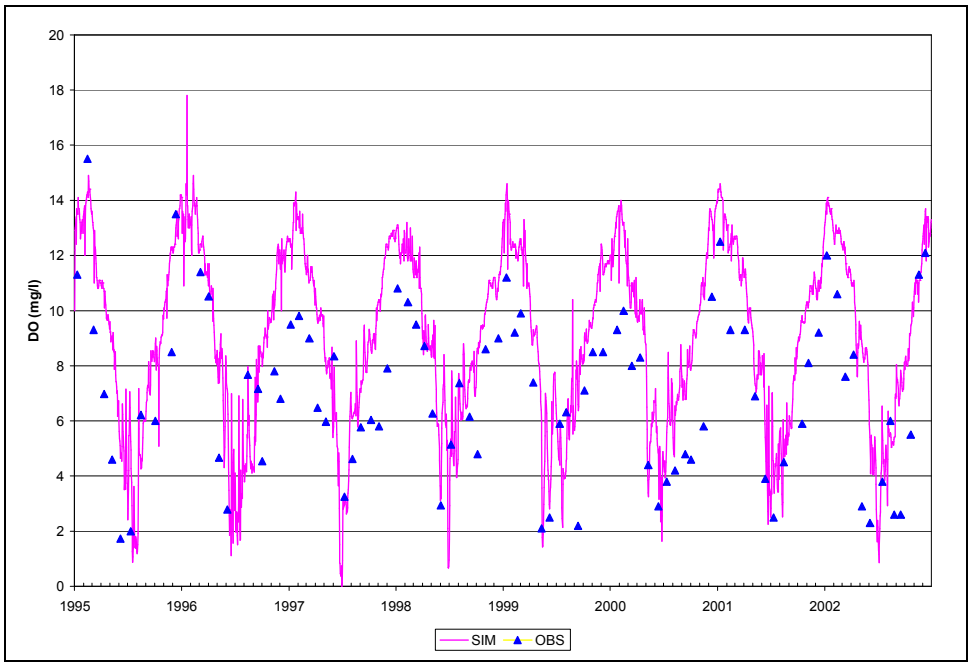

Figure C.4. Time Series of Observed and Simulated DO, Calibration Scenario, ANA08

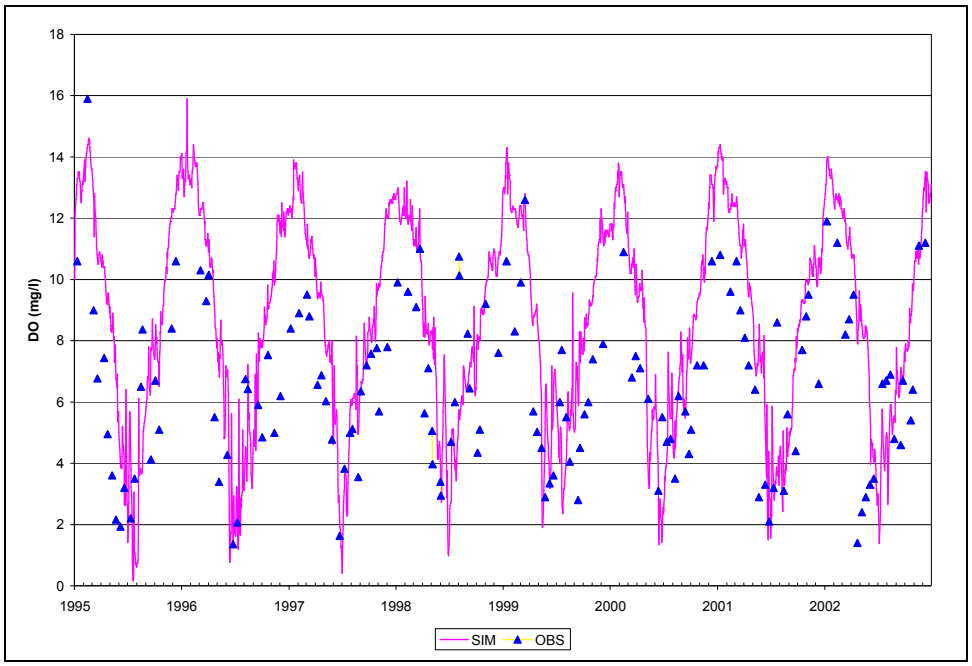

Figure C.5. Time Series of Observed and Simulated DO, Calibration Scenario, ANA14

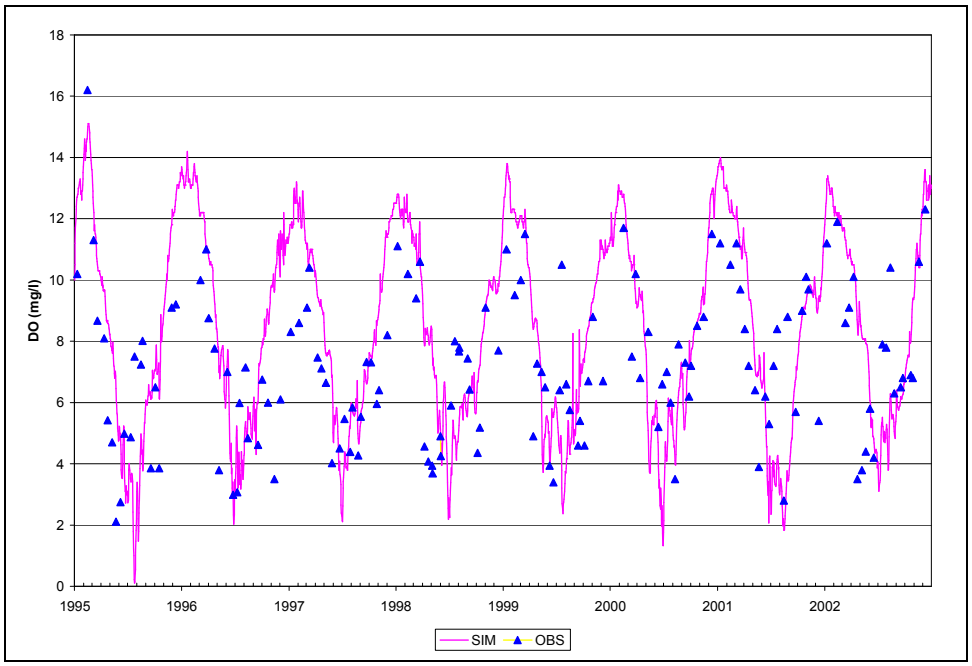

Figure C.6. Time Series of Observed and Simulated DO, Calibration Scenario, ANA21

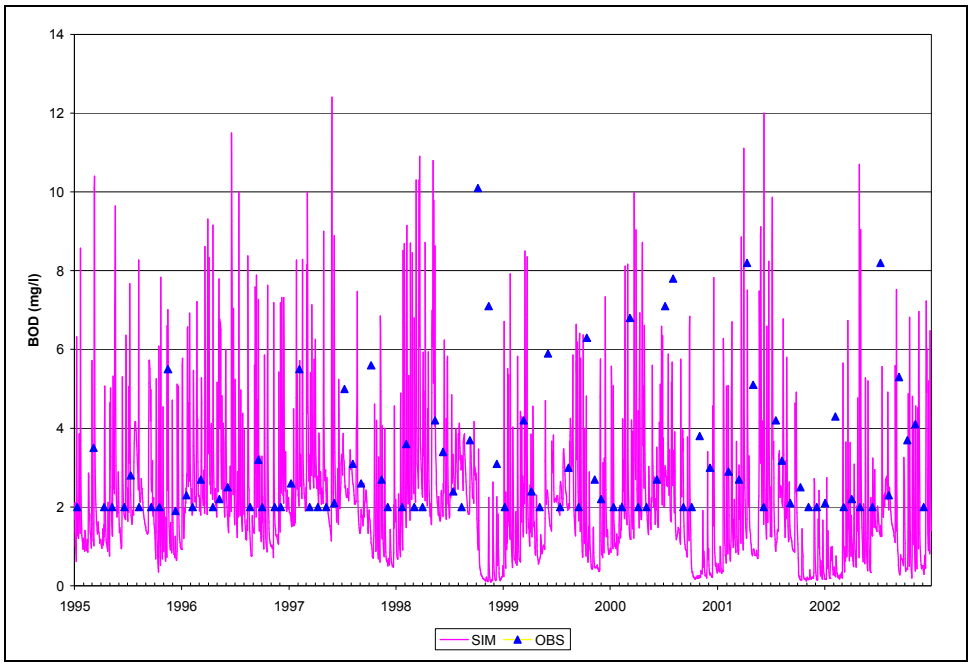

Figure C.7. Time Series of Observed and Simulated BOD, Calibration Scenario, ANA0082

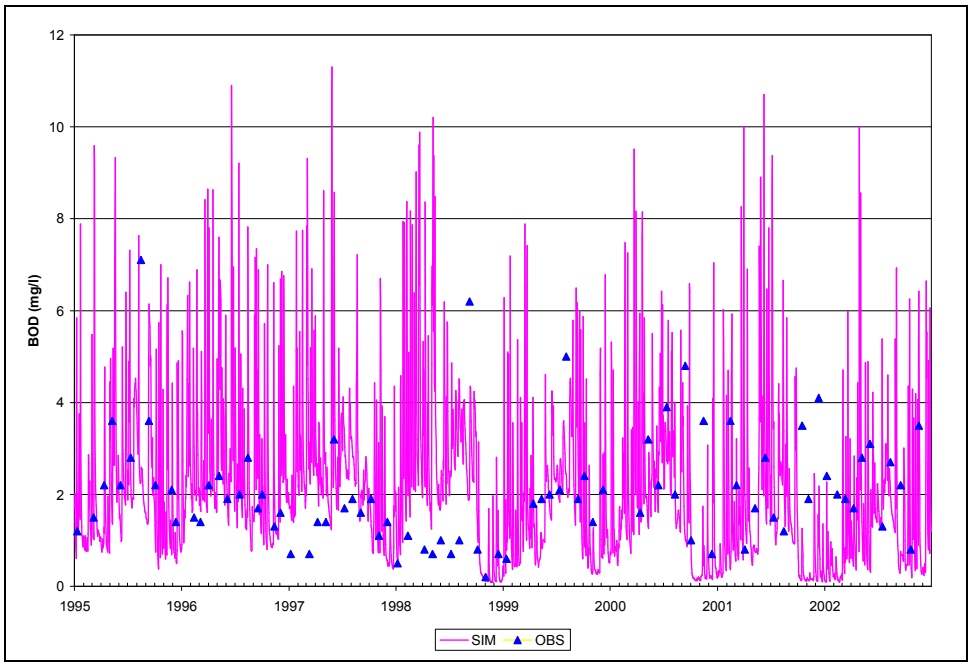

Figure C.8. Time Series of Observed and Simulated BOD, Calibration Scenario, ANA30

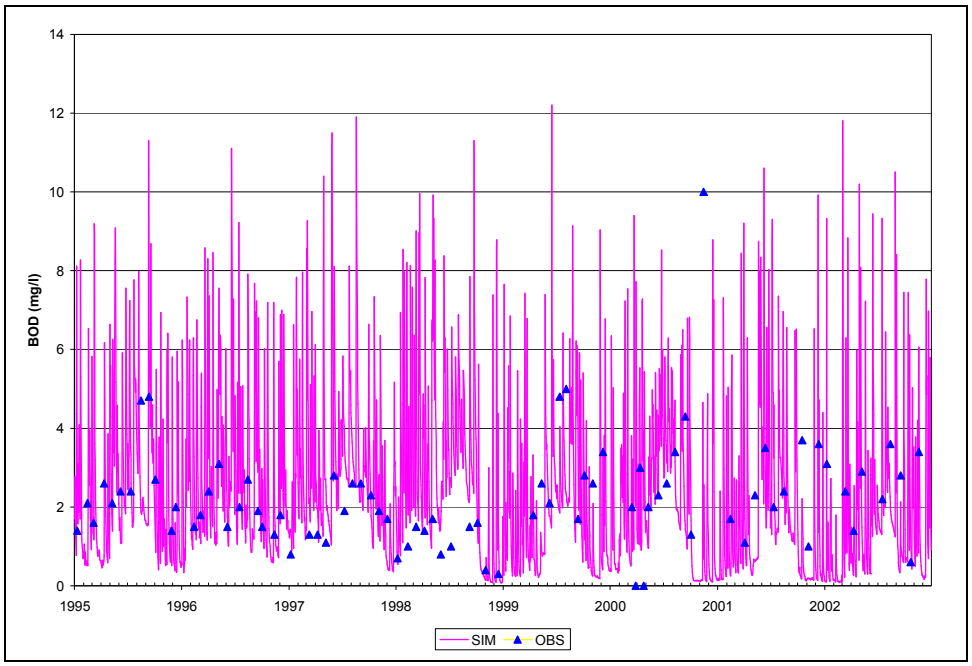

Figure C.9. Time Series of Observed and Simulated BOD, Calibration Scenario, ANA01

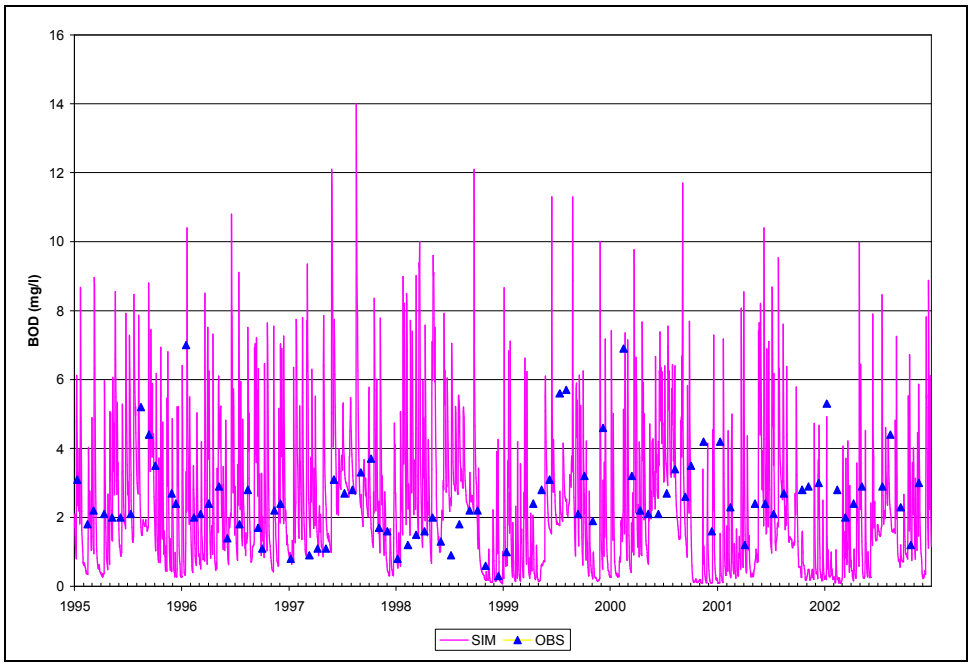

Figure C.10. Time Series of Observed and Simulated BOD, Calibration Scenario, ANA08

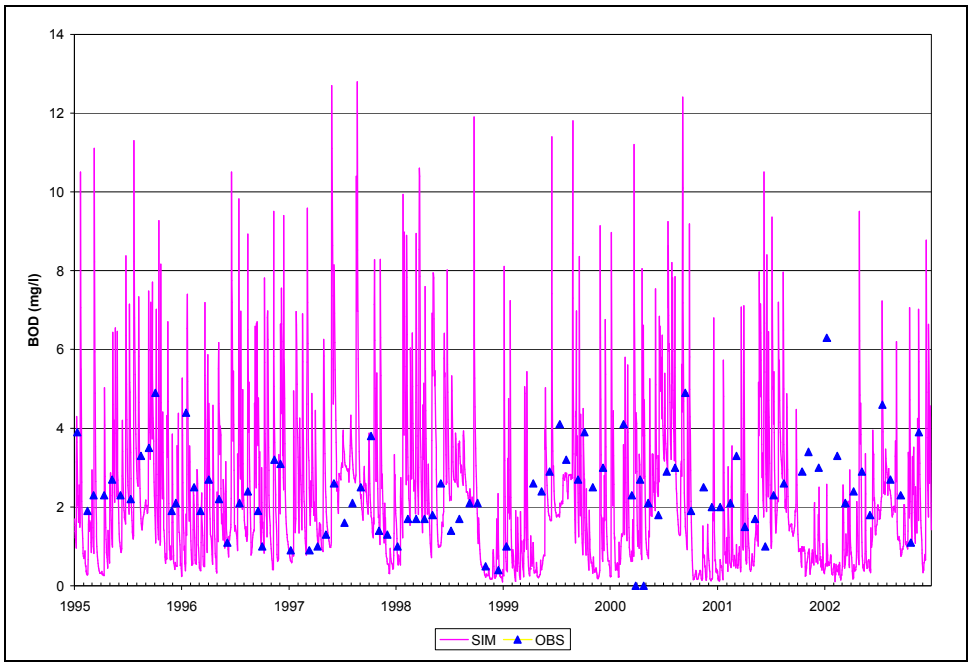

Figure C.11. Time Series of Observed and Simulated BOD, Calibration Scenario, ANA14

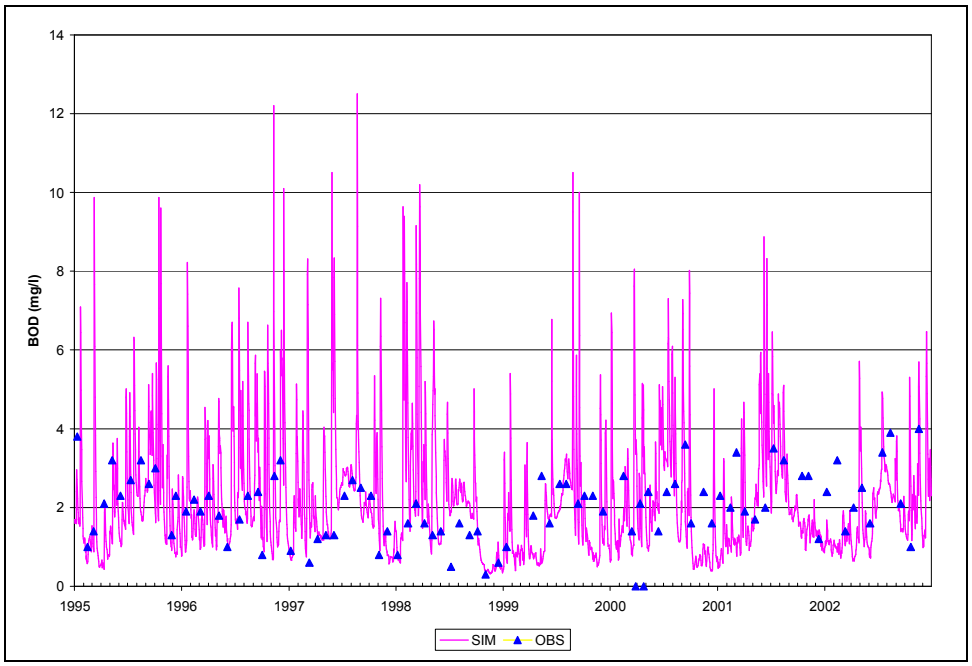

Figure C.12. Time Series of Observed and Simulated BOD, Calibration Scenario, ANA21

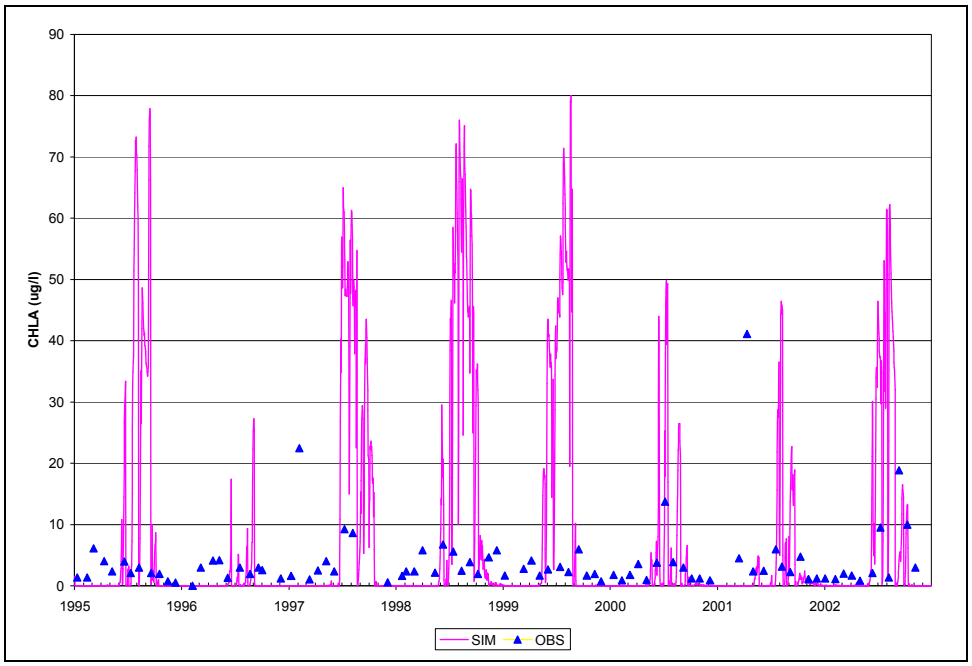

Figure C.13. Time Series of Observed and Simulated CHLA, Calibration Scenario, ANA0082

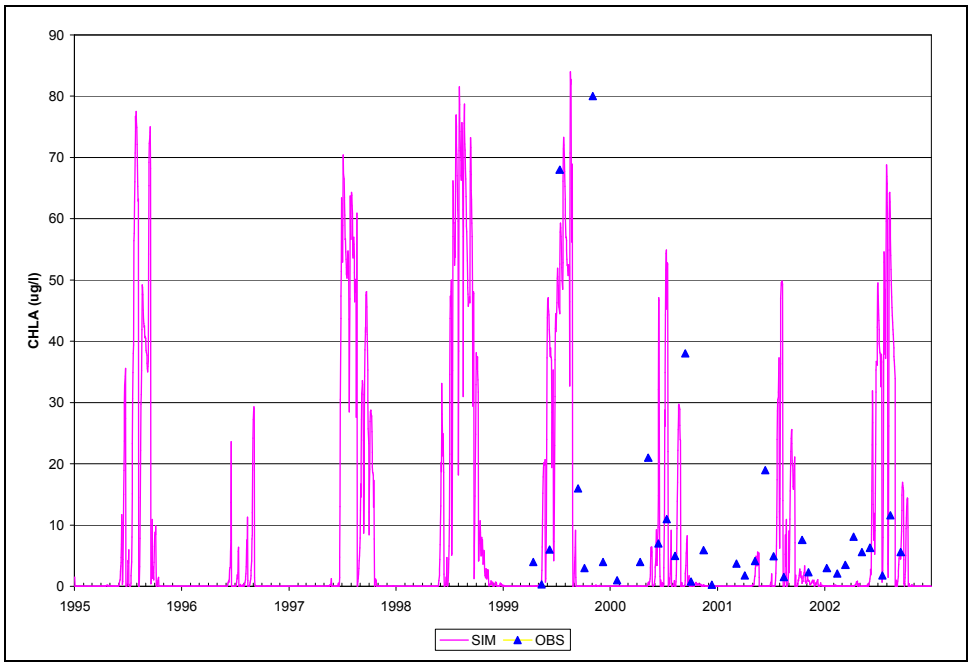

Figure C.14. Time Series of Observed and Simulated CHLA, Calibration Scenario, ANA30

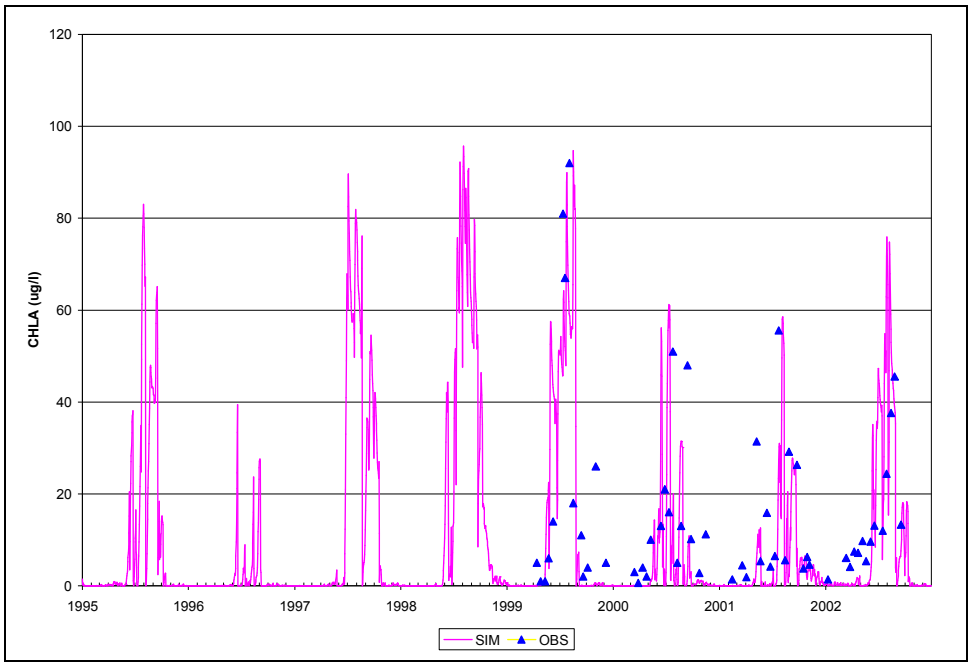

Figure C.15. Time Series of Observed and Simulated CHLA, Calibration Scenario, ANA01

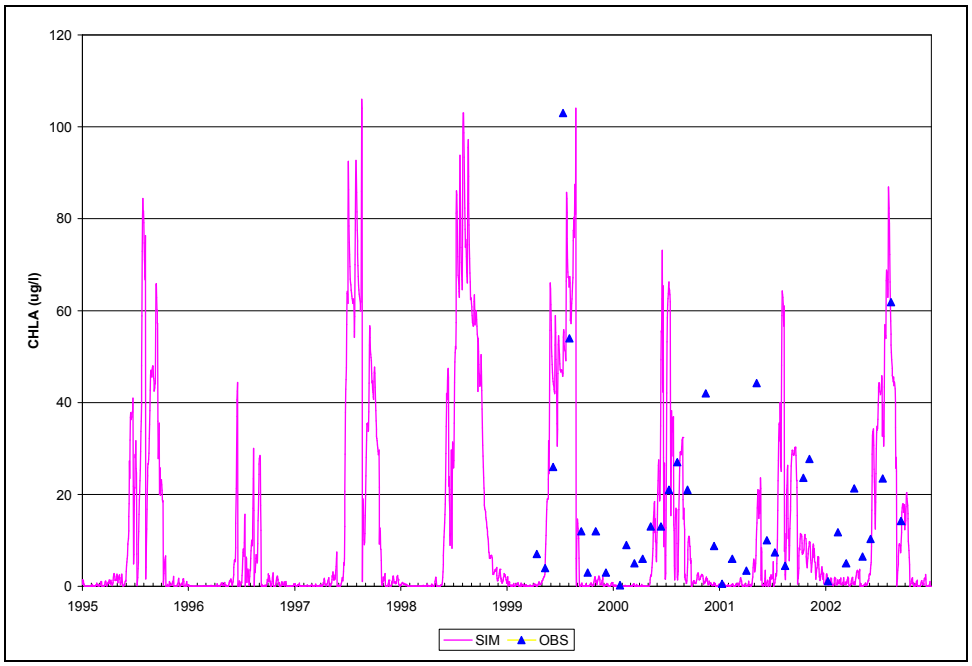

Figure C.16. Time Series of Observed and Simulated CHLA, Calibration Scenario, ANA08

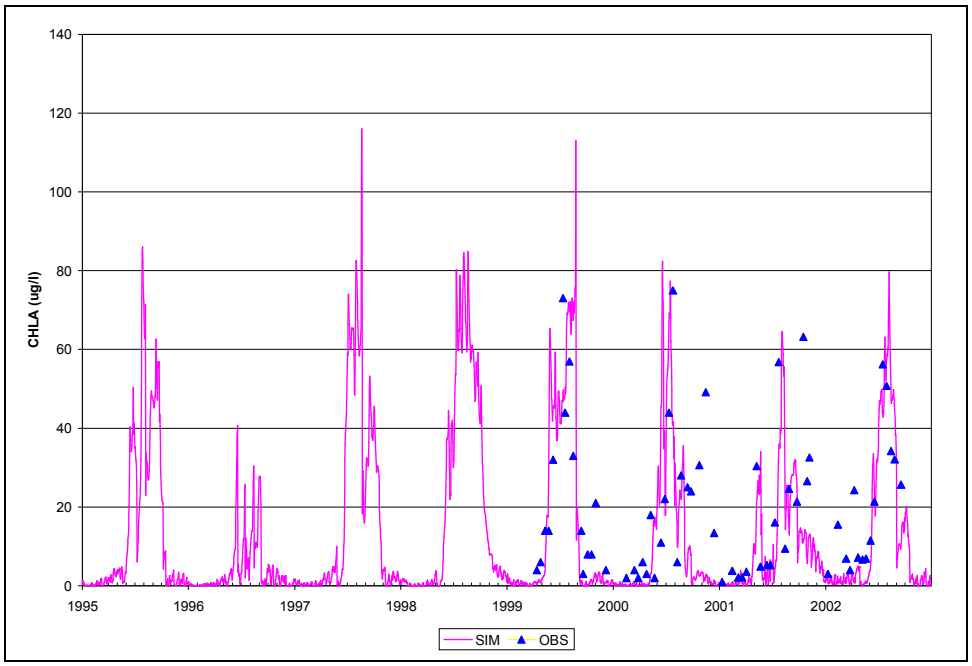

Figure C.17. Time Series of Observed and Simulated CHLA, Calibration Scenario, ANA14

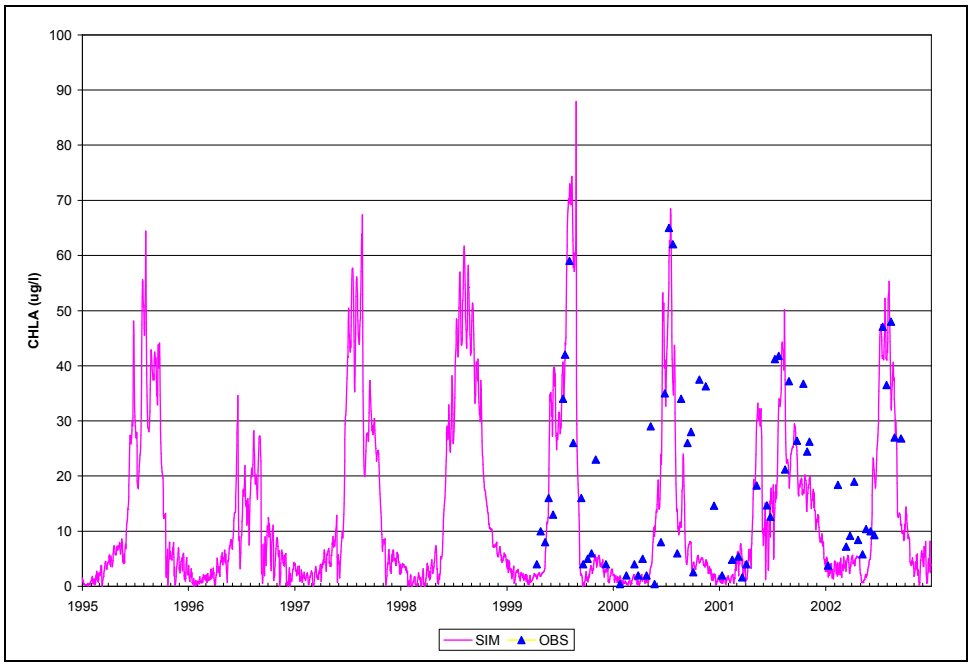

Figure C.18. Time Series of Observed and Simulated CHLA, Calibration Scenario, ANA21

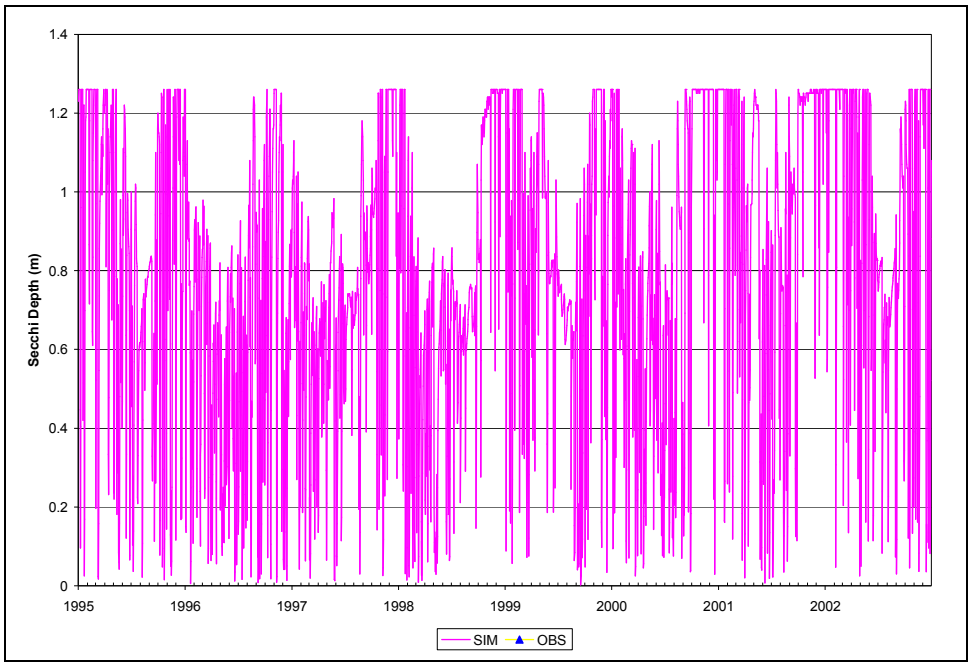

Figure C.19. Time Series of Observed and Simulated SECCHI DEPTH, Calibration Scenario, ANA0082

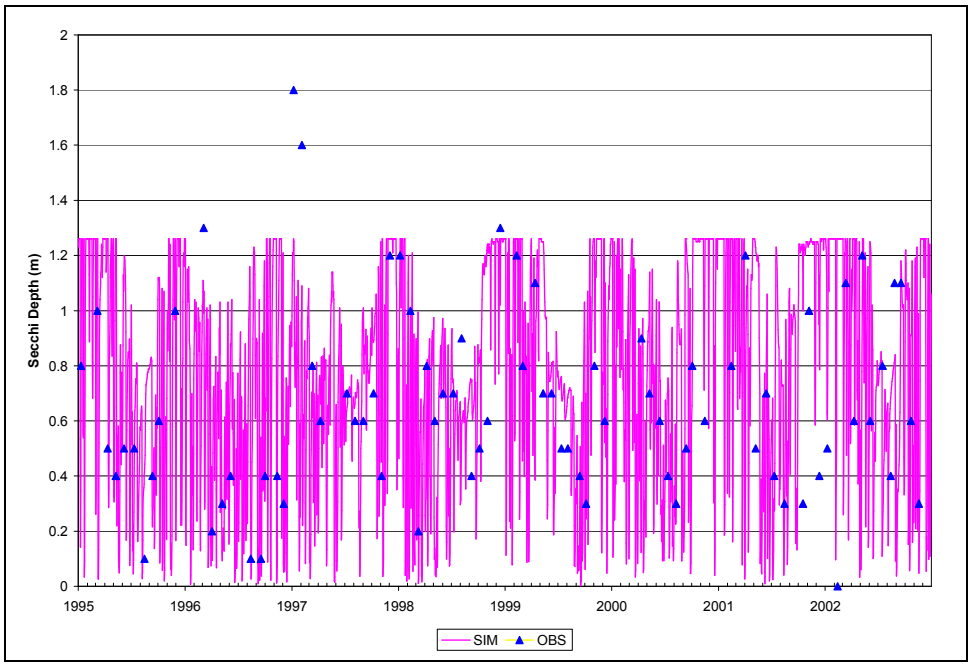

Figure C.20. Time Series of Observed and Simulated SECCHI DEPTH, Calibration Scenario, ANA30

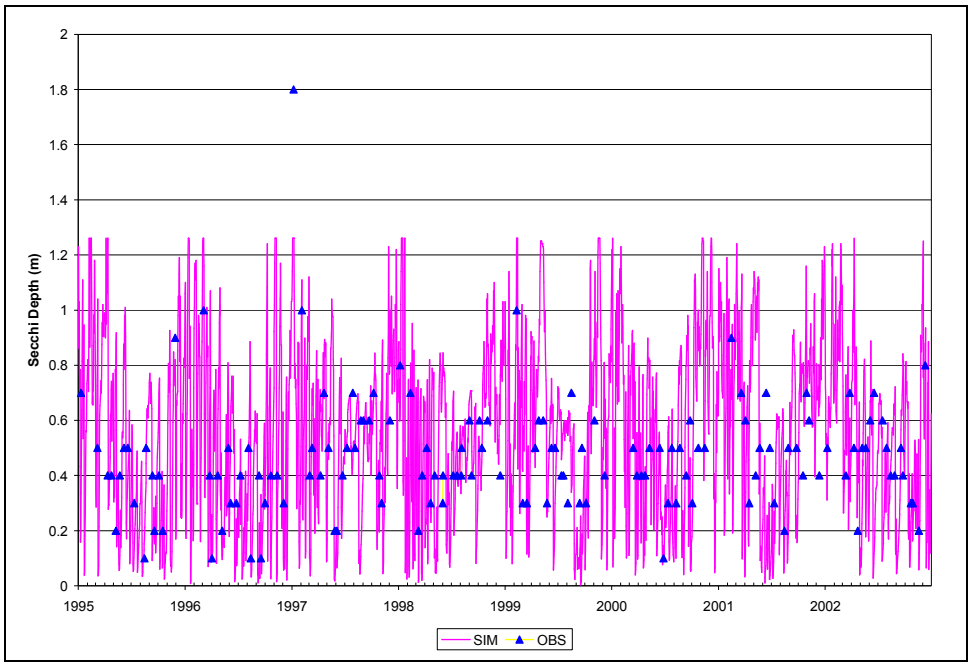

Figure C.21. Time Series of Observed and Simulated SECCHI DEPTH, Calibration Scenario, ANA01

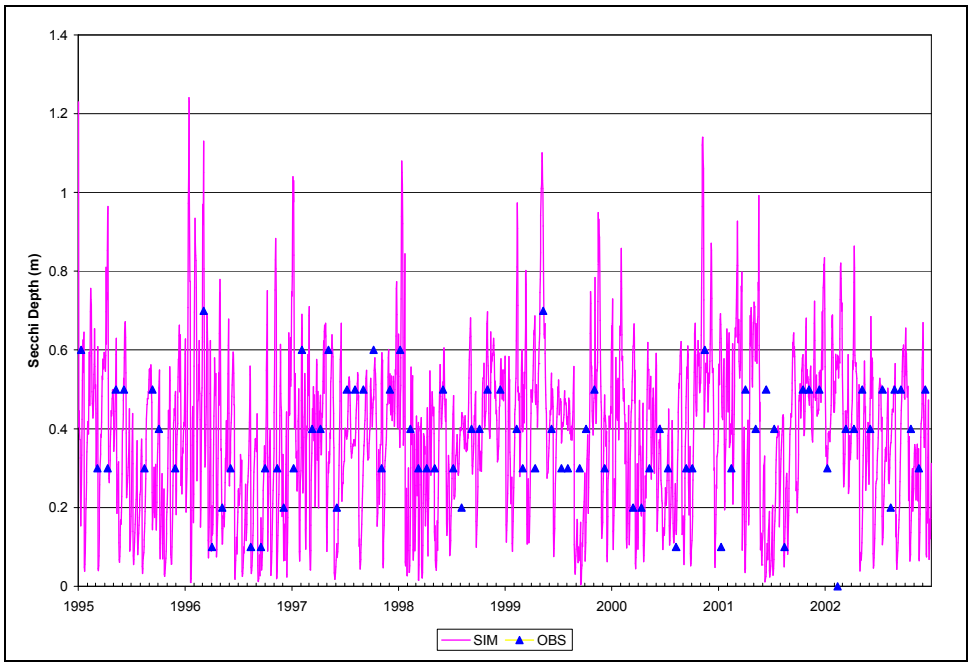

Figure C.22. Time Series of Observed and Simulated SECCHI DEPTH, Calibration Scenario, ANA08

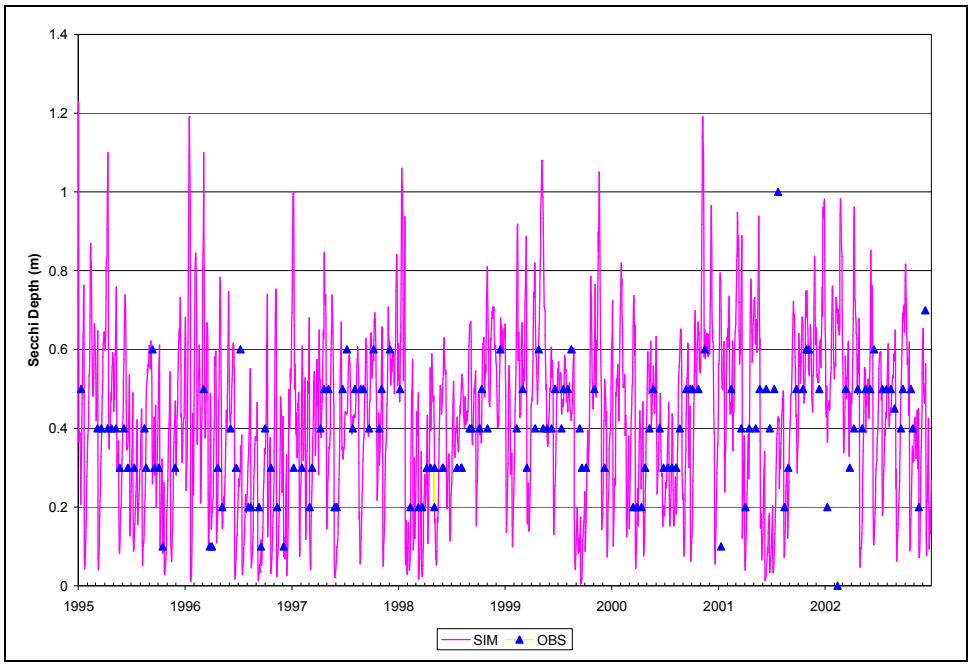

Figure C.23. Time Series of Observed and Simulated SECCHI DEPTH, Calibration Scenario, ANA14

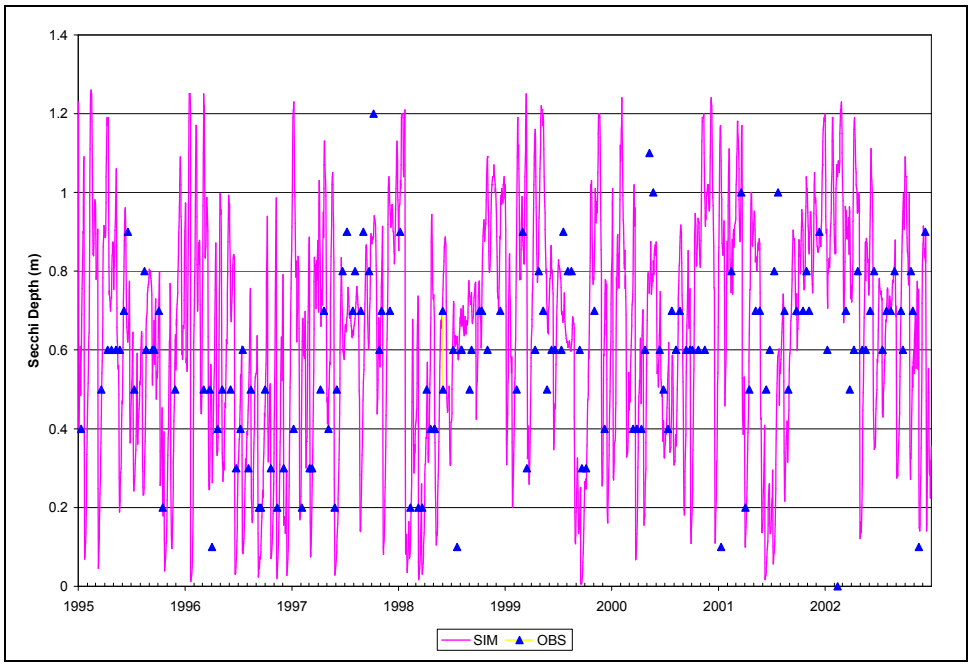

Figure C.24. Time Series of Observed and Simulated SECCHI DEPTH, Calibration Scenario, ANA21

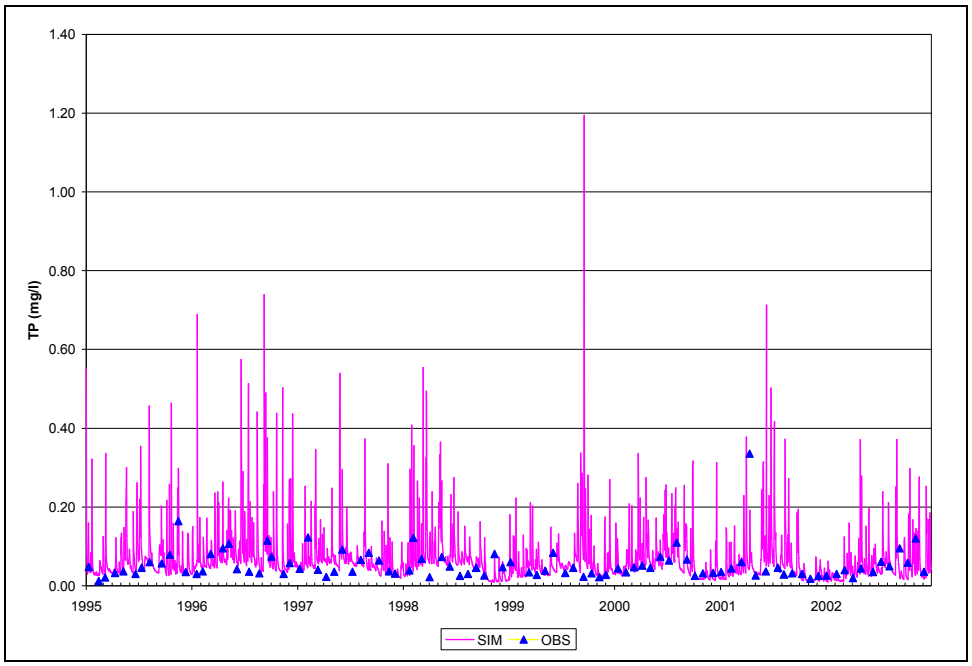

Figure C.25. Time Series of Observed and Simulated TP, Calibration Scenario, ANA0082

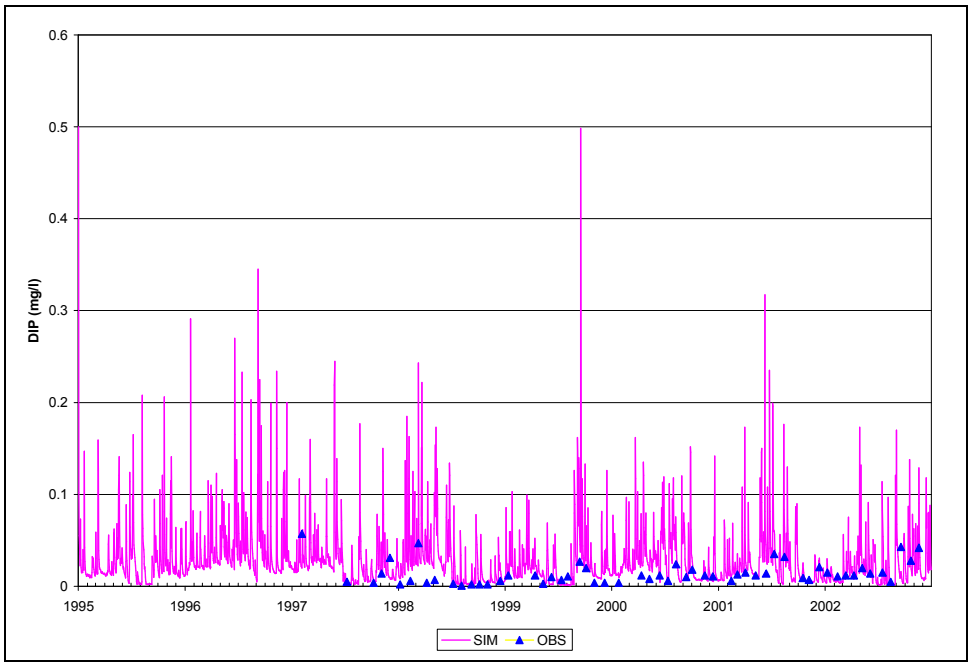

Figure C.26. Time Series of Observed and Simulated DIP, Calibration Scenario, ANA30

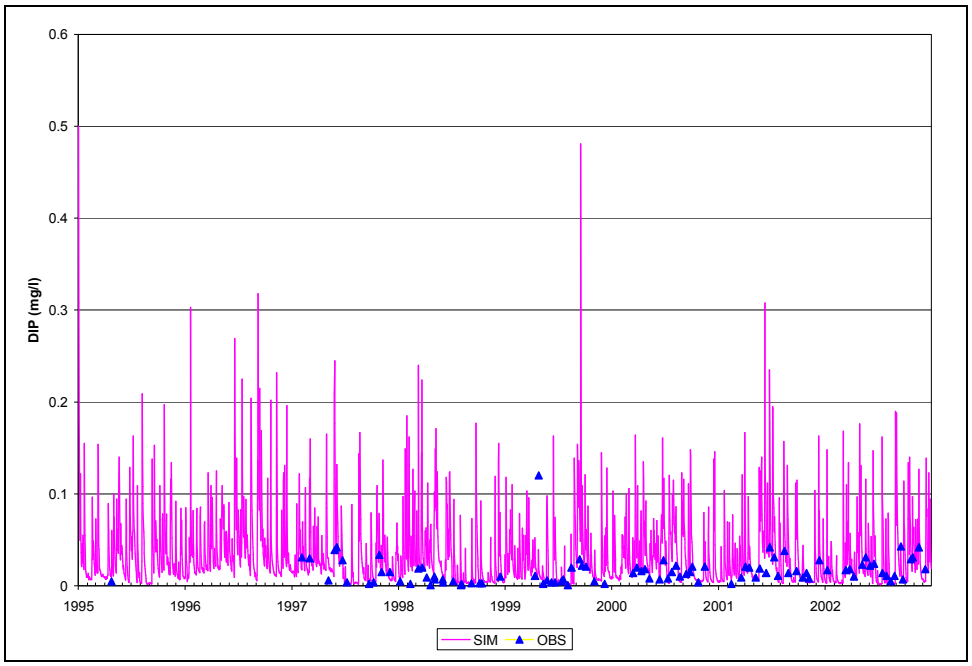

Figure C.27. Time Series of Observed and Simulated DIP, Calibration Scenario, ANA01

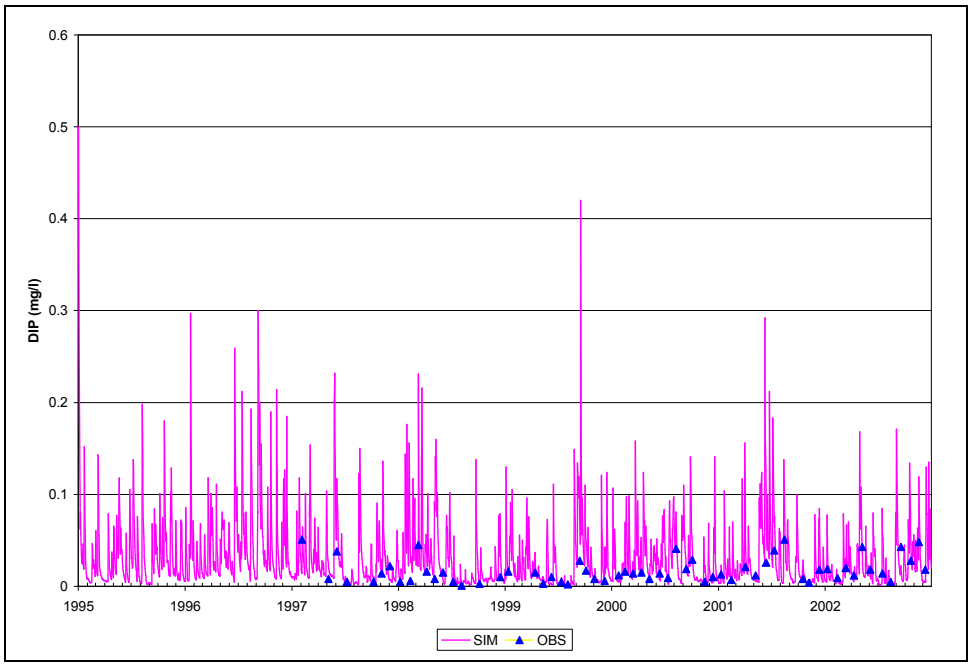

Figure C.28. Time Series of Observed and Simulated DIP, Calibration Scenario, ANA08

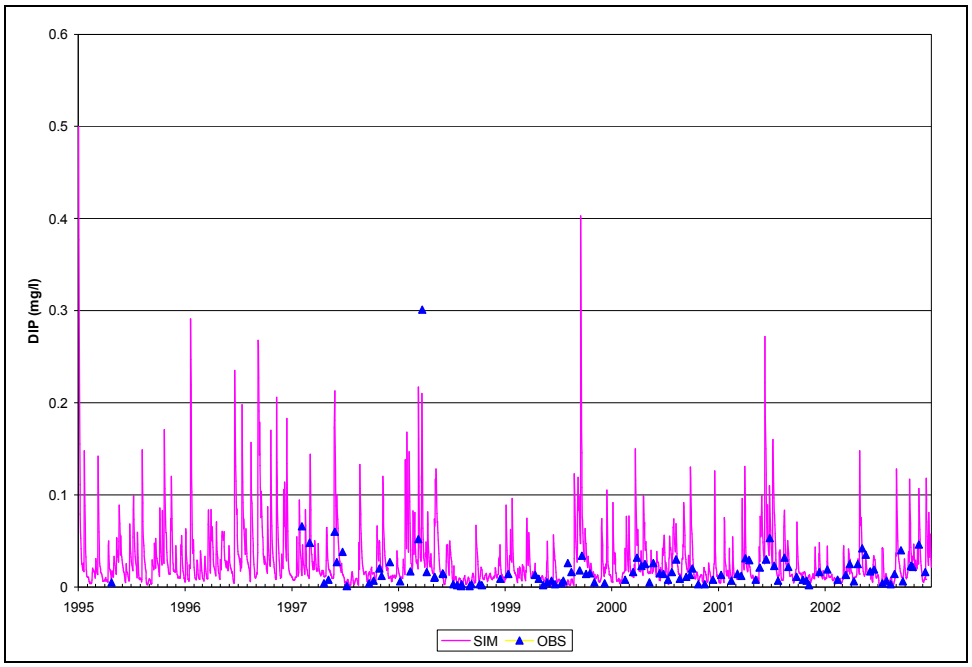

Figure C.29. Time Series of Observed and Simulated DIP, Calibration Scenario, ANA14

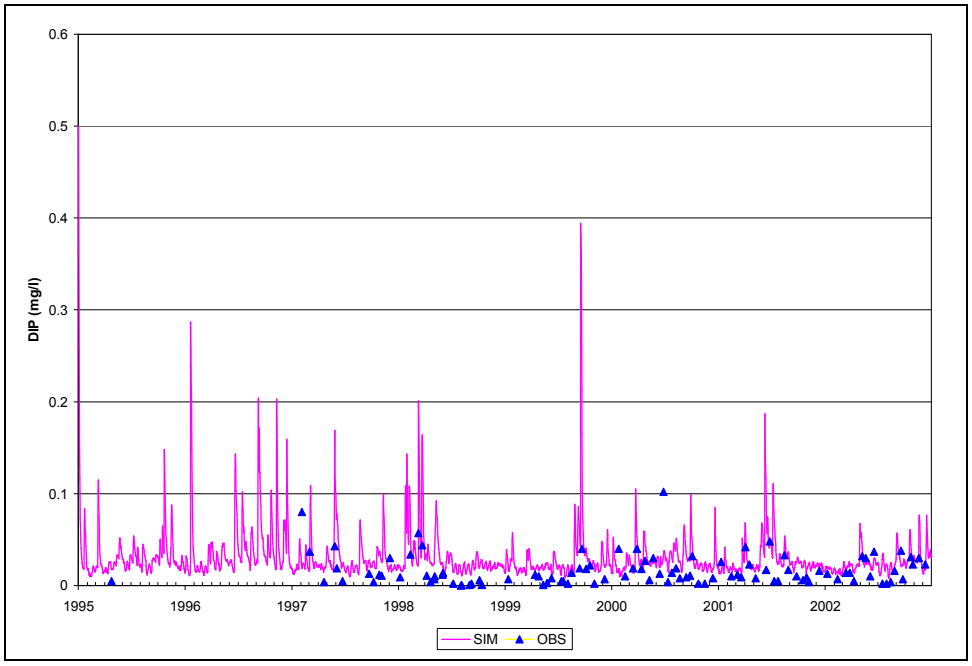

Figure C.30. Time Series of Observed and Simulated DIP, Calibration Scenario, ANA21

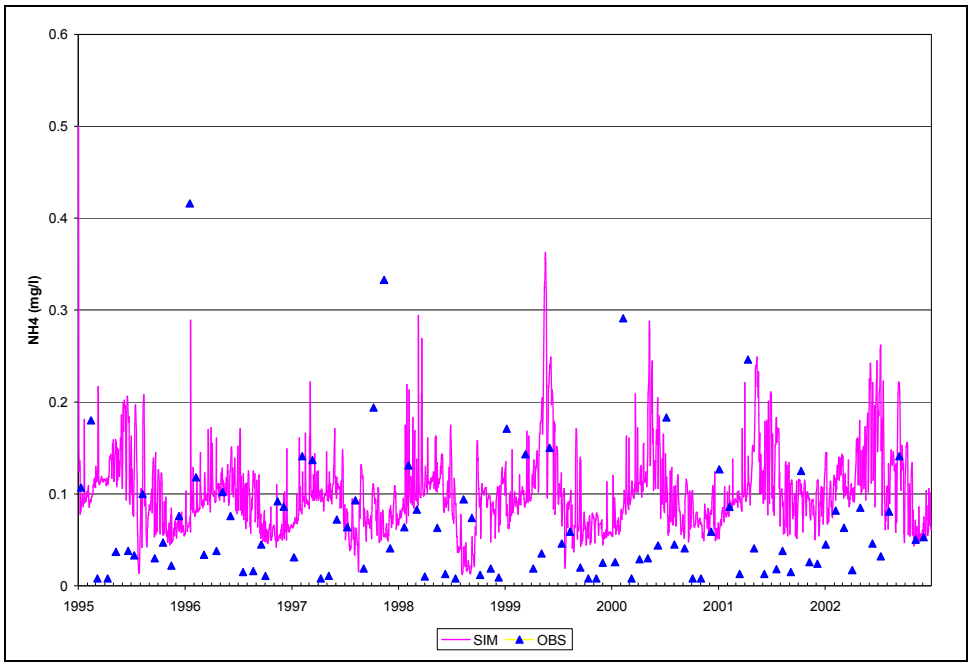

Figure C.31. Time Series of Observed and Simulated NH4-N, Calibration Scenario, ANA0082

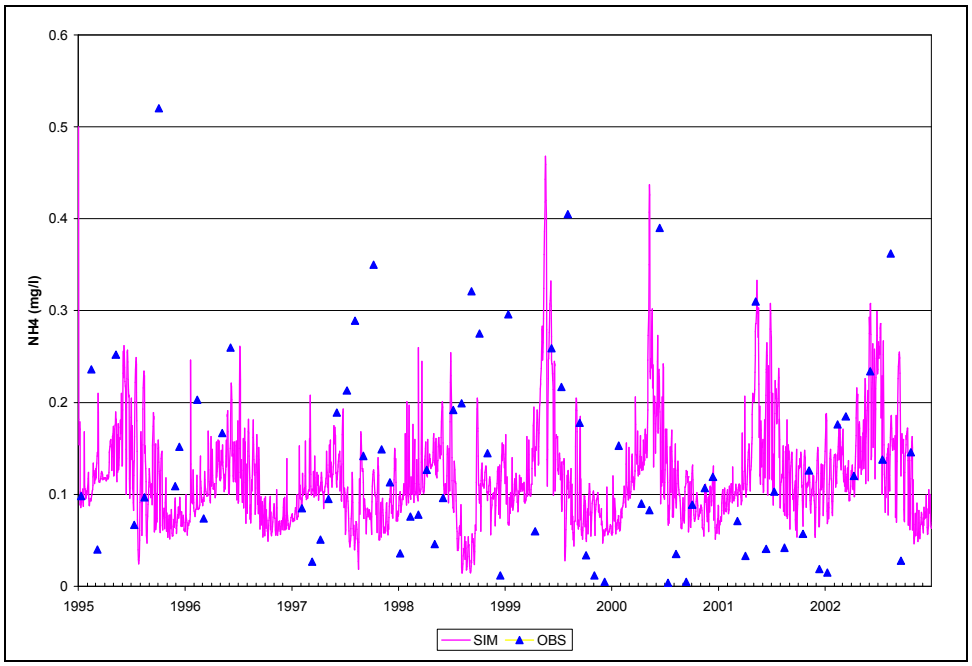

Figure C.32. Time Series of Observed and Simulated NH4-N, Calibration Scenario, ANA30

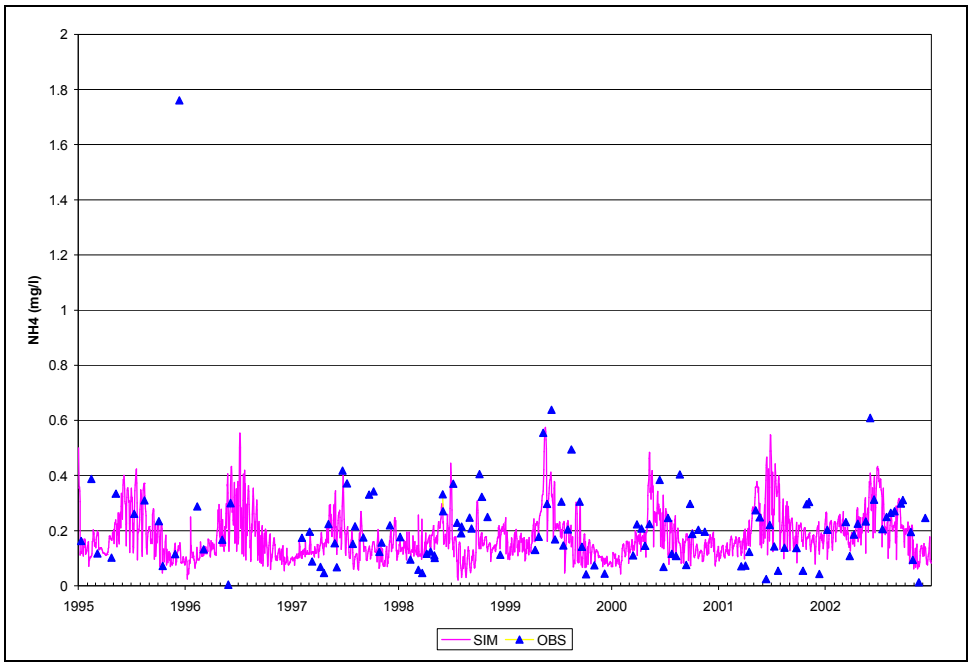

Figure C.33. Time Series of Observed and Simulated NH4-N, Calibration Scenario, ANA01

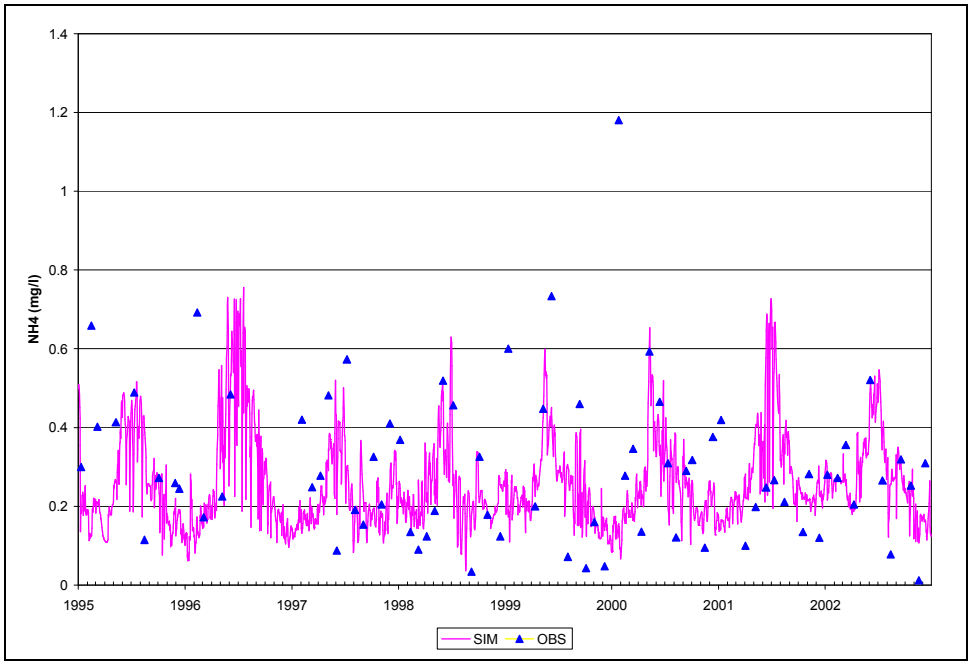

Figure C.34. Time Series of Observed and Simulated NH4-N, Calibration Scenario, ANA08

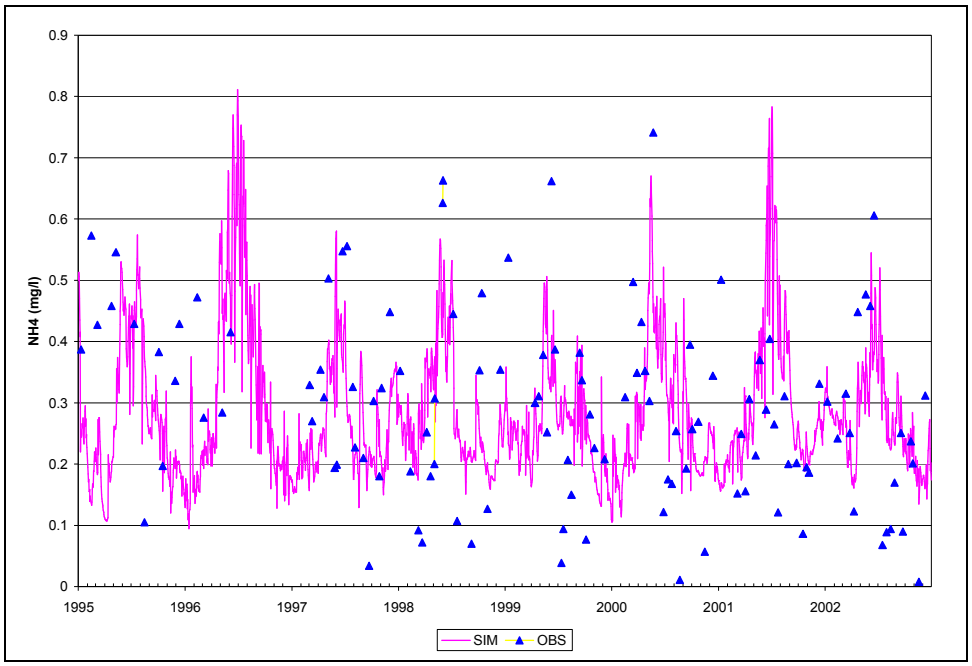

Figure C.35. Time Series of Observed and Simulated NH4-N, Calibration Scenario, ANA14

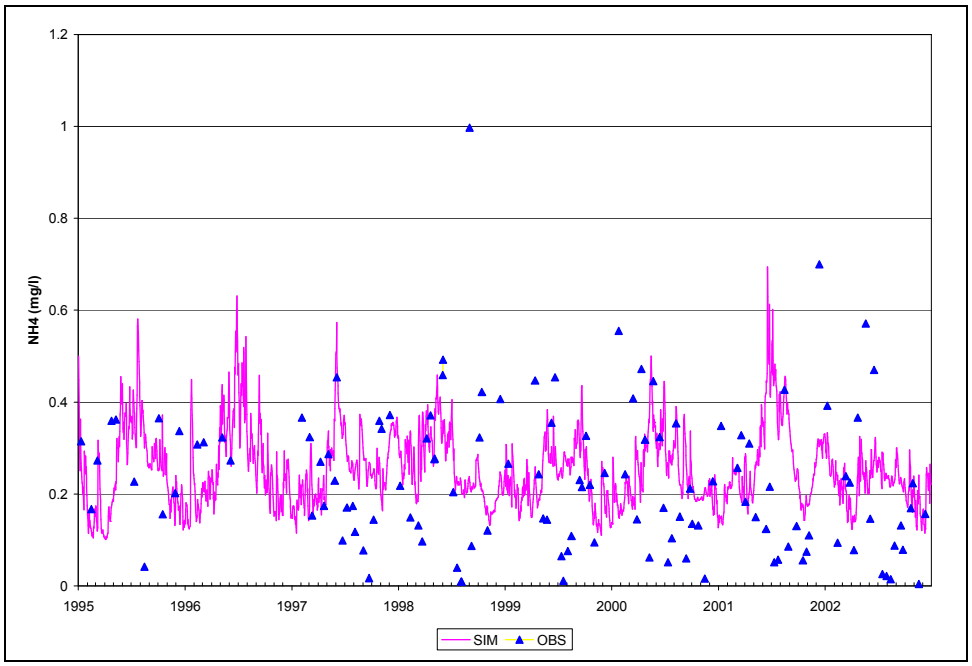

Figure C.36. Time Series of Observed and Simulated NH4-N, Calibration Scenario, ANA21

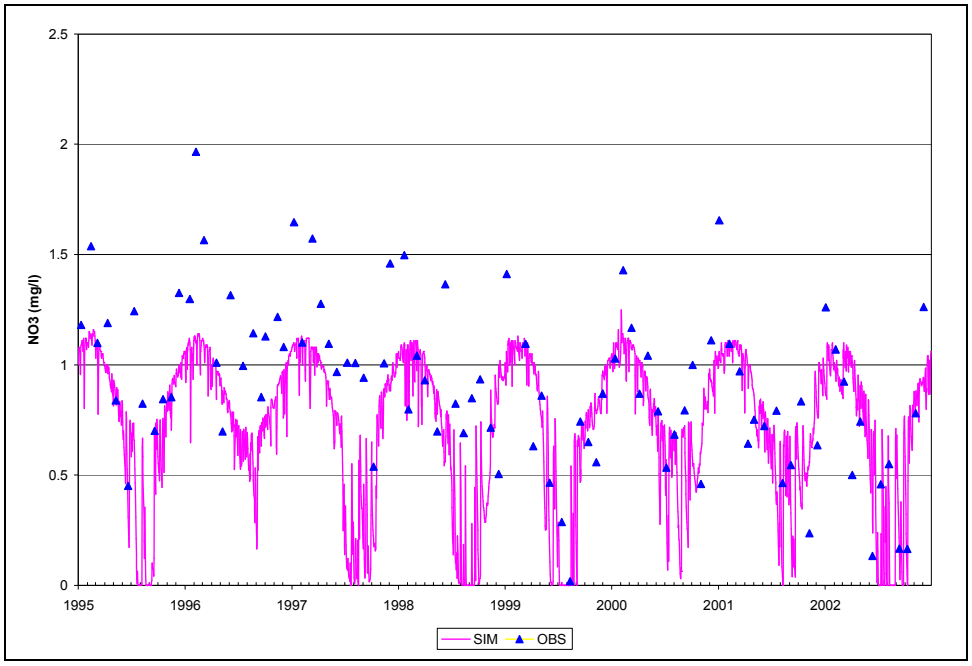

Figure C.37. Time Series of Observed and Simulated NO3-N, Calibration Scenario, ANA0082

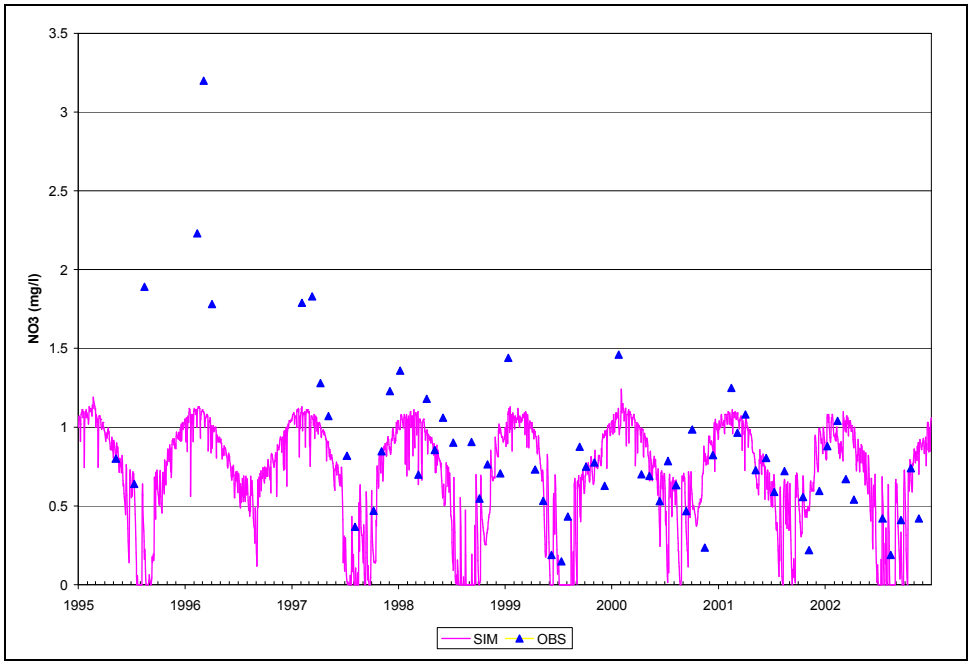

Figure C.38. Time Series of Observed and Simulated NO3-N, Calibration Scenario, ANA30

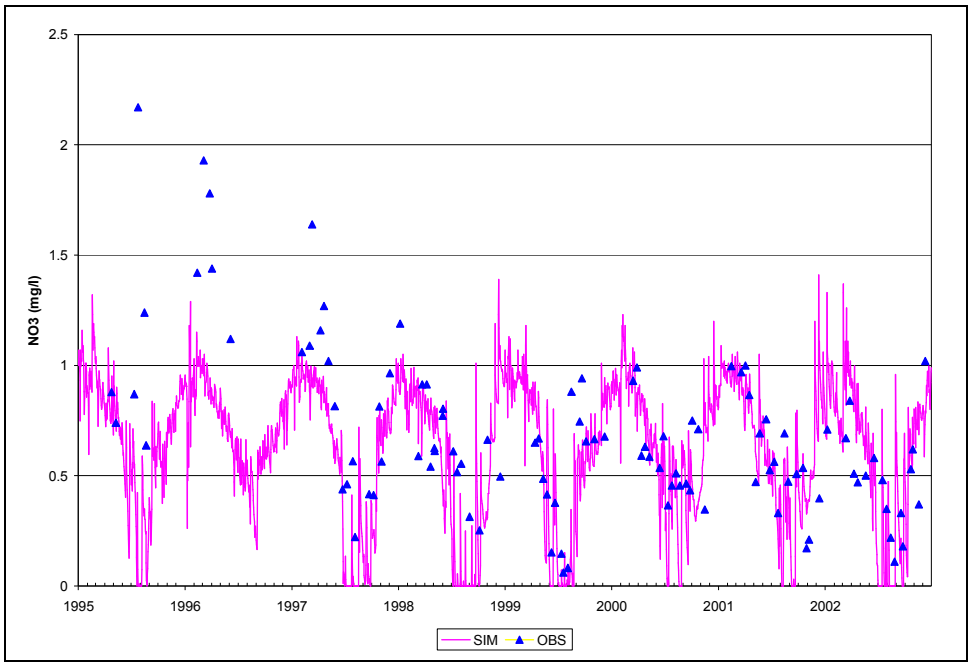

Figure C.39. Time Series of Observed and Simulated NO3-N, Calibration Scenario, ANA01

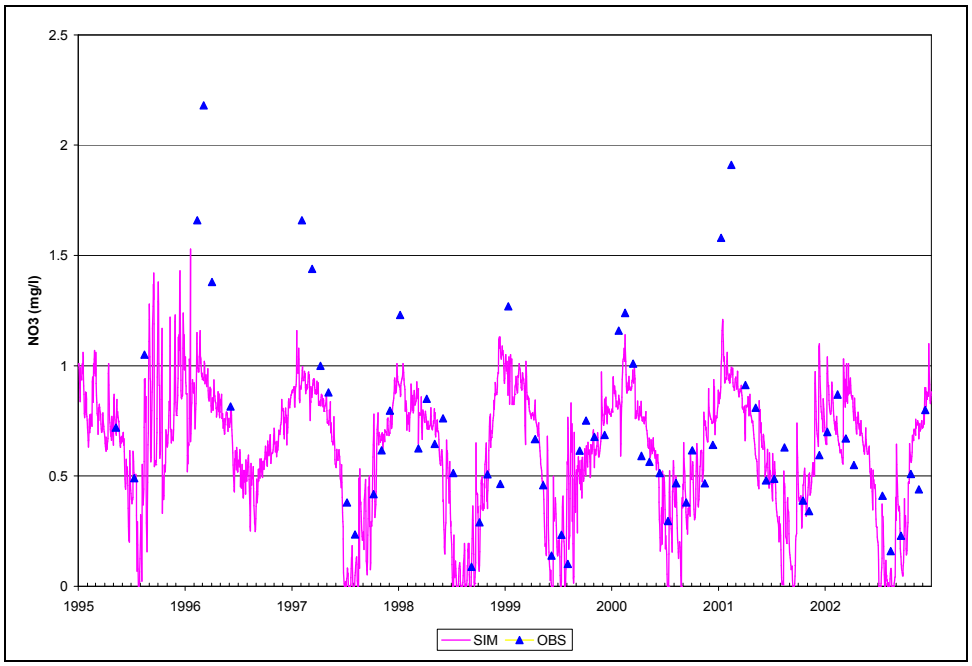

Figure C.40. Time Series of Observed and Simulated NO3-N, Calibration Scenario, ANA08

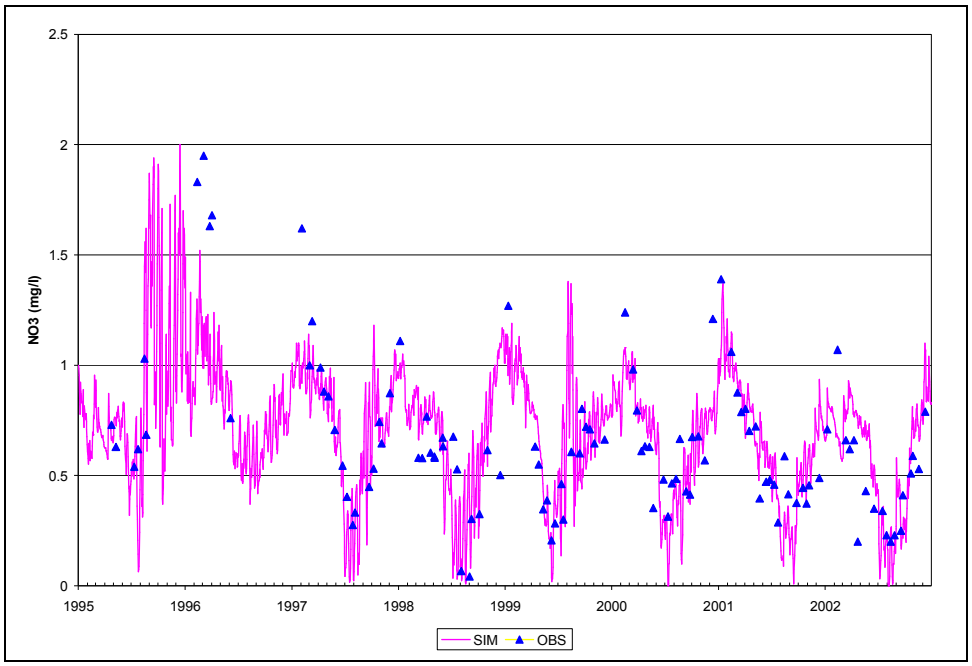

Figure C.41. Time Series of Observed and Simulated NO3-N, Calibration Scenario, ANA14

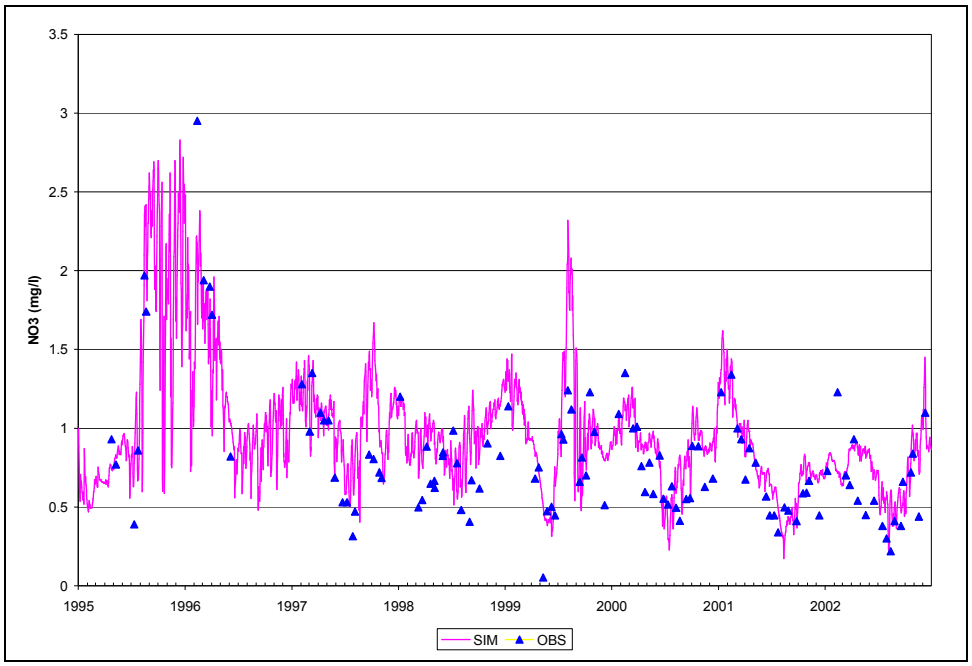

Figure C.42. Time Series of Observed and Simulated NO3-N, Calibration Scenario, ANA21